Driving Factors for Levelized Cost of Energy in Floating Wind Farms

Fredrik von Schlanbusch
Asgeir Sorteberg

A Preliminary Master's Thesis
ENERGI399
Geophysical Institute
University of Bergen

June 1, 2022

UNIVERSITY OF BERGEN
GEOPHYSICAL INSTITUTE

This master's thesis is written at the Geophysical Institute at the University of Bergen in the study program Energy under the supervision of Professor Asgeir Sorteberg.

I would like to extend my gratitude to Professor Asgeir Sorteberg, who has guided me and been available to my disposal at every step of this project. I would also like to thank Ph.D. candidate Ida Marie Solbrekke, who has helped me gain access to data produced by her during the work with her Ph.D.

Abstract

This thesis presents a method for calculating LCOE for offshore floating wind farms. A method has been created that aims to do a life cycle cost analysis, with emphasis on the cost of installation and transportation, and the cost of operation and maintenance for. The method was created to carry out a sensitivity analysis on the effects of various wind farm parameters such as water depth, distance to harbor, wind farm lifetime, capacity factor, wake loss, and the number of wind turbines in the wind farm, on the LCOE of the wind farm. The method was also created to see differences in cost between the three floating platform types: Spar Buoy, Tension Leg Platform, and Semi-Submersible Platform.

In 2010 NVE looked at the suitability of 15 locations outside the Norwegian cost for offshore wind farms, Espegren et al. (2010). Four of these locations had water depth suitable for floating platforms. In 2012 another report was published by NVE, looking at the economic suitability of wind farms in the 15 locations, Sydness et al. (2012). The data used in their report has not been made publicly available.

In this thesis, data from the dataset NORA3, described by Solbrekke and Sorteberg (2021), has been used, together with a method for calculation of LCOE, to compare the economic potential with that found by NVE for the four locations suitable for floating wind farm, Utsira Nord, Stadthavet, Frøyabanken, and Træna Vest.

The results presented in this thesis, points in the same direction as that found by NVE, with some variations. The results presented in this thesis shows the locations Utsira Nord, and Stadthavet as the most economically viable locations, with an LCOE about 15 to 20 €/MWh lower than that found for Frøyabnaken, and Træna Vest.

The results of the sensitivity analysis shows that the capacity factor of a location should be a decisive factor when building a wind farm with low LOCE is the goal. Other factors such as being able to extend the lifetime of the wind farm, and keeping the distance from the wind farm to a port short, was also shown to have a significant effect on lowering the LCOE. The distance to harbor was found to have a great impact on LCOE for large distances. Out of the wind farm parameters investigated, water depth was found to have the

least amount of impact on LCOE.

Contents

1 Nomenclature **3**

2 Introduction **8**
2.1 Thesis Relevancy 8
2.2 Problem Statement 9
2.3 Outline of the Thesis 9
2.4 Background literature 10
2.4.1 The Economics of Floating Wind 11
2.4.2 Wind tubines 13
2.4.3 Floating Pltatforms 18
2.5 Aim of the thesis 21
2.6 Previous work 21

3 Data **26**
3.1 Data used in power estimation 26
3.2 Location descriptions 27
3.2.1 Utsira Nord 31
3.2.2 Stadthavet 31
3.2.3 Frøyabanken 36
3.2.4 Træna Vest 37
3.2.5 Comparison between locations 39

4 Method **43**
4.1 Assumptions 43
4.2 Calculation of Energy Production 44
4.3 Cost models 47
4.3.1 Choise of supporting articles for the cost model 49
4.3.2 Cost model for C_{Dev}, C_{Manuf}, and C_{Decom} 51
4.3.3 Cost model data for $C_{I\&T}$ and $C_{O\&M}$ 53
4.3.4 Cost model for installation of floating platforms and wind turbines 56

4.3.5 Cost model for cables, substations, and moorings . . . 66
4.3.6 Cost model for O&M . . . 70
4.3.7 Claculation of LCOE . . . 76

5 Results **79**
5.1 Effects of the wind farm parameters on LCOE . . . 81
5.2 Locations . . . 92
5.3 Comparisons with the findings in the NVE reports . . . 94
5.3.1 Capacity factor comparison . . . 96
5.3.2 Annual energy production comparison . . . 96
5.3.3 LCOE deviation from mean comparison . . . 97
5.4 LCOE compared with Maienza et al. (2020) . . . 98

6 Discussion **100**
6.1 Discussion of assumptions . . . 100
6.2 Discussion of the method . . . 102
6.2.1 Choice of cost categories to impact LCOE . . . 102
6.2.2 Choice of supporting articles for the method used . . . 104
6.3 The results . . . 105
6.3.1 Floating platform types . . . 105
6.3.2 Effects of $C_{O\&M}$ on the results . . . 107
6.3.3 Effects of wind farm parameters on LCOE . . . 107
6.3.4 Locations . . . 118
6.3.5 Comparison of results with NVE report, Sydness et al. (2012) . . . 119

7 Conclusion **121**

A Parameter explanation for tables 4.2, 4.3, and 4.4 **135**

B Enlarged figures **138**

Chapter 1

Nomenclature

A_{GIS} - Gas Insulated Switchgear GIS plan area
A_{TS} - Plan area of transformer
$A_{IP,1}$ - The area needed for storing the floating platforms during the installation process
$A_{IT,1}$ - The hired area of the port required for one wind turbine
$A_{ITS,4,1}$ - The total area of the port that needs to be hired for storage of the substation components during the installation of the substations
A_{TS} - The plan area of the transformer
C_{Decom_avg} - Average decommissioning cost of five articles and one master's thesis found in 4.1
C_{Decom} - Decommissioning costs
C_{Dev_avg} - Average development cost of five articles and one master's thesis found in 4.1
C_{Dev} - Development costs
Cf - Capacity factor
C_{fix} - Sum of C_{Dev}, C_{Manuf}, and C_{Decom}
$C_{I\&T}$ - Installation and transportation costs
$C_{IMA,1}$ - AHV cost
$C_{IMA,2}$ - The cost of direct labour
C_{ITS} - The total cost of installing all cables needed for the wind farm
$C_{ITS,1}$ - The cost of installing the array cables
$c_{ITS,1}$ - The daily rental cost of the cable laying vessel (CLV)
$C_{ITS,2}$ - The cost of installing the export cable
$C_{ITS,3}$ - The cost of installing the onshore cables
$c_{ITS,3}$ - Unit installation cost
$C_{ITS,4}$ - The total cost of the installation process of the substations
$C_{ITS,4,1}$ - The cost associated with the port procedure regarding the substation

$C_{ITS,4,2}$ - The cost of transportation regarding the substations
$C_{ITS,4,3}$ - The cost of installing the substations at the wind farm location
$C_{ITS,5}$ - Cost of installing the onshore substation
$C_{ITS,5,1}$ - Cost of soil preparation for the onshore substation
$C_{ITS,5,2}$ - The foundation cost for the onshore substation
C_{IMA} - The cost of installing anchors and moorings
$c_{IMA,1}$ - The daily rental cost of the anchor handling vehicle (AHV)
$c_{IMA,2}$ - The cost of the direct labor associated with the installation
C_{IP} - Cost of transporting and installing the floating platforms
$C_{IP,1}$ - The port procedure cost for the floating platforms
$C_{IP,2}$ - The transportation cost for the floating platforms
$C_{IP,3}$ - The cost of installation at sea for the floating platforms
C_{IT} - Cost of transporting and installing the wind turbines
$C_{IT,1}$ - The port procedure cost for the wind turbines
$C_{IT,2}$ - The transportation cost for the wind turbines
$C_{IT,3}$ - The cost of installation at sea for the wind turbines
$C_{ITS,3}$ - The cost of the installation of the onshore cables
$c_{ITS,3}$ - the installation cost per meter of installed onshore cable
$C_{ITS,5,3}$ - Cost of cranes during the installation process for the onshore substation
c_{line} - cost of moorings per meter of mooring line
C_{Manuf} - Manufacturing costs
C_{Manuf_avg} - Average maufacturing cost of five articles and one master's thesis found in 4.1
C_m - Manufacturing cost of moorings
$C_{O\&M}$ - Operation and maintenance costs
C_c - Daily cost of cranes
c_t - Daily cost tug
c_b - Daily cost barge
c_{tm} - Mobilization cost tug
c_{bm} - Mobilization cost barge
C_{cm} - Mobilization cost crane
c_c - Cost of port crane
$c_{BT,3}$ - Number of wind turbines per travel 3
cos_L - cosines of the angel between the mooring line and the water surface
c_s - Hiring cost of storage area
c_{cv} - Cost of crew vessel
$c_{O,4}$ - Insurance cost per power unit
$c_{O,5}$ - Transmission cost per power unit
$C_{O,1}$ - The cost of calendar-based preventative maintenance

$C_{O,2}$ - The cost of unplanned corrective maintenance
$C_{O,3}$ - The annual cost of renting the maritime state property
$C_{O,4}$ - The annual insurance cost
$C_{O,5}$ - The annual transmission cost based on the capacity of the wind farm
$C_{O,2,1}$ - The annual cost of all minor unplanned corrective maintenance events
$C_{O,2,2}$ - The annual cost of all major unplanned corrective maintenance events
$c_{O,5}$ The cost of transmission per installed MW of power capacity at the wind farm
d_{pl} - Draft
d_p - Average distance from within wind farm location to closest harbor
d_{ip} - Inferior pontoon diameter floater
E_{el} - Energy production over wind farm lifetime
E_f - Export cable annual failure rate
E_{anno} - The annual energy production
FRC - The fixed charge rate
I - The initial investment
k_t - Downtime
$k_{ITS,1}$ - Installation rate of array cables
$k_{ITS,2}$ - Installation rate of export cables
$k_{ITS,1}$ - The installation rate of the CLV in m/day
$k_{ITS,2}$ - The installation rate for export cables of the CLV
LCOE - Levelized cost of energy
LCC - Life cycle cost
L_P - Number of mooring lines per platform
l_{TS} - Electric transformer lengt
l_{GIS} - Gas insulated Switchgear leangth
l - length of platform
l_f - Maximum freeboard
l_b - Turbine blade length
ℓ - Rent percentage of wind farm revenue
l_1 - The length of the array cables
l_2 - the length of the export cable
$min_{UCMpct.}$ - The minor unplanned corrective maintenance events as a percentage of the total unplanned corrective maintenance events
NVE - Norges vassdrags- og energidirektorat
NORA3-WP - 3-km Norwegian Reanalysis
n_S - Number of substations in the wind farm
n_{UCM} - The annual number of all unplanned corrective maintenance events
N_T - Number of wind turbines in the wind farm
$n_{BT,1}$ - Number of wind turbines per travel 1

$n_{BT,2}$ - Number of wind turbines per travel 2
n_c - Number of cranes w/o storage area
n_t - Number of tug vessels
n_b - Bumber of barge vessels
n_1 - Number of electric array cables
n_2 - Number of electric export cables
n_3 - Number of electric onshore cables
n_{cs} - Number of floating cranes w/ storage area for transportation
$n_{BP,1}$ - Number of floating platforms per boat, 1
$n_{BP,2}$ - Number of floating platforms per boat, 2
$n_{BP,3}$ - Number of floating platforms per boat, 3
n_{TS} - The number of transformers
n_{TS} - The number of transformers
n_1 - The number of electric cables used for the array cables
n_2 - The number of electric cables used for the export cable
n_M - The total number of moorings at the wind farm
n_{CBM} - The annual number of calendar-based maintenance events
P - Average power output of a turbine
PE - Price per unit energy
Pr - Rated power of a turbine
$r_{IMA,1}$ - The installation rate of anchors installed per day
r - The real discount rate
SB - Spar Buoy
SSP - Semi-Submersible Platform
TLP - Tension Leg Platform
T_{pc} - Wind farm power capacity
t_{LT} - Time to load turbines in the vessel
t_{iT} - Time between movements while OWT is installed
t_{imT} - Time to install WT offshore with lifts
t_{iP} - Time for installing and lifting offshore
t_{imP} - Time between movements while installing
t_{LP} - Time to load platform in vessel
$t_{IT,1}$ - The time needed to hire the port per wind turbine
$t_{A,1}$ - Time waiting for the barge during the port procedure
$t_{A,2}$ - Time waiting for the tug during the port procedure
$t_{A,3}$ - Time wating for the crane during the port procedure
$t_{A,4}$ - Time spent using the floating crane
$t_{A,5}$ - The operation time during the installation process of the floating crane
$t_{A,6}$ - The operation time during the installation process of the barge
$t_{A,7}$ - The operation time during the installation process of the tug

$t_{A,8}$ - The operation time during the installation process of the floating crane
$t_{A,9}$ - The operation time during the installation process of the floating crane
t_{LIOS} - Time lift substation, load on vessel
$t_{IT,1}$ - Sum of $t_{A,3}$ and $t_{A,4}$
$t_{IP,1}$ - The number of days the port has to be rented during the installation of the floating platforms
t_{LOS} - The time to load all substations during the port procedure
t_{LIOS} - The time to load one substation into vessel
$t_{ITS,4,1}$ - The time needed to hire the port during the installation process
t_{LOS} - The time needed to load the substations onto the carrying vessel
T_{pc} - The total power capacity of the wind farm
UCM - unplanned corrective maintenance
v_t - Speed of barge and tug vessels
v_{t1} - Speed of floating crane
v_{cv} - Crew vessel speed
w_d - Average water depth
WF_{LT} The lifetime of the wind farm
WL - Wake loss

Chapter 2

Introduction

2.1 Thesis Relevancy

In 2012 a report was written by NVE (Norges vassdrags- og energidirektorat), Sydness et al. (2012). The report looked at 15 different sites on the coast of Norway for production of offshore wind energy. 11 out of the 15 different sites that were looked at by NVE at the time are located in shallow water areas where fixed foundation turbines would be utilized. As the water depth is thought to be a significant contributor to the cost of building offshore wind farms, NVE has assumed that, since locations that will use floating solutions are located in deeper waters, these farms would need to be built out with at least 1000 MW capacity to reduce unit cost of production.

The data used by NVE in their report has not been made publicly available. As the economics of offshore wind power production continues to improve, and the interest in building out the Norwegian offshore wind energy production capacity increases, there is an increased need of getting a better understanding of the suitability of wind farms in these areas. Since the data used by NVE is not publicly available, this thesis will investigate the locations Utsira Nord, Træna Vest, Frøyabanken, and Stadthavet, using the publicly available dataset NORA3-WP, and see how the expected energy production compares with that found by NVE, Sydness et al. (2012). I also want to investigate how the parameters depth, distance to harbor, number of turbines, type of turbine, type of floating platform, wake loss, and wind farm lifetime influence the cost of building wind farms in these locations.

The overall objective of this thesis is to contribute to more knowledge about the various wind farm parameters being investigated, and how they influence

the cost of wind farms over their lifetime.

Hence, the research done in this thesis will be of interest for policy makers, organizations, companies, and stakeholders with interest in offshore wind on the Norwegian coast.

2.2 Problem Statement

The research in this thesis will be supported by the following questions:

How is the levelized cost of energy (LCOE) affected by the distance to port, the number of wind turbines in a park, the wake effect, the water depth, capacity factor and the wind farm lifetime?

Can we add to the understanding that we have from research done by for example Myhr et al. (2014), and Shafiee et al. (2016) on how different parameters influence LCOE for offshore wind farms?

Can we improve our understanding of available resources for production of wind energy and are there areas better suited for wind farms than others regarding LCOE?

Are there any significant changes in the possible energy production in the different areas looked at by NVE when using the data from NORA3-WP?

To answer these questions, data from NORA3-WP will be used to find the expected energy production of the four locations, Utsira Nord, Træna Vest, Stadthavet and Frøyabanken. The resulted data will further be used in combination with parameters such as the distance to port, the number of wind turbines in a park, the wake effect, the water depth, the capacity factor, and the wind farm lifetime. These parameters will be used to look at how they affect the levelized cost of energy for wind farms, in combination with three different turbines of different rated power and three different platform types.

2.3 Outline of the Thesis

This thesis will first, in chapter 2, present some basic concepts within offshore floating wind that is useful to understand when reading this thesis. At the

end of the chapter a summary of the findings regarding LCOE in offshore wind farms found in other articles is presented. Further, the data that has been used in the calculations of LCOE in this thesis is presented in chapter 3, before a method chapter, outlining the method that has been created in this thesis to calculate LCOE for floating wind farm, in chapter 4. Finally, the results found when using the data presented in chapter 3 together with the method for calculating LCOE from chapter 4, is presented in chapter 5. These results is further discussed in chapter 6, before a conclusion is given in chapter 7. A list of figures and tables are found after the last chapter, and finally, at the end of the thesis, Appendix A, and B is found.

2.4 Background literature

The development of offshore wind energy is still in an early phase. Therefor there still has not been done an adequate amount of research around floating offshore wind. This leads to the need to make assumptions when looking into the different factors that play a role in the cost of offshore wind. As of May 2022, there are three operational floating wind farms in the world. These are Hywind Scotland with five turbines and 30 MW installed capacity, Equinor (2022a), WindFloat Atlantic with three turbines and 20 MW installed capacity, EDP (2022), and Kincardine with six turbines and 50 MW installed capacity, Cobra (2022). There also exists a couple of single operational turbines around the world. Because there does not exist floating wind farms of the same size as that of bottom fixed windfarms, the available data for costs within the floating offshore wind industry is still quite limited. Therefore, a lot of research that has been done within the area has been based on simulations.

A lot of the literature used to support the work with this thesis are articles proposing various cost models for floating offshore wind. Considering the various parameters regarding the wind farm investigated in this thesis (the distance to port, the capacity factor, the number of wind turbines in a park, the wake effect, the water depth, and the wind farm lifetime), I have decided to put special emphasis on papers and articles discussing the parts of the life cycle cost (LCC) that are the most affected by variations in the selected parameters. This will be papers, and articles that discuss cost models for installation, transportation, and operation and maintenance (O&M) costs.

To look at LCOE, I need to get an understanding of the LCC of an offshore wind farm. I have decided to divide the LCC into five cost-categories which

will be discussed further in chapter 4. Two of the cost categories are installation costs and operation and maintenance costs. Maienza et al. (2020) and Bjerkseter and Ågotnes (2013), are two articles that has been used to develop the cost model used in this thesis. These two articles have developed cost models for the installation and transportation of the wind turbines and the floating platforms, the installation of cables, and the yearly operation and maintenance costs associated with an offshore wind farm. These are the costs that are the most affected by variations in the different wind farm characteristics being looked at in this thesis.

The NVE Report, Sydness et al. (2012), is a central part of the literature used to write this thesis. From the report I have collected information about coordinates for areas that would be interesting to investigate regarding floating offshore wind. I have also been using this report to compare the potential energy outputs of the various areas being investigated to that of the energy output calculated in this thesis. When deciding on the size of the wind farms in the areas being investigated in this thesis, I have based this on the assumed maximum power capacity in megawatts (MW), suggested for each area in the NVE report. For most areas that is 1500 MW. This number is being used in order to have a point of reference when comparing possible energy production between the areas being investigated. I am aware that building floating offshore wind farms of this scale is not realistic today. The reason for this is that the maximum possible effect assumed by NVE would mean building wind farms on a scale yet to be seen in any offshore wind farm, floating or bottom-fixed. Today there exists one offshore wind farm with more than 1 GW installed capacity, built in 2019. Three other farms with more than 1 GW installed capacity are under construction. 10 years ago, the greatest offshore wind farm had an installed capacity of 500 MW.

Judging by the trends in the size of offshore wind farms that has been built the last 15 years, we can assume that farms with the 1500 MW effect being used in the analysis of this thesis, or greater effect will probably be built within the coming years and decades. The greatest proposed project to date is located in South Korea and has a planned effect of 8 GW.

2.4.1 The Economics of Floating Wind

Offshore wind farms are highly capital demanding infrastructure projects. Depending on the size of the wind farm the cost of just the manufacturing of

all the turbines, platforms and parts needed for the farm can cost upwards of billions of euros.

In this thesis the economic metric that will be used to compare windfarms is called Levelized cost of energy (LCOE). LCOE is an effective way of comparing economic feasibility of energy producing technologies with each other as well as comparing different energy producing power plants of the same technology, for example two different wind farms. LCOE is an effective way of comparing power plants because it is given in currency units per energy unit produced, commonly in €/MWh. Therefore, a power plant's LCOE showcases how much it needs to sell its energy for. This way the investors of the power plant know when they will break even on their investment during the power plant's lifetime. If the energy produced is sold for an average amount lower than that of the power plant's LCOE, the facility will lose money over its lifetime. However, if the energy is sold for an average price higher than the power plant's LCOE the facility will make money during its lifetime.

Seeing how the effectiveness of LCOE as an indicator to compare power plants with each other, you can see how LCOE also can be used to compre different types of energy production with each other. By looking at the LCOE of a power plant, one can compare the economic feasibility for that of a coal power plant with an offshore wind farm, or the economic advantages of one wind farm over another farm in a different location. It is because of the effectiveness of LCOE as a tool to compare the cost of energy for different power plants that it is useful.

In this thesis LCOE will be calculated as defined by Lerch et al. (2018). They have defined LCOE as in equation 2.1.

$$LCOE = \frac{LCC}{E_{\text{el}}} \tag{2.1}$$

Where LCC is life cycle cost in euros, and E_{el} represents total energy production over the wind farm's life cycle in MWh.

Life cycle cost (LCC) is a way of measuring an asset's, or in this case the wind farm's total cost over its lifetime. This includes all costs associated with the wind farm: initial investments in infrastructure to maintenance and finally removal of the farm after its lifetime. Lerch et al. (2018) defines LCC

as the sum of development costs (C_{Dev}), manufacturing costs (C_{Manuf}), installation and transportation costs ($C_{I\&T}$), operation and maintenance costs ($C_{O\&M}$) and decommissioning costs (C_{Decom}). LCC is calculated as shown in equation 2.2.

$$\text{LCC} = C_{\text{Dev}} + C_{\text{Manuf}} + C_{\text{Transport}} + C_{\text{Instal}} + C_{\text{O\&M}} + C_{\text{Decom}} \tag{2.2}$$

These five costs include all costs associated with an offshore wind farm throughout its lifetime. Development costs includes costs associated with the planning and development phase where the wind farm is designed, the construction of the farm is planned and a strategy for the operation and maintenance phase is laid out. Manufacturing costs includes all costs associated with the purchase and manufacturing of all physical components of the offshore wind farm. This primarily means the purchase of wind turbines, offshore floating platforms, off- and onshore substations and floating platforms for the offshore substations, array cables, export cables, onshore export cables, as well as anchors and moorings. Installation and transportation costs includes costs associated with the transportation of wind turbines and offshore floating platforms to the location of the offshore wind farm from a nearby harbor, installation of the wind turbines onto the floating platforms at the wind farm location, the installation of cables, substations, anchors, and moorings. Finally, the decommissioning costs includes all costs associated with the removal and decommissioning of all wind farm components.

2.4.2 Wind tubines

The development of wind turbine technology has been moving the industry in the direction of bigger turbines for the past two decades, and the trend is not showing signs of slowing down as shown in figure 2.1, where we can seee that bigger and bigger turbines take up a larger share of the turbines installed.

From wind turbines with the effects of 1-2 MW in the early 2000s, to the largest turbine that have currently been built with an effect of 14 MW, Simens Gamesa (2022a). The trends of making continuously larger turbines over the years is a trend partly fueled by the emergence of offshore wind turbines. One

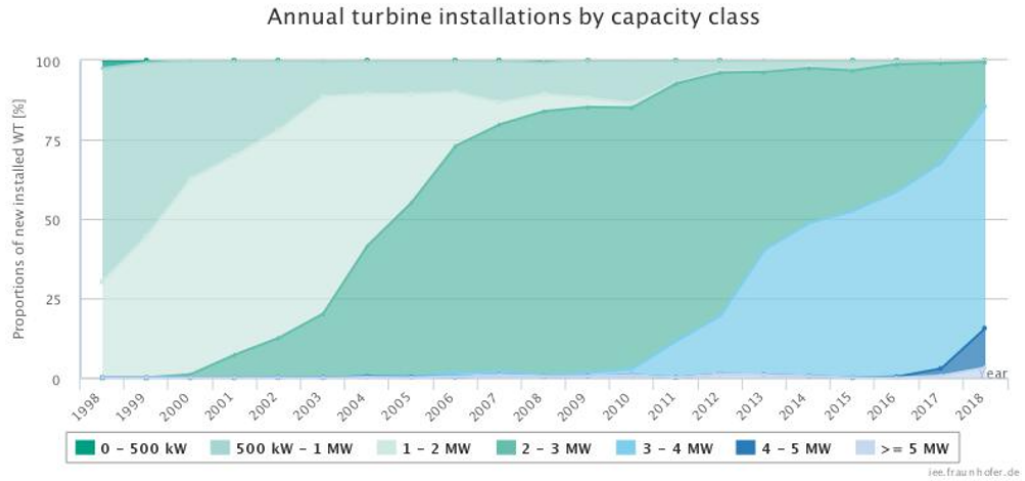

Figure 2.1: *Proportion of new installed wind turbines each year by wind turbine rated power for onshore wind. Each color represents the share of total annual installed capacity for each "power capacity group" ranging from 0-500 kW, all the way to greater than 5 MW turbines. Figure is taken from Wind Monitor (2022a).*

problem with onshore wind turbines is that the turbine blades must be made in one solid piece and therefore also must be transported from the production site to the wind farm as one piece. This makes for some difficult logistics when it comes to transportation as wind turbines get larger and the blades gets longer. Offshore wind turbines on the other hand can be produced in factories by the sea and then easily carried by ship to a port located near the offshore wind farm. The fact that offshore wind turbines are leading the way when it comes to the increase in installed rated power for wind turbines can be seen when comparing Figure 2.1 and figure 2.2. Here you can see that the 5 MW rated power turbines make up a much larger portion of the newly installed wind turbines for offshore wind compared with the onshore wind.

Before we continue this section, I would like to define some important concepts regarding wind energy that is important to have a common understanding of when reading this thesis.

Power curve: Every different model of wind turbines has a power curve that corresponds to that model of wind turbine. The curve shows how the turbines power output vary with the wind speed. Examples of power curves can be seen in figure 2.3.

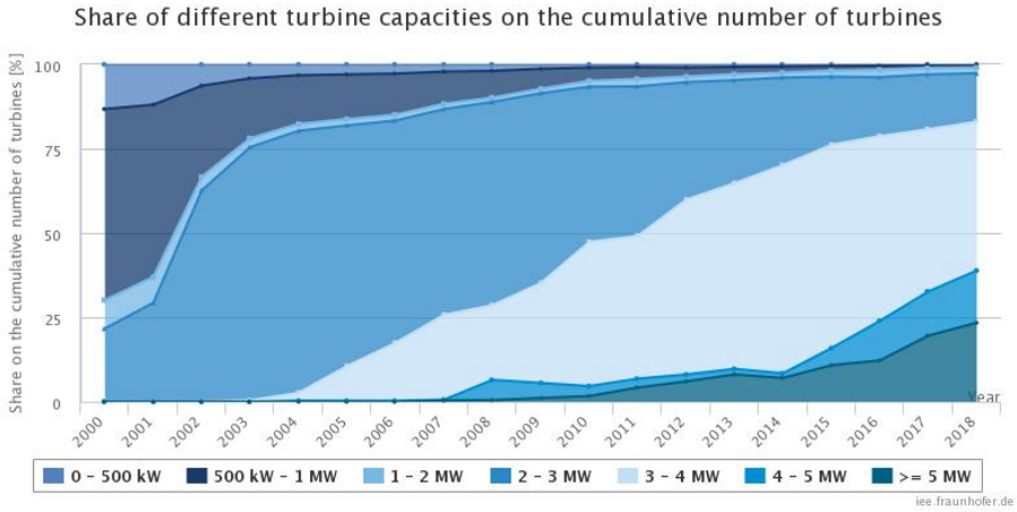

Figure 2.2: *Proportion of annualized installed offshore wind turbines categorized by wind turbine rated power. Each color represents the share of total annual installed capacity for each "power capacity group" ranging from 0-500 kW, all the way to greater than 5 MW turbines. Figure is taken from Wind Monitor (2022b).*

Rated wind speed: A turbine's rated wind speed is the wind speed at which the turbine is designed to not increase its power output with an increasing wind speed, but rather keep a constant power output.

Rated power: A turbine's rated power is a turbine's maximum power output. The rated power of a wind turbine is given by the turbine's rated wind speed, at which the turbine will keep a constant power output with increasing wind speed.

Capacity factor: A turbine's average power output, divided by its rated power. It is given by equation 2.3:

$$Cf = \frac{P}{Pr} \tag{2.3}$$

Where: Cf = capacity factor, P = average power output of a turbine, and Pr = The rated power of a turbine.

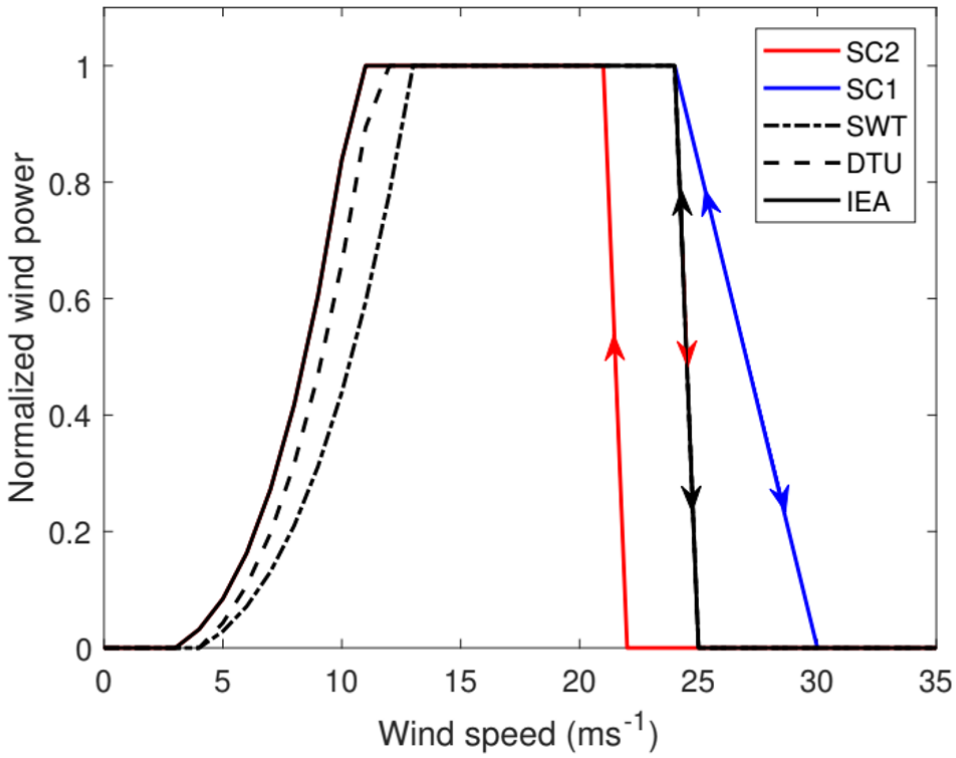

Figure 2.3: *The graph shows the power curves of three wind turbine types: the 6 MW SWT-6.0-154 turbine, the 10 MW DTU-10.0-Reference turbine, and the 15 MW IEA-15-240-RWT turbine. The solid line represents the 6 MW turbine, the dashed line represents the 10 MW turbine, and the dash-dot line represents the 15 MW turbine. The figure shows normalized wind power on the y-axis, and wind speed on the x-axis, and is useful to compare the cut-in wind speeds of each turbine. The black arrowed line represents the cut-out wind speed. The red, and blue arrowed lines represent storm control 1, and 2, and are nor relevant for this thesis. Figure from Solbrekke and Sorteberg (2021).*

In figure 2.3 the power curve of three different wind turbines is shown. SWT is a wind turbine with a rated power of 6 MW, DTU is a 10 MW turbine, and IEA is a 15 MW turbine. These turbines will be presented in the next section. Notice how the line from the larger turbine starts to increase at earlier wind speeds than the smaller turbine. This is due to the larger turbines having lower a cut-in speed than the smaller turbines. This allows the larger wind turbines to utilize the wind at lower wind speeds, and therefore increase the total time during a year they can produce energy. This means the larger wind turbines generally have larger capacity factor than smaller turbines.

In this thesis I will investigate three different wind turbines in my analysis of the LCOE of the various wind farm locations. The turbines will have the rated power of 6, 10 and 15 MW. In the following part these three turbines will be described, followed by a description some of their specifications, such as rotor diameter, and rated wind speed.

SWT-6.0-154

The 6 MW turbine is called SWT-6.0-154 and is produced by Siemens Gamesa Renewable Energy, Simens Gamesa (2022b). It is a wind turbine produced specifically for offshore use. The nacelle is designed to withstand the harsh offshore conditions with the use of a direct drive gearbox that has fewer moving parts compared to a traditional gearbox and will not be worn down as easily in the offshore weather. The turbine has a rotor diameter of 154 meters, blade lenght of 75 m, Simens Gamesa (2022b). This thesis assumes a blade diameter of 0,5 m, and tower diameter of 6 m in calculations using these parameters. SWT-6.0-154 is shown in figure 2.4.

DTU-10.0-Reference

The 10 MW turbine that will be discussed in this thesis is called DTU-10.0-Reference. It is, as its name suggest, a reference turbine. Meaning it is designed for the purpose of "providing a publicly available representative design basis for next generation of new optimized rotors" as described by Bak et al. (2012). It is designed specifically for academic use, and not for industrial production. The turbine is designed at the Technical University of Denmark (DTU). It has a rated power of 10MW and a rotor diameter of 178,3 m, 86,3 m, Bak et al. (2012). This thesis assumes a blade diamter of 0,5 m, and a tower diameter of 6 m in calculations using these parameters.

Figure 2.4: *Five SWT-6.0-154 are used in Hywind Scotland, the first commercial floating wind farm ever to be built. Here represented by a SWT-6.0-154 from Hywind Scotland. Other turbines from the farm can be seen in the background. Picture from Wind Europe (2022)*

IEA-15-240-RWT

The last turbine that will be discussed in the this chapter is IEA-15-240-RWT. Like the DTU turbine, IEA-15-240-RWT is also a reference turbine with a publicly available design, made for academic purposes. It is designed as a collaboration between National Renewable Energy Laboratory (NREL), sponsored by the U.S. Department of Energy, and the Technical University of Denmark (DTU), sponsored by the European Union's H2020 Program, through the second work package of International Energy Agency (IEA) as described by Gaertner et al. (2020). It has a rated power of 15 MW, a rotor diameter of 240m, and a blade length of 117 m, Gaertner et al. (2020). This thesis assumes a blade diamter of 0,5 m, and a tower diameter of 6 m in calculations using these parameters.

2.4.3 Floating Pltatforms

Floating platforms for wind turbines are a relatively new concept, although the technology of floating platforms has been used in the offshore industry, especially the offshore oil and gas industry, for decades. The first ever prototype of a floating offshore wind turbine connected to the grid was a single

2,3 MW turbine located outside the island of Karmøy, Norway. It was built by Equinor and connected to the grid in 2009. The floating platform chosen for this concept was a spar buoy floating platform, which will be described in the next section. As described in the beginning of this chapter, as of May 2022 there exists three operational floating wind farms in the world. Hywind tampen will be located outside Scotland and is currently the largest floating wind farm under construction and will consist of 11 turbines, giving the farm a total capacity of 95 MW, Equinor (2022b).

The three types of floating platforms discussed in this thesis are Spar Buoy (SB), Semi-Submersible Platforms (SSP) and Tension Leg Platforms (TLP). These are the most discussed platforms in academic articles. The three floating wind farms mentioned in the beginning of the chapter use one of these three platform types. Kincardine, located outside Scotland and WindFloat Atlantic, located on the coast of Portugal uses SSP, EDP (2022), Cobra (2022). Hywind Scotland located outside Scotland uses SB, Equinor (2022a). The planned Hywind Tampen will use SB, Equinor (2022b). The platforms for Hywind Tampen was recently completed and ready for use as of May 2022.

Spar Buoy

A Spar Buoy floating platform for wind turbines is the simplest of the three platforms discussed in this thesis. It consists of a single cylinder where the turbine is mounted, as seen in figure 2.5. The top part of the cylinder is buoyant and is what causes the turbine and the platform to float. The lower part of the cylinder is made up of an extremely heavy ballast so that the center of gravity stays below the center of buoyancy. This part is made to keep the structure and the wind turbine in a stable upright position. The SB is anchored to the bottom with three mooring lines at an angel. In the method used for calculating LCOE in thesis the SB moorings are assumed to be made of a steel chains, Energy Facts (2022).

Tension Leg Platform

A Tension Leg Platform has a central column and arms that are connected to the seabed with moorings, seen in figure 2.6. The structure is highly buoyant and therefor gets its stability from the tension in the moorings that pulls the buoyant structure down. The moorings rise vertically from the seabed. In the method used for calculating LCOE in this thesis the TLP discussed will

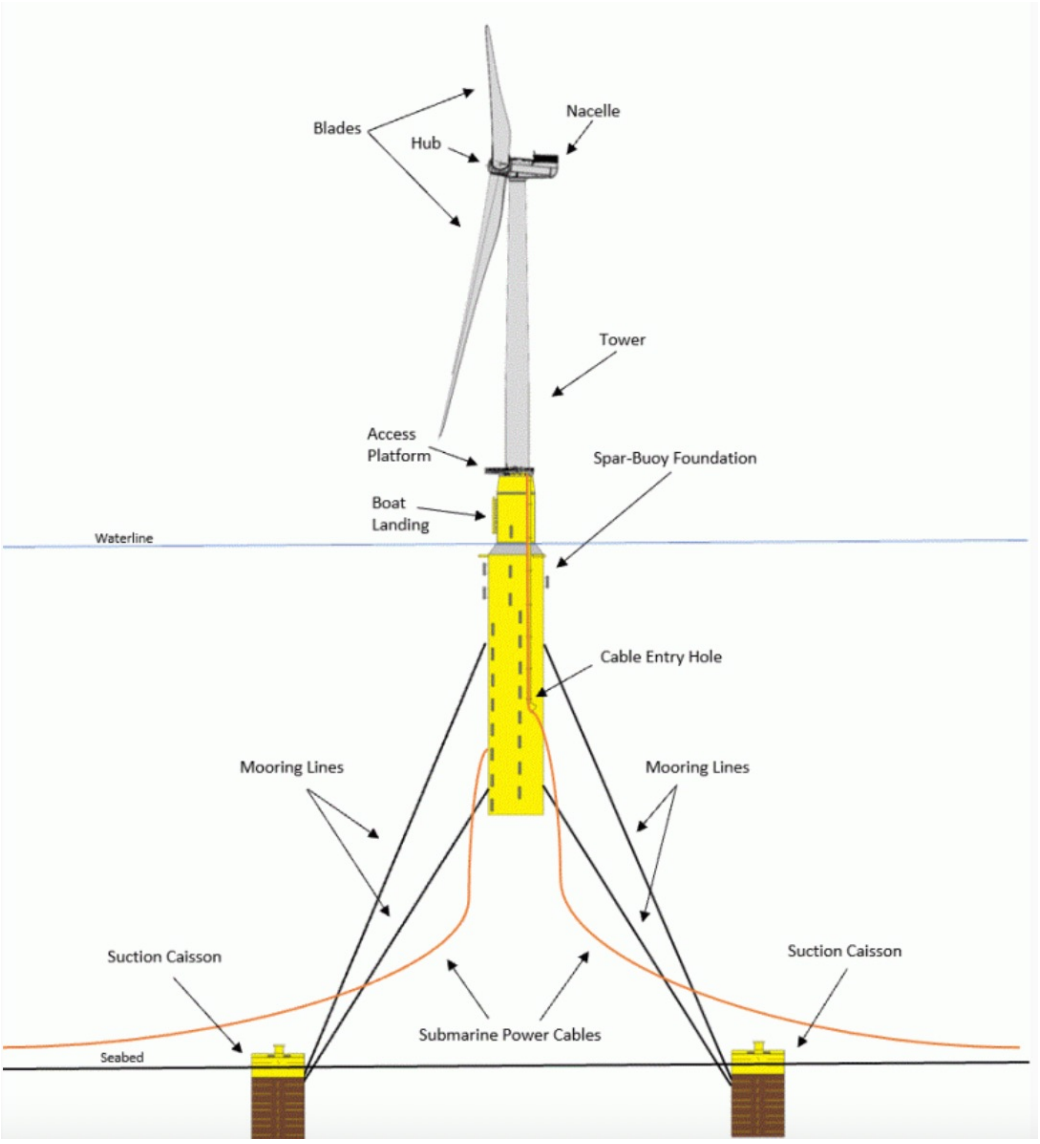

Figure 2.5: *The Figure shows a wind turbine installed on a Spar Buoy. Most of the SB stays under the water surface, using its weight to balance the wind turbine. The moorings can be seen as black angled lines. They connect the turbine to the anchors holding the turbine in place. The figure from Energy Facts (2022)*

be assumed to have eight moorings made from synthetic fiber ropes, Energy Facts (2022).

Semi- submersible platform

Semi-submersible platform is built by connecting columns together, usually three of them in a triangle formation that keeps the structure stable. This can be seen in Figure 2.7. The columns are connected by submerged pontoons that keep the structure floating. The turbine is placed on top of one of the columns. The platform is kept in place by anchors connected to the platform by moorings. The platform will usually be equipped with either six or three mooring lines, Energy Facts (2022). A detailed description of the platform can be seen in figure 2.8. the method used for calculating LCOE in this thesis I will assume the use of six mooring lines made with steel chains.

2.5 Aim of the thesis

The aim of this thesis is to do an LCOE-estimate for offshore wind energy on the Norwegian coast based on the data set NORA3-WP, to look at differences between some areas investigated in the NVE report from 2010, Espegren et al. (2010), to do a sensitivity analysis of what parameters cause these differences, as well as any differences in the production estimate from the NVE report from 2012, Sydness et al. (2012).

2.6 Previous work

Before I present the data that has been used during the work with this thesis in the next chapter, I want to present some research that has previously been done in the field of estimation of LCOE for floating wind farms. Some of the research presented in this section will be used to compare the results found in this thesis.

The foundation for this thesis is based on locations for potential offshore wind farms identified by NVE in their report by Espegren et al. (2010). In this report 15 potential locations for wind farms were identified. Four of those locations was suitable for floating wind farms. Further work by NVE resulted in a report, Sydness et al. (2012), where the economic potential of

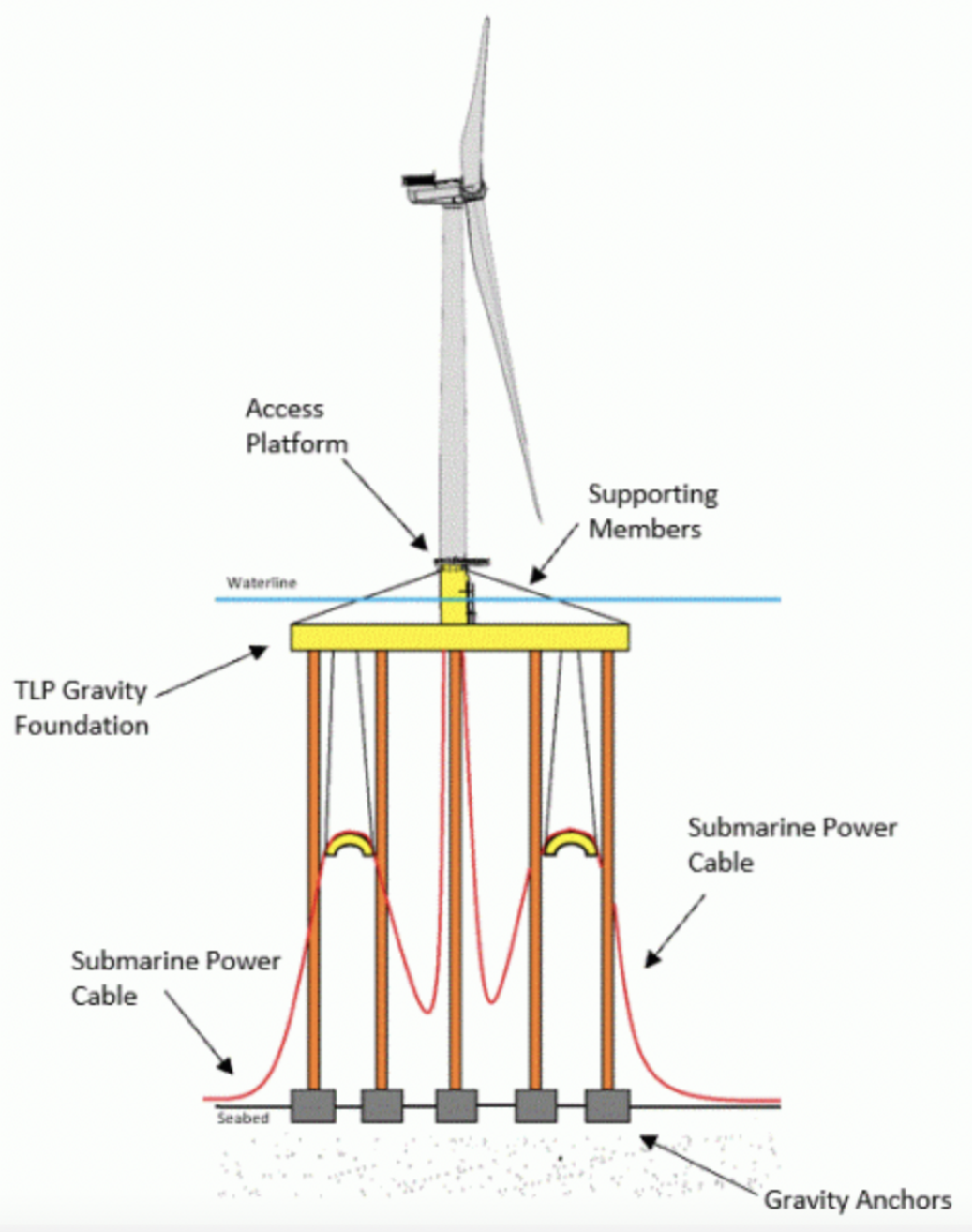

Figure 2.6: *The figure shows a wind turbine installed on a Tension Leg Platform. The platform, seen as a yellow structure on the figure, has high buoyancy keeping the structure afloat. The high buoyance creates tension on the moorings, which raises vertically from the seabed, keeping the floating platform connected to the anchors. Figure from Energy Facts (2022)*

Figure 2.7: *The picture shows three wind turbines in the WindFloat Atlantic wind farm outside Portugal. All three wind turbines are installed on Tension Leg Platforms. Picture from EDP (2022)*

these locations was analyzed. This report found an LCOE for each of the 15 areas that was investigated. The value in terms of €/MWh that was found is not presented in their report. However, a percentage change from the 15 locations' mean LCOE is presented for each location. This will be further explained in chapter 5. These results will be used when comparing the results found in this thesis.

Myhr et al. (2014) has looked at how variations in water depth, distance to harbor, number of wind turbines in a wind farm, lifetime of the wind farm, steel costs, load factor, and discount rate affected the LCOE of the wind farm. The article looks at the cost of energy trough a life cycle analysis, similar to that which will be carried out in this thesis. In the article LCOE is found to vary between 130 and over 200 €/MWh for the various wind farm designs that is investigated. LCOE is found to be highly sensitive to variations within all parameters mentioned, including water depth, distance to harbor, number of wind turbines in a wind farm, lifetime of the wind farm, steel costs, load factor, and discount rate.

Shafiee et al. (2016) has, like Myhr et al. (2014), investigated the effects of various wind farm parameters on LCOE. These parameters include capacity

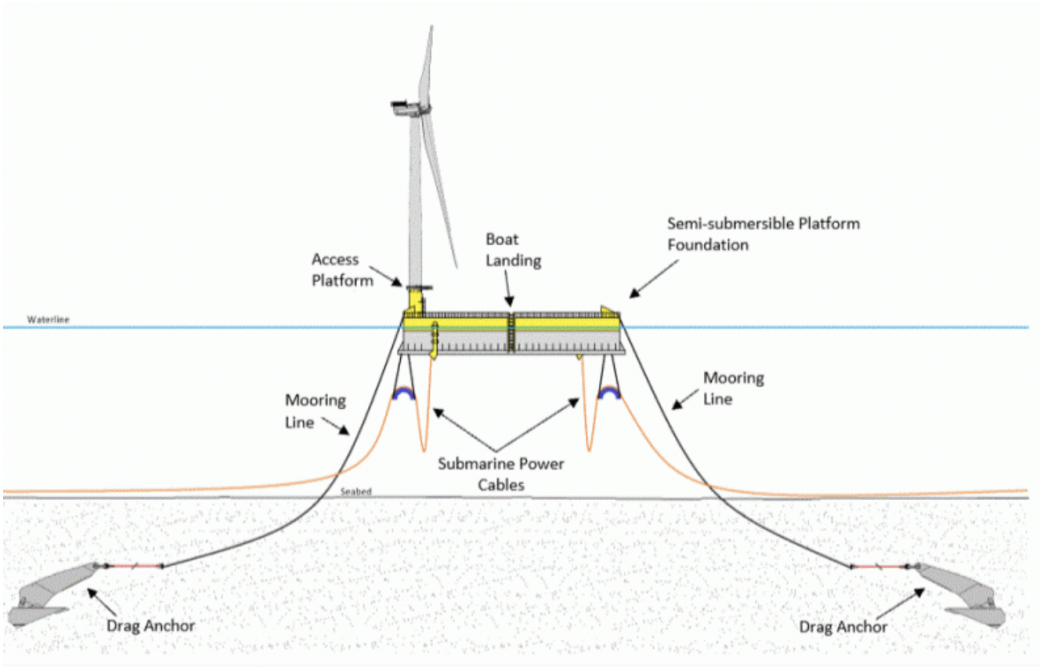

Figure 2.8: *The figure shows a wind turbine installed on a Semi-Submersible Platform. As seen, the platform is partly under, and partly over the water surface, hence the name "Semi-Submersible". The mooring lines can be seen stretching to the seabed with slack in the lines. Picture from Energy Facts (2022)*

of the offshore wind farm, site location, interest rate, and the quality of fault detection. The article points to the installed capacity of a wind farm, the distance from shore, and the fault detection capability of a condition monitoring system as parameters of the wind farm that influence the LCOE.

Maienza et al. (2020) has investigated how LCOE is affected by the same three different floating platform types that will be investigated in this thesis. The research paper has aimed to develop a cost model for offshore floating wind farms, using the most resent available datasets, and parametric equations from literature within the field of floating wind LCOE calculations. For the cases investigated in the article, an average LCOE of 97,4 €/MWh is found. It also concludes that the Semi-Submersible Platform is the most cost effective out of the three platforms that is investigated.

Chapter 3

Data

In this chapter I am going to discuss the data used to estimate LCOE in this thesis. This includes data about the physical world, such as distances from harbor, transformer, and shore for the locations that will be investigated for the potential of establishing floating wind farms. It also includes weather data used to calculate the potential for energy production.

3.1 Data used in power estimation

To calculate the LCOE in this thesis I need an estimate of the energy production that can be expected from each location that is being analyzed. The energy production for the locations has been estimated using a dataset called NORA3-WP, which is described in Solbrekke and Sorteberg (2021). This is a wind dataset with a resolution of 3 km^2. The dataset consists of data covering wind resources and wind power in the north sea, Baltic sea, and part of the Norwegian and Barents sea. The dataset stretches from 1996 until 2019 at the time of writing this thesis, but the period it covers will be extended in the future, Solbrekke and Sorteberg (2021). From the raw data in NORA3-WP a few datasets have been created regarding wind turbines. One dataset that has been created by Ida Marie Solbrekken during her work with her PhD is a dataset containing the calculated capacity factor for the three wind turbines SWT-6.0-154, DTU-10.0-Reference and IEA-15-240-RWT. This dataset is used in this thesis to estimate energy production. The dataset contains data about the capacity factor, as described in 2.3. The capacity factor used for calculations in this thesis is based on hourly wind speeds and is calculated as a monthly average for each month between January 1996 and December 2019. The data has the same horizontal resolution

as the original NORA3-WP dataset, meaning every 3 km^2 will have a corresponding value for the capacity factor. The capacity has been calculated for all three turbines mentioned above. It is therefore possible to do production estimates for all three turbines directly from the data. Figure 3.1 shows a map where the colored area displays the area that the dataset covers. The figure shows how the capacity factor varies. Between on- and offshore the difference is especially visible.

3.2 Location descriptions

The locations that will be discussed in this thesis are Utsira Nord, Stadthavet, Frøyabanken and Træna Vest. These locations are all colored pink in Figure 3.2. With deep waters, these four locations are all suitable for floating offshore wind farms.

In table 3.1 key data for all locations are presented. The data seen in the table have been derived from five datasets with data describing capacity factor, water depth, distance to harbor, distance to shore, and distance to a transformer. The datasets contain data about distance from any point to the closest harbor, closest transformer, and closest point on the shoreline. The data has been derived from the datasets NORA3-WP (capacity factor) Solbrekke and Sorteberg (2021), GEBCO Grid (water depth) GEBCO (2021), geonorge (NVE) (transfomrers) Geonorge (2022), geonorge (Kystverket) (Distance to shore) Kartverket (2022), and geonorge (NMA) (distance to harbor) Kystverket (2022). This data will be presented in more detail in the following sections, describing each location for itself. The harbors used in the dataset Kystverket (2022) consists of 32 main harbors, and is described by BarentsWatch (2012) as "Stamnettshavner" translated to "Main network ports".

The following sections will present key data from each of the four locations being investigated in this thesis, in order from south-most location, to the northern most location, as seen in Figure 3.2. For each location I will present a summary of what NVE has said about the locations in their report, Sydness et al. (2012). I will present a map of the location, and some figures showing depth, and distances to shore, transformer, and harbor regarding each location. The coordinates used to collect the data in this thesis are calculated from degrees, minutes, and seconds coordinates, to longitude and latitude using the coordinates found in the NVE reports, Espegren et al. (2010) and

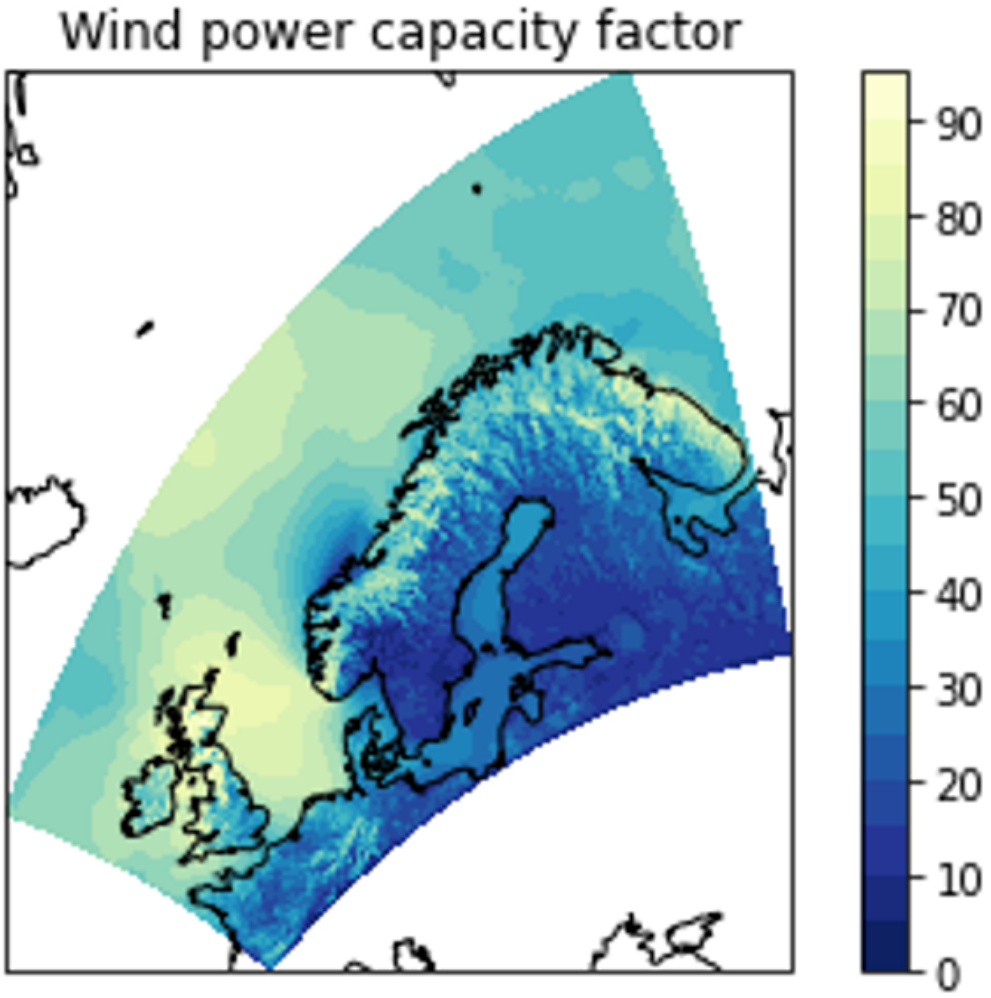

Figure 3.1: *The total area the NORA3-WP dataset covers is shown with color. The map shows capacity factor for a 6 MW turbine. The color representing the capacity factor can be seen in the legend, where the capacity factor is a percentage between 0 and 90 %. A low capacity factor is shown in dark blue, while the color gets lighter with higher capacity factor.*

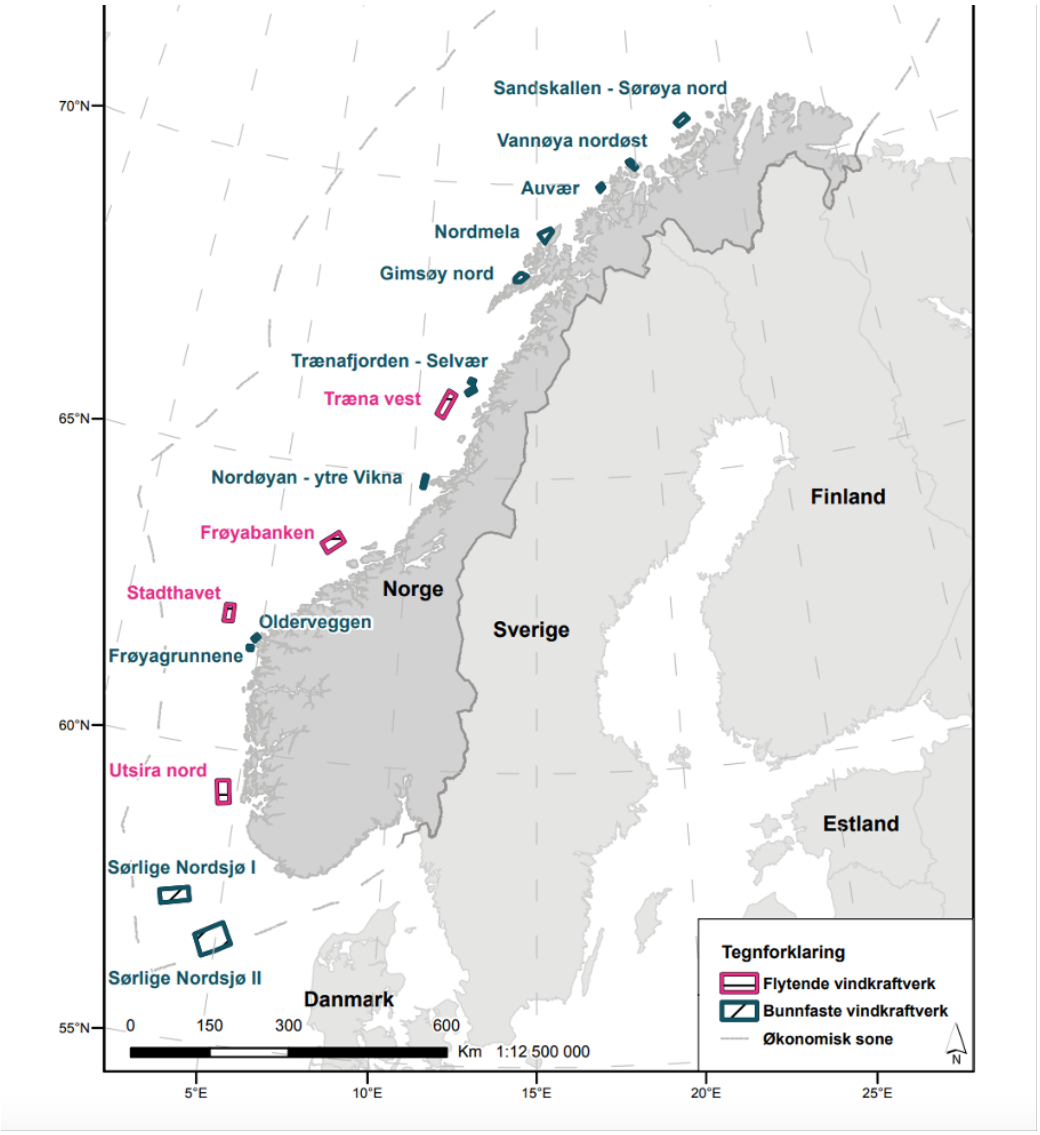

Figure 3.2: *All 15 locations analyzed by NVE. The locations with deep waters, suitable for floating wind are colored pink. Picture from NVE's 2010 report, Espegren et al. (2010).*

Områdedata

	Utsira Nord	Stadthavet	Frøyabanken	Træna Vest
Turbine capacity factor (%)				
6 MW	46,4	48,7	40,8	42,6
10 MW	54,4	56,3	48,3	50,8
15 MW	59,5	61,2	53,3	56,2
Distance to harbor (km)				
Average	45,4	81,9	72,7	131,8
Closest	33	69,5	59,5	114,3
Furthest	57,6	93,3	86,1	149,5
Depth (m)				
Average	265	207	207	269
Shallowest	229	174	165	195
Deepest	283	251	311	331
Distance to transformer (km)				
Average	39,2	84	51,6	57,7
Closest	24,7	71,7	40,9	36,4
Furthest	54,5	95,4	64,4	73,9
Distance to shore (km)				
Average	21,8	71,3	46,3	42,4
Closest	7,6	60,4	35,8	22
Furthest	34,6	81,2	58,7	57,3

Table 3.1: *Key data for the locations Utsira Nord, Stadthavet, Frøyabanken and Træna Vest. Turbine capacity factor is a measure of the average capacity factor each location, using 6 MW turbines, 10 MW turbines, and 15 MW turbines. Distances is shown for the average, closest and furthest distance to the closest harbor, transformer, and shoreline. The capacity factor data is gathered from the dataset NORA3-WP, Solbrekke and Sorteberg (2021). The distance to harbor data is gathered from the geonorge (NMA) dataset, Kystverket (2022). The water depth data is gathered from the GEBCO Grid, GEBCO (2021). The distance to transformer data is gathered from geonorge (NVE) dataset, Geonorge (2022). The distance to shore data is gathered from the geonorge (POD - Norge 1:50000 (land)) dataset, Kartverket (2022)*

Sydness et al. (2012).

3.2.1 Utsira Nord

NVE has concluded that for a 1500 MW farm at Utsira Nord, a production of 6210 GWh can be expected using a capacity factor of 47 %, Sydness et al. (2012). They have concluded that the building of a wind farm in the area could have significant negative effects for shipping, as well as Norwegian defense interests. The north-western part of the location is currently being used as a military firing range. The eastern-most part of the location is also heavily trafficked with vessels traveling along the Norwegian coast. These are the most significant negative consequences of establishing a wind farm at the Utsira Nord location, Sydness et al. (2012).

Utsira Nord is the southern-most location of the four chosen locations, located on the west coast, outside of the city of Haugesund. The location and the coordinates can be seen on the map in Figure 3.3.

Some key data for Utsira Nord can be found in Table 3.1. As a reminder, the investigated dataset includes capacity factors for one wind turbine of 6, 10 and 15 MW rated power, hence we can note that the capacity factor for the 6 MW turbine is about the same as the one used by NVE in their report, Sydness et al. (2012). For the larger turbines the capacity factor increases significantly. Two other metrics that will be important in this thesis is the distance to harbor and water depth. Distance to shore, and transformer is of less significance in the equations for calculating LCOE, presented chapter 4. These two distances is therefore not described as detailed as the water depth and distance to harbor in the following sections. The average distance to a harbor at Utsira Nord is 45,4 km. The average depth is 264,7 m. In figure 3.4 one can get an overview of how the depth, and distances to shore, harbor, and transformer is distributed within the Utsira Nord location.

3.2.2 Stadthavet

NVE has concluded that a 1500 MW wind farm at Stadthavet would be able to produce 6348 MWh each year. They have assumed a capacity factor of 48 %, Sydness et al. (2012). They have concluded that the establishment of a wind farm in the area would have significant negative effects for fishing industry in the area, as well as one species of fish, the Blue Ling species. The Norwegian directorate of fisheries has recommended not to build in the

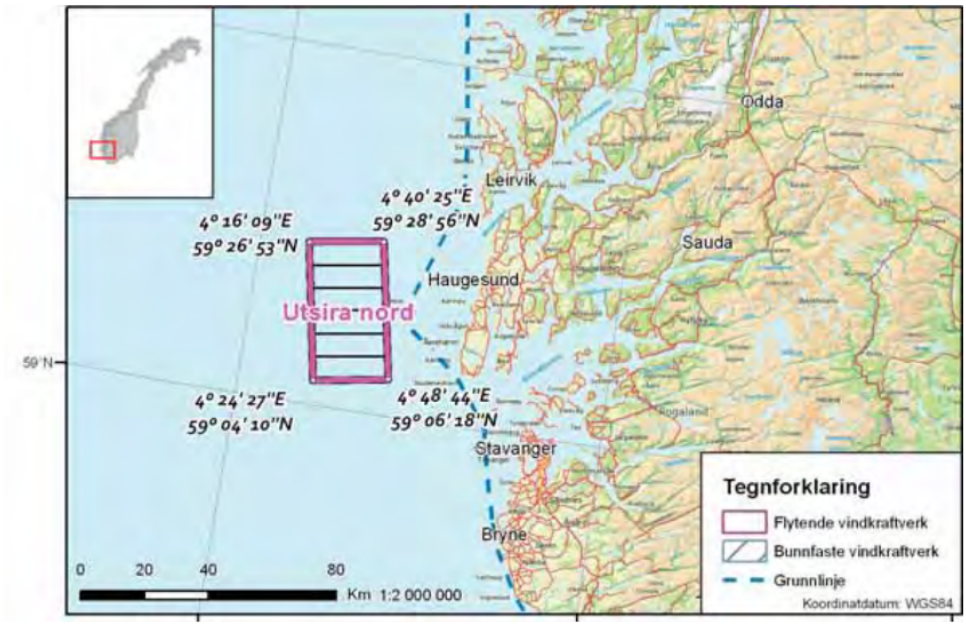

FIGUR 40-1:
Geografisk lokalisering av Utsira nord.

Figure 3.3: *The location of Utsira Nord with location coordinates. Picture from NVE's 2012 report, Sydness et al. (2012).*

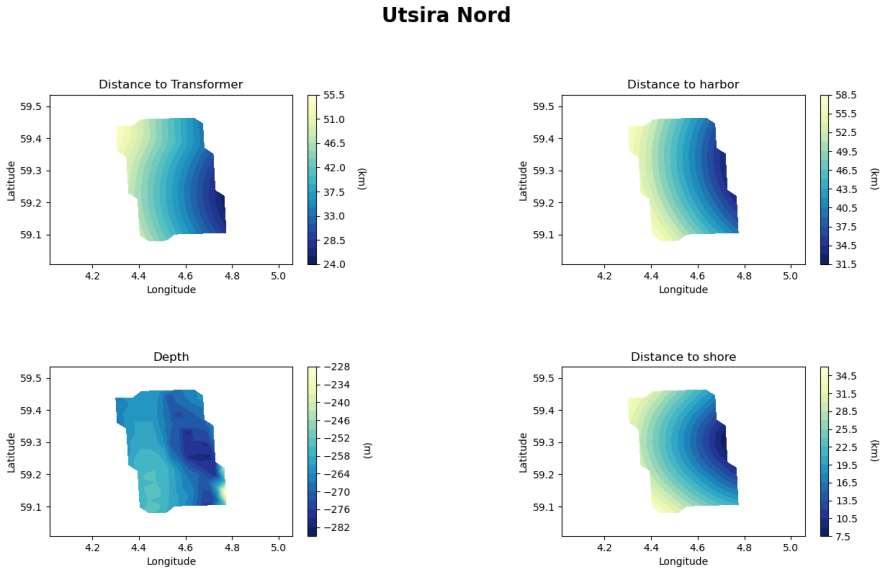

Figure 3.4: *Key data for Utsira Nord. The table show the closest distance to transformer, harbor, shore, and the water depth. Longitude and latitude for the mapped area are displayed on the x- and y-axis respectively. The legends display distance as lighter color the larger the distance is. Distance is displayed in km. Water depth is displayed as lighter colors the shallower it gets. Water depth is displayed as meters below sea level.*

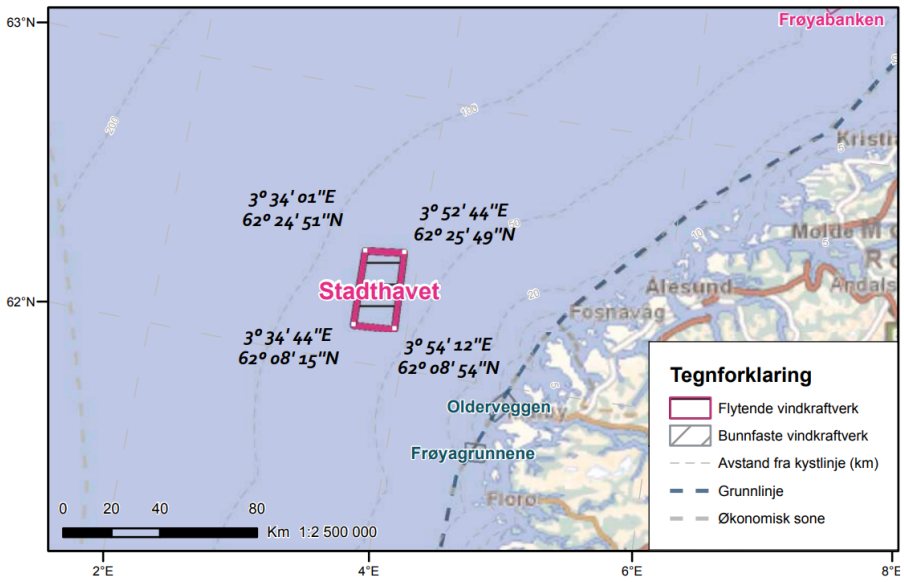

Figure 3.5: *The location of Stadthavet with location coordinates. Picture from NVE's 2010 report, Espegren et al. (2010).*

northern-most part of the location, to avoid conflicts with the fishing industry. The location is also problematic for the fish species Blue Ling, who has a significant amount of its only known spawning grounds for this species in Norway within the location, Sydness et al. (2012).

Stadhavet is located in the northern part of western Norway, just west of Ålesund. A map of the location can be seen on figure 3.5, together with the location's coordinates.

Some key data for the Stadthavet can be found in table 3.1. We can note that the capacity factor found using NORA3-WP is 48,7 % when using a 6 MW turbine, about the same as the capacity factor used by NVE. The average distance to harbor is 81,9 km, almost double that of Utsira Nord. The average depth is 206,5 km. In figure 3.6 one can get an overview of how the depth, and distances to shore, harbor, and transformer is distributed within the location.

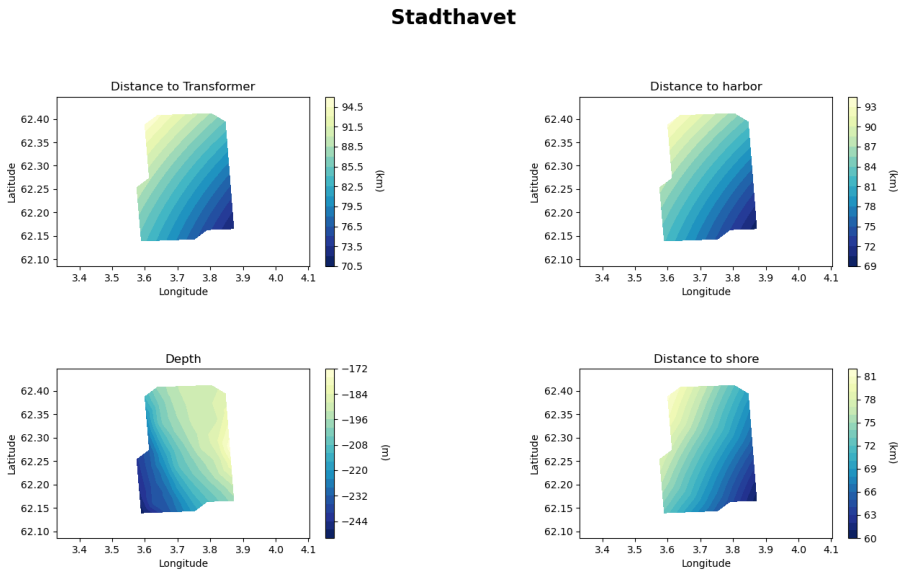

Figure 3.6: *Key data for Stadthavet. The table show the closest distance to transformer, harbor, shore, and the water depth. Longitude and latitude for the mapped area are displayed on the x- and y-axis respectively. The legends display distance as lighter color the larger the distance is. Distance is displayed in km. Water depth is displayed as lighter colors the shallower it gets. Water depth is displayed as meters below sea level.*

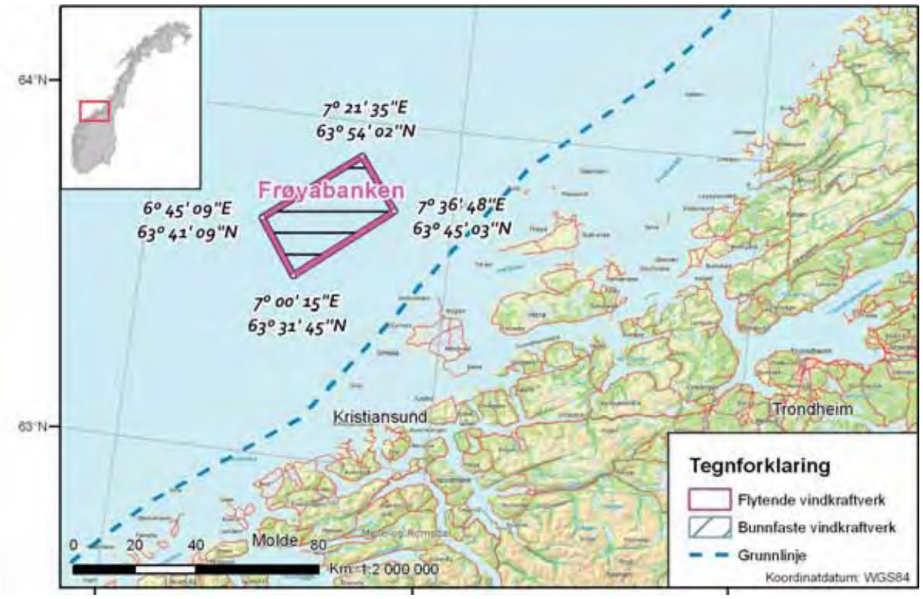

FIGUR 37-1:
Geografisk lokalisering av Stadthavet.

Figure 3.7: *The location of Frøyabanken with location coordinates. Picture from NVE's 2012 report, Sydness et al. (2012).*

3.2.3 Frøyabanken

The capacity factor found in NVE's report is 42 % for a 1500 MW wind farm. The annual energy production for a farm of this size is calculated to be 5508 GWh, Sydness et al. (2012). The only significant negative impact from establishing a wind farm in this area is on the shipping industy. There is a lot of activity from shipping to the various oil rigs located in the area. Also, an extra reported possible effect of the establishment of a wind farm in this location could complicate the process of sailing into the harbor of Kristiansund for large vessels, Sydness et al. (2012).

Frøyabanken is located off the coast of the middle of Norway, north of the city of Kristiansund. The location, together with coordinates for the location can be seen in the map in figure 3.7.

Key data for the location can be found in table 3.1. The capacity factor

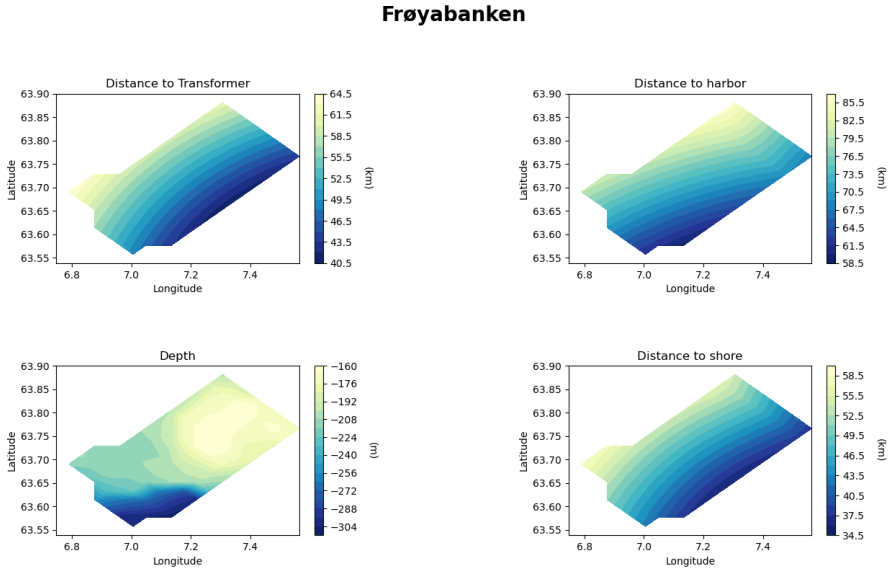

Figure 3.8: *Key data for Frøyabanken. The table show the closest distance to transformer, harbor, shore, and the water depth. Longitude and latitude for the mapped area are displayed on the x- and y-axis respectively. The legends display distance as lighter color the larger the distance is. Distance is displayed in km. Water depth is displayed as lighter colors the shallower it gets. Water depth is displayed as meters below sea level.*

used for Frøyabanken for 6 MW turbines in this thesis is 40,8 %. This is just below the capacity factor used by NVE. The average distance to a harbor for Frøyabanken is 72,7 km. The average depth at the location is 207,4 m. In figure 3.8 one can get an overview of how the depth, and distances to the closest shoreline, harbor, and transformer is distributed within the location.

3.2.4 Træna Vest

Træna Vest is the last location that will be investigated in this thesis. NVE has reported a capacity factor of 44 % and an annual energy production of 5615 GWh for a 1500 MW wind farm for this location, Sydness et al. (2012). The location has significant negative impacts reported on shipping and fishing industry in the area. There are significant amounts of heavy ship traffic within the location. The Norwegian Coastal Administration has recommended that no wind farms should be built within the location. Building of a wind farm within this location would lead to traffic having to avoid the

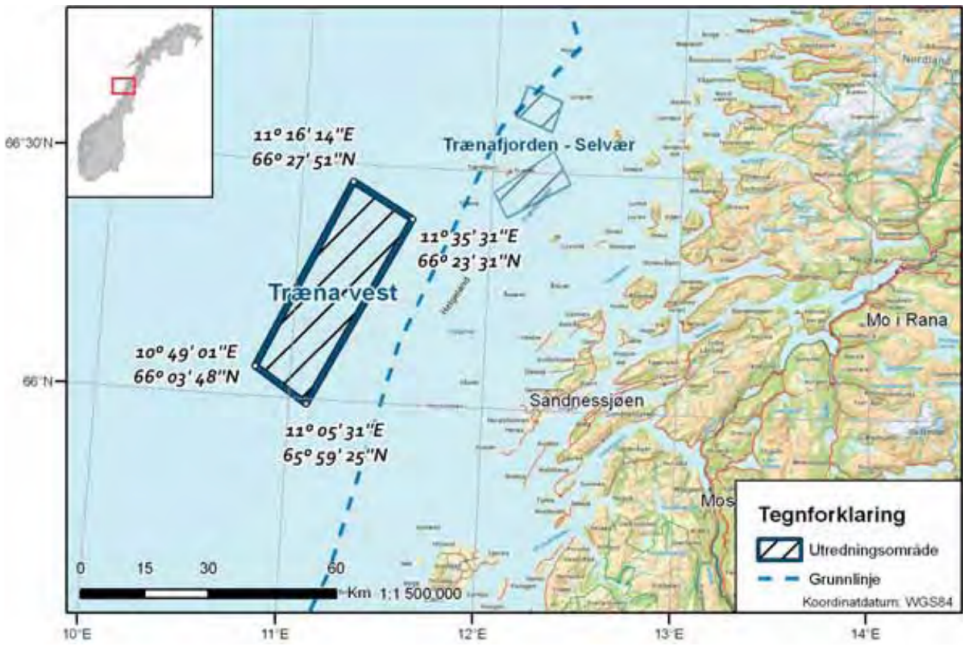

FIGUR 34-1:
Geografisk lokalisering av Træna vest.

Figure 3.9: *The location of Træna Vest with location coordinates. Picture from NVE's 2012 report, Sydness et al. (2012)*

area getting increased expenditures going towards fuel. The location has also got a lot of traffic from fishing boats, many of which are under 11 meters and are therefore not tracked, Sydness et al. (2012).

Træna Vest is the northern-most of the four locations. The location lays off the coast of Nordland county, in the southern-most part of northern Norway.

Key data for Træna Vest can be found in table 3.1. From the table we can find that the average capacity factor within the location is 42,6 % for a 6 MW turbine. The average distance to a harbor is 131,8 km. This is the furthest from a harbor for any of the four locations being investigated in this thesis. The average depth is 269,4 m. This is also the deepest average depth of any of the four locations, though just 4 meters deeper than Utsira Nord. In figure 3.10 one can get an overview of how the depth, and distances to shore, harbor, and transformer is distributed within the location. In the following section there will be an overview of the data, from the four locations, compared with

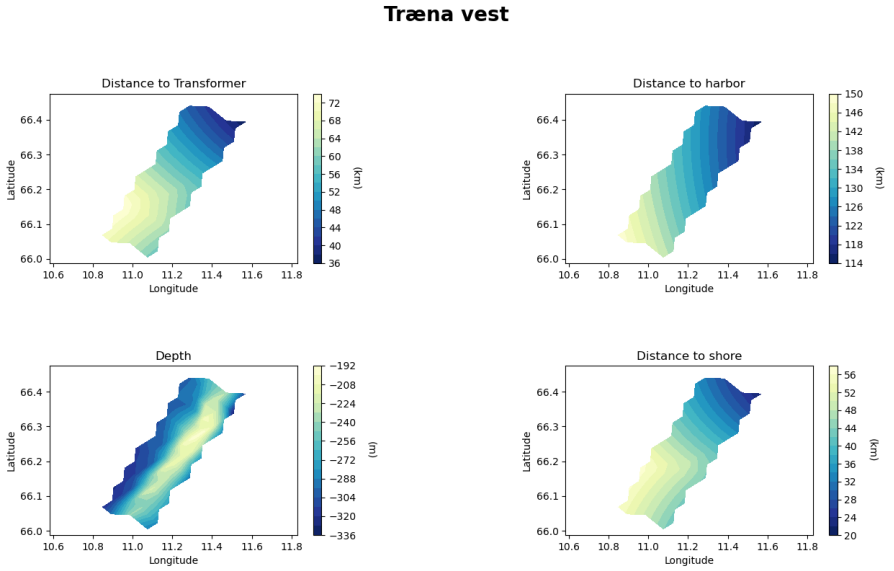

Figure 3.10: *Key data for Træna Vest. The table show the closest distance to transformer, harbor, shore, and the water depth. Longitude and latitude for the mapped area are displayed on the x- and y-axis respectively. The legends display distance as lighter color the larger the distance is. Distance is displayed in km. Water depth is displayed as lighter colors the shallower it gets. Water depth is displayed as meters below sea level.*

each other.

3.2.5 Comparison between locations

To get a clearer picture of the data presented in the previous section, this section will look at how the data from the four locations compare with each other. The three data categories that have the biggest impact on the cost model for LCOE, water depth, capacity factor and distance to harbor will be shown in this section.

In Figure 3.11 one can see how the variability in depth differs between the four locations. Utsira Nord clearly has the least variability in depth with only 54 m between the shallowest and deepest point. Frøyabanken on the other hand has the most variability in depth with a difference of 146 m. In this thesis variability in depth does not influence the results of the LCOE, but the variability could be interesting to take note of for stakeholders looking

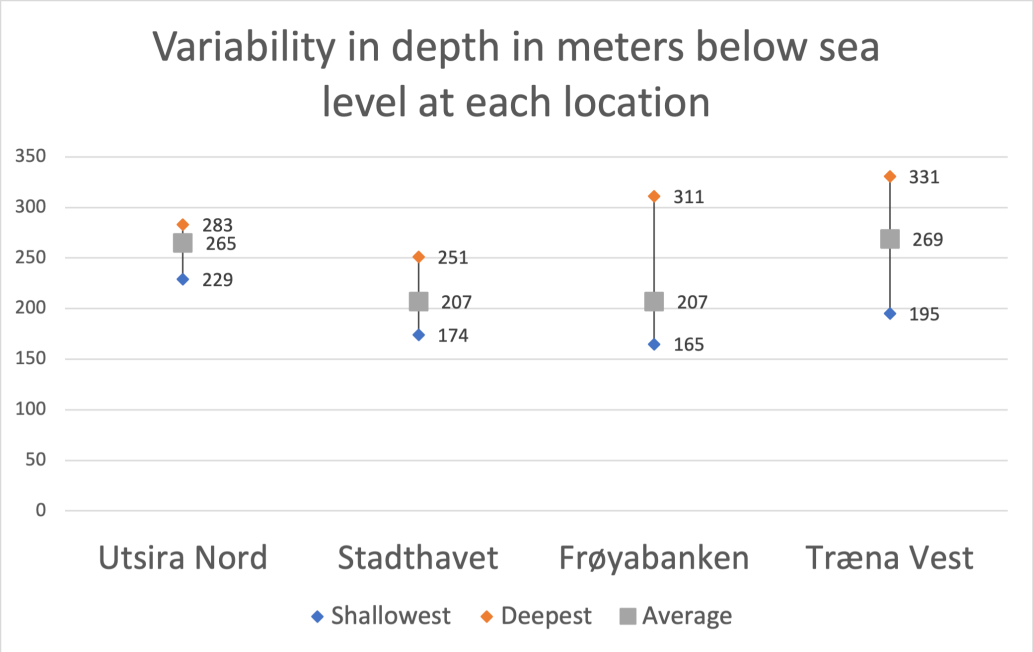

Figure 3.11: *The figure show water depth at Utsira Nord, Stadthavet, Frøyabanken, and Træna Vest. The y-axis display water depth as meters below sea level (MBSL). For each location the water depth at the shallowest point is marked with a blue square, the average water depth is marked with a gray square, and the deepest water depth is marked with an orange square.*

into developing any of these locations.

For the capacity factor, as seen in Figure 3.12, the change from one turbine to another is about the same for each location. One can also note that there seems to be two locations with relatively higher capacity factors, Utsira Nord and Stadthavet, while Frøyabanken and Træna Vest has a comparatively lower capacity factor for all three turbine types. The difference in capacity factor between the three turbines come from the lower cut-in wind speed for the larger turbines, as can be seen in the power curves for the three turbines in Figure 2.3.

Figure 3.13 shows the difference in distance to the closest harbor between the four locations. From this table the difference when it comes to distance to harbor between the locations is clearly large. We can also note that Træna Vest is a clear outlier with an average distance almost double that of Frøyabanken and Stadthavet, and almost three times as far from a harbor as

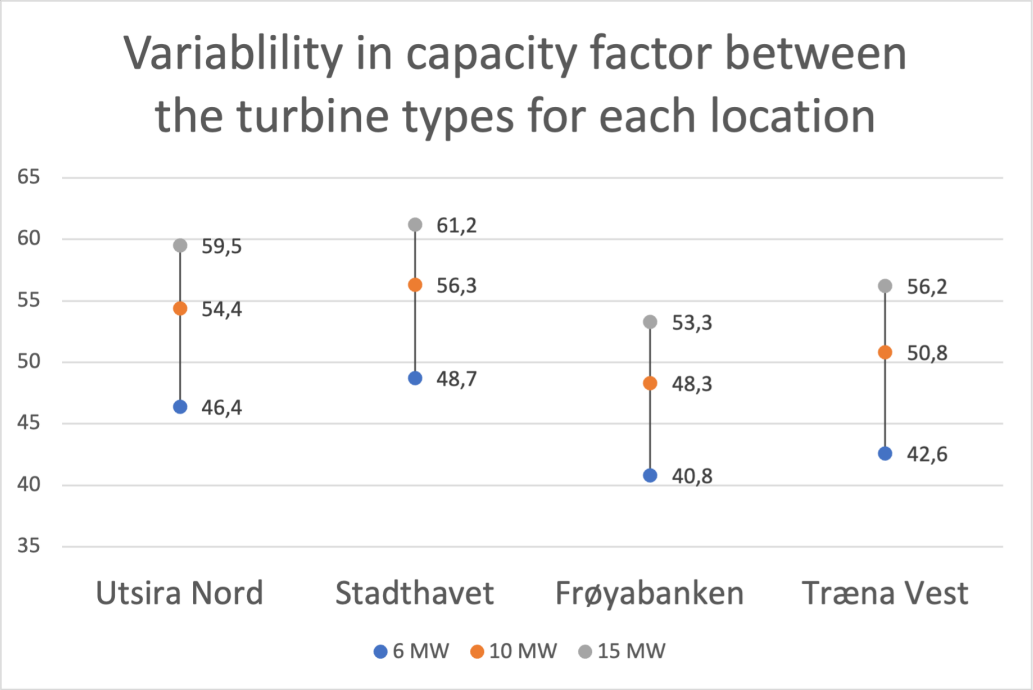

Figure 3.12: *The figure show capacity factor at Utsira Nord, Stadthavet, Frøyabanken, and Træna Vest. The y-axis display capacity factor as a percentage (%). The capacity factor is shown for three wind turbines. For each location the capacity factor for the 6 MW turbine is marked with a blue square, the capacity factor for the 10 MW turbine is marked with a gray square, and the capacity factor for the 15 MW turbine is marked with an orange square.*

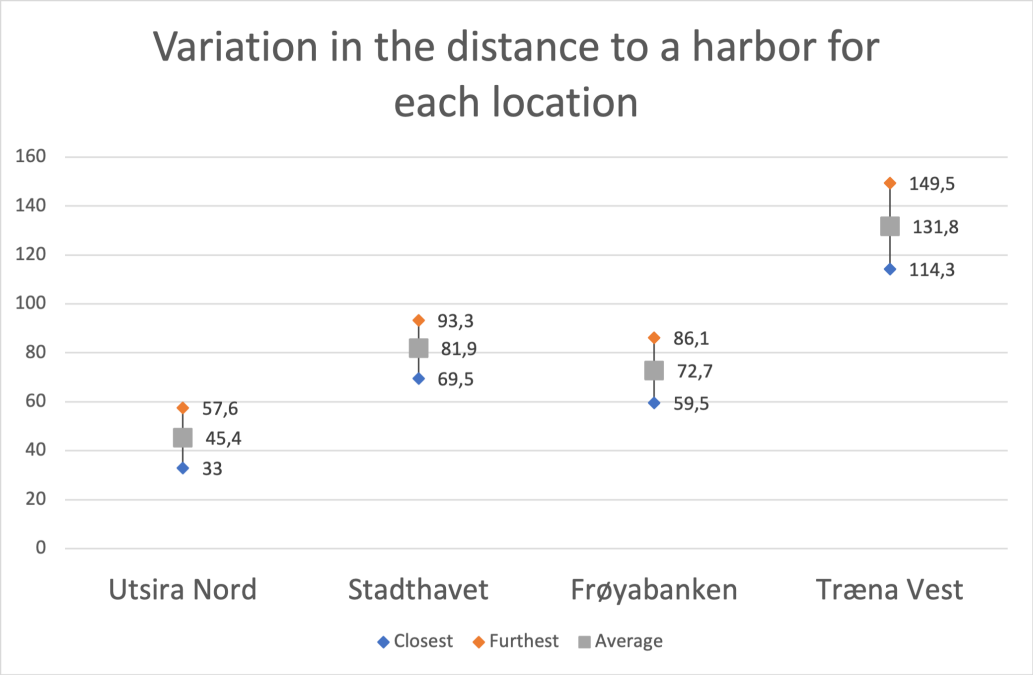

Figure 3.13: *The figure show distance to the closest harbor at Utsira Nord, Stadthavet, Frøyabanken, and Træna Vest. The y-axis display distance in kilometers (km). For each location the closest distance to harbor within the location is marked with a blue square, the average distance to harbor within the location is marked with a gray square, and the furthest distance to harbor within the location is marked with an orange square.*

Utsira Nord on average. When comparing the distance to shore for all locations in Table 3.1 it is not clear that Træna Vest should be an outlier in the distance to harbor since the distance to shore is shorter than for two of the other locations. The reason for this is that Træna Vest is located on a streach of the coastline that is far from any of the harbors in the main network ports.

Chapter 4

Method

I will in this chapter go over the method used to calculate LCOE in this thesis. This includes the method of calculating the estimated energy production for a potential wind farm location, and the calculation of the LCC for a wind farm. I will start the chapter with going over some assumptions that has been made in order to do these calculations.

4.1 Assumptions

I will in this section list all assumptions that has been made to be able to follow the calculations in the next sections. All assumptions will be discussed in chapter 6.

1. There has been assumed no loss of power in any of the cables in the wind farm. That includes array cables, export cables, and onshore cables. Myhr et al. (2014) describes a power loss of 1,8 % from electrical arrays. This loss is assumed to be neglectable.

2. The angel between the water surface and the mooring lines has been assumed to be a fixed angel, of approximately 73 degrees for the SSP, and approximately 70 degrees for the SB. These numbers come from dividing the water depth by the mooring length found in Maienza et al. (2020). This division results in the cosines of the angel between the water surface and the mooring lines. In reality, the mooring lines are not straight lines between the floating platform and the seabed, but rather curves with varying radius, and the calculations of mooring line lengths are complex calculations, therefore this simplification has been

used in this thesis. For the TLP the angel between the water surface and the mooring lines is 90 degrees. The mooring lines are assumed to be connected to the TLP at 50 meters below the water surface. This number comes from subtracting the water depth from the mooring line length of the TLP used by Maienza et al. (2020).

3. A loss of power of 10 % due to wake loss has been assumed for the wind farms investigated in this thesis.

4. For the operation and maintenance phase of the cost calculation, there has been assumed that maintenance is carried out throughout the whole year, and not mainly in the summer months, which would have been a more realistic scenario.

5. I want to be able to see the effects of increasing water depth on mooring costs. There has therefor been assumed that mooring costs make up the same amount of the total manufacturing cost as in Maienza et al. (2020). In Maienza et al. (2020) mooring costs make up 3 % of the manufacturing cost. Therefore, In this thesis 3 % of the manufacturing cost has been removed and replaced with a calculated cost of manufacturing moorings, which varies with water depth.

6. In terms of maintenance, on all cables in the wind farm there has been assumed a maintenance time of 24 hours to repair any failures.

4.2 Calculation of Energy Production

In this section I will show the method used in this thesis to calculate energy production for a wind farm.

One of the main calculations in this thesis is the calculation of the potential energy production for each location being investigated. As stated in equation2.1, the Levelized cost of energy (LCOE) is composed of two elements: total energy production over the wind farms lifetime (E_{el}), and Life cycle cost (LCC). LCOE is what this thesis wants to investigate, naturally energy estimation is an important part of that investigation, as it is defined as the denominator in the fraction in the equation describing the calculation of LCOE, equation 2.2.

Energy production in this thesis is understood as the generation of electricity from wind turbines. It is important to keep in mind that all locations for

wind farms being investigated in this thesis are potential. Meaning none of the locations are being used for energy production as of May 2022.

The estimation of energy production is done using the dataset for capacity factor based on NORA3-WP, as described in Solbrekke and Sorteberg (2021). The dataset includes calculated capacity factors for one wind turbine of 6, 10 and 15 MW rated power. The average capacity for each month from January 1996 until December 2019 is calculated for the specific location that we want to estimate energy production of. The monthly energy production is found in equation 4.1, and can be calculated as follows:

$$E_{\text{month}} = \frac{Cf \cdot Pr \cdot N_T \cdot t \cdot (1 - WL)}{1000 \frac{MWh}{GWh}} \tag{4.1}$$

Where Cf is the Capacity factor given as a value between 0 and 1, Pr is the rated power given in MW, N_T is the number of wind turbines in the wind farm, t is the number of hours in the month corresponding to the same month as the Cf and WL is the assumed wake loss for the wind farm given as a number between 0 and 1.

Using by the corresponding capacity factor for every month from 1996 until 2020 from NORA3-WP, together with the above equation, a graph displaying the potential energy production of a location in the same time period can be produced, as seen in figure 4.1.

For the energy production used when calculating LCOE, an average energy production of all months in the available period of the dataset has been used and then multiplied with the assumed lifetime of the wind farm to get the total energy production over the wind farm's lifetime. This calculation is described in equation 4.60, which describes the method for calculating LCOE used in this thesis.

For the four locations being investigated in this theis, Utsira Nord, Frøyabanken, Træna Vest, and Stadthavet, a dataset containing potential monthly energy production as shown in Figure 4.1 above has been created. An average of the potential energy production from each location has been used and then multiplied with the assumed lifetime of the wind farm to get the total energy production over the wind farm's lifetime. As mentioned, this is shown in equation 4.60, in the end of this chapter.

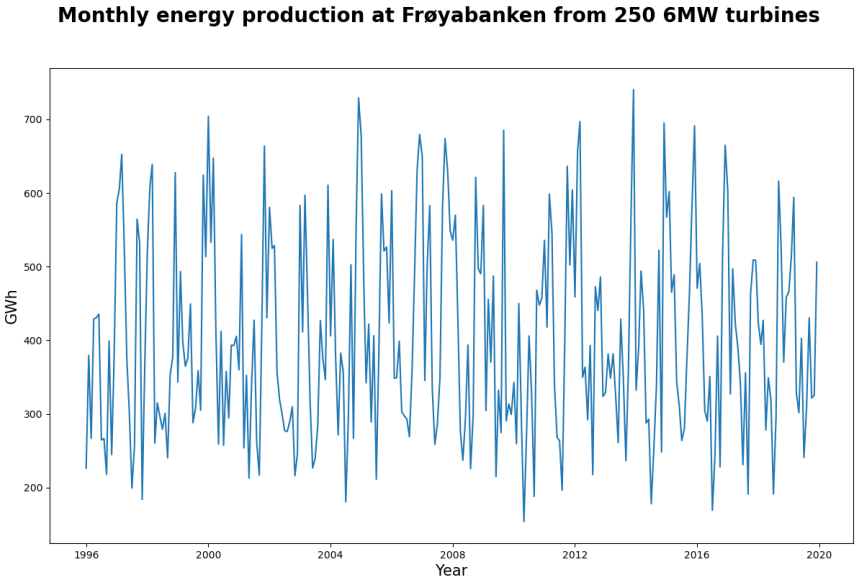

Figure 4.1: *The graph shows potential monthly energy production for a 1,5 GW capacity wind farm with 250 6 MW turbines, located at Frøybanken. The y-axis shows the monthly energy production in GWh. The time is shown in years on the x-axis, but keep in mind that the energy production is monthly values. Energy production can be seen to spike and crash every year. This is due to the winter months being naturally windier than the summer months, and thereby the production being significantly higher during the winter, than the summer.*

4.3 Cost models

In the following section I will describe the life cycle cost model that has been created. In addition to describing the cost model, I will also present the method for calculating the LCC.

In the previous section, the first half of the equation for LCOE, energy production, was discussed. The second half of the equation for LCOE consist of LCC. Calculating LCC for an infrastructure project of the size of a floating wind farm is a complex task. Based on this I have decided to make some simplifications when calculating LCC for a wind farm in.

These simplifications is made regarding the following: LCC is divided in five cost categories in this thesis, as shown in equation 2.1. These five cost categories are the cost of development (C_{Dev}), the cost of transportation and installation ($C_{I\&T}$), the cost of manufacturing (C_{Manuf}), the cost of operation and maintenance ($C_{O\&M}$), and the cost of decommissioning (C_{Decom}). The calculations regarding C_{Dev}, C_{Manuf}, and C_{Decom} have been simplified in this thesis, and these simplifications will be specified in the following paragraphs.

In this section I will describe how LCC has been calculated in this thesis, and the simplifications that has been made. In chapter 6 I will desicuss why I believe these simplifications could be done without sacrificing the accuracy of the results that is needed to achieve the goals of this thesis. I will also describe how $C_{I\&T}$ and $C_{O\&M}$ have been calculated. In chapter 6 I will discuss why these costs have been calculated more thoroughly.

The calculation of LCC has been done by developing a cost model for floating wind. As an overview, the cost model has been developed so that three of the costs associated with LCC will be fixed costs. These are C_{Dev}, C_{Manuf}, and C_{Decom}. A slight expetion is made to C_{Manuf}, which 3 % of the cost will vary with water depth. This expetion will be described in the following sections. The two remaining costs $C_{I\&T}$, and $C_{O\&M}$ will vary with parameters that can be changed to the specific wind farm being investigated.

When developing the cost model, it is important to keep in mind the objectives of the thesis: to look at how certain wind farm parameters influence the LCOE of floating wind farms. These parameters are water depth, distance

to harbor, number of turbines, wake loss, capacity factor, and wind farm lifetime. With this in mind, I have made the simplifications of setting C_{Dev}, C_{Manuf}, and C_{Decom} to fixed values that only change if the power capacity of the wind farm being investigated is changed. This is due to these three cost categories being less sensitive to changes in the wind farm parameters being investigated, then $C_{I\&T}$ and $C_{O\&M}$. A discussion of the decision to make this simplification is provided in 6.

As mentioned above, the three costs categories development and project management, manufacturing, and decommissioning have been simplified to fixed values only influenced by the size of the wind farm. The simplification will mean that these costs will not be calculated regarding the parameters specific for each of the potential wind farms investigated. Instead, I have looked at the three cost categories mentioned and seen how the costs have been distributed for wind farms investigated in previous literature. Specifically the articles: Maienza et al. (2020), Ioannou et al. (2018), Rinaldi et al. (2021), Bjerkseter and Ågotnes (2013), and Castro-Santos and Diaz-Casas (2015) and one other master's thesis: Hvidevold and Karlsen (2020). To do this, I have looked at the projected costs of development and project management, manufacturing, and decommissioning made in this literature. I have then extrapolated the power capacity of the wind farms used in the literature, to a 1500 MW wind farm. The costs found for each of the three cost categories (C_{Dev}, C_{Manuf}, and C_{Decom}) have been scaled according to the extrapolation done for the power capacity for each article. Then, an average of the extrapolated costs within each cost category has been used. The costs found in the literature as well as the average costs that has been calculated can be found in Table 4.1.

In this thesis I will mostly discuss wind farms of the size 1500 MW power capacity. If a wind farm of a different power capacity is being discussed, C_{Dev}, C_{Manuf}, and C_{Decom} will be scaled according to the size of the wind farm by dividing by 1500 MW, and multiplying by the relevant power capacity. This will be shown in equation 4.2.

It should be noted that there is one slight exception to the simplification in the case of the manufacturing cost. This is to be able to account for the change in LCOE with variations in depth. To do this I have decided to make the manufacturing of moorings into a varying cost, included in C_{Manuf}. In Maienza et al. (2020), mooring costs make up 3 % of the total manufacturing cost. In this thesis I have removed 3 % of the total average manufacturing cost.

The average cost for all five categories can be seen in Table 4.1, together with the extrapolated costs found in four different articles and two master theses. $C_{I\&T}$, and $C_{O\&M}$ can be found in the table, even though these average costs are not used to calculate LCC in this thesis. They are there as a reference to compare the costs of these two categories that will be calculated later in the thesis.

The values seen in table 4.1 have all been adjusted for inflation. Though this adjustment increases the values some, it is reasonable to think that some of these costs has been lowered due to advancement in technology and manufacturing methods since the writing of many of the articles. These lower costs are hard to quantify and will not be taken into consideration. It is also worth noting the large variations between the articles listed in table 4.1, within each cost category. These variations could come from the poor data basis that exists for offshore wind energy, as such source of power is still in its early years of development, as well as different methods for calculating the costs of offshore wind energy.

4.3.1 Choise of supporting articles for the cost model

I will in this section describe the choice of supporting articles that has been used when creating the cost model for the method of calculating LCOE.

I want to investigate the effects of water depth, distance to harbor, number of turbines, type of turbine, wake loss, and wind farm lifetime on the wind farm's LCOE. To do this, I first had to determine which of the five cost categories that make up LCC are the most affected by these parameters. To a certain degree they are all affected, but I decided that that $C_{I\&T}$, and $C_{O\&M}$ would be the most appropriate costs to see the variations in LCOE that the parameters would cause. The reason for this decision will be discussed more thoroughly in chapter 6, but in short, they were chosen for the impact I believed they would have on LCOE, with regards to variations in the parameters compared with the three other cost categories.

Cost model for installation and transportation

The cost of installation and transportation contains costs associated with the installation of floating platforms at sea, as well as installation of wind

Authors	Maienza et al. (2020)	Ioannou et al. (2018)
Dev		672 802 500
Manuf	6 396 493 680	3 120 690 000
IT	673 015 200	917 226 000
OM	1 233 840 000	4 626 804 750
Decom	259 526 160	401 752 200
Authors	Rinaldi et al. (2021)	Castro-Santos and Diaz-Casas (2015)
Dev		111 197 025
Manuf		3 406 773 150
IT		296 261 775
OM	6 791 202 000	1 707 182 775
Decom	339 866 010	
Authors	Bjerkseter and Ågotnes (2013)	Hvidevold and Karlsen (2020)
Dev	349 440 000	225 144 000
Manuf		
IT	263 760 000	1 219 530 000
OM	5 502 000 000	3 517 875 000
Decom	178 080 000	574 149 000
	Average	
Dev		339 645 881
Manuf		4 307 985 610
IT		673 958 595
OM		3 896 484 088
Decom		350 674 674

Table 4.1: *The table show values for costs of development costs (C_{Dev}), manufacturing costs (C_{Manuf}), installation and transportation costs ($C_{I\&T}$), operation and maintenance costs ($C_{O\&M}$) and decommissioning costs (C_{Decom}). The table shows values in euros (€) collected from five articles and one master's theses, referenced in the table. The values have been adjusted after they were collected and cannot be found as they are shown in this table in their respective papers. The values have first been adjusted for inflation since the year of the publication of the respective paper. The values have been extrapolated from the power capacity of the wind farm being investigated in the respective paper, to a 1,5 GW wind farm (The power capacity of the farms investigated in this thesis). The values seen under "Average" is an average of the values from the articles, for each category. Note that $C_{I\&T}$ and $C_{O\&M}$ are not used to calculate LCC in this thesis. They are there as a reference to compare the costs of these two categories that will be calculated later in the thesis.*

turbines onto the floating platforms. It also contains the costs for the transportation of floating platforms and turbines from the nearest harbor to the location of the wind farm. Lastly, it contains costs for installation of cables, moorings, and anchors. The method used for calculating these costs will be shown in section 4.3.4.

For this part of the cost model regarding $C_{I\&T}$, I have chosen to utilize a cost model developed by Maienza et al. (2020). This cost model uses parameters for the wind farm that will be investigated, together with various costs, such as vessel costs, found in Table 4.2, and 4.3. Parameters for a reference wind turbine can be found in Table 5.1

Cost model for Operation and Maintenance

The cost of operation and maintenance contains all costs associated with the daily operation of the wind farm. They also include costs for all maintenance that must be done on the infrastructure of the wind farm. These costs are calculated as a yearly expenditure, and then added up according to the expected lifetime of the wind farm.

For this part of the cost model, I decided not to look at Maienza et al. (2020). Instead, I have looked at the method used by Bjerkseter and Ågotnes (2013). They have based their work on a specialized cost calculating software associated with wind energy, developed by the Energy Research Centre of the Netherlands. The cost values that are used in this software are unfortunately not publicly available, so I have followed the method as described by Bjerkseter and Ågotnes (2013) and estimated some values and found some values for different costs in other sources. How this has been done will be explained in detail in section 4.3.6.

The following sections will describe the equations used in the calculation of the LCC.

4.3.2 Cost model for C_{Dev}, C_{Manuf}, and C_{Decom}

I will in this section describe the method used to calculate the cost of development and project management, C_{Dev}, the cost of manufacturing, C_{Manuf}, and the cost of decommissioning, C_{Decom}. The sum of these costs is called

fixed costs, C_{fix}, and can be calculated as follows:

$$C_{fix} = \frac{\left(C_{Dev_{avg}} + C_{\text{Decom }_{avg}} + (C_{\text{Manufavg }} \cdot 0,97) + C_m\right) \cdot T_{pc}}{1500MW} \tag{4.2}$$

Where C_{Manuf} has been multiplied with 0,97 to remove the fixed cost of mooring manufacturing, T_{pc} is the total power capacity of the wind farm, C_m is the manufacturing costs of the moorings. The cost of manufacturing the moorings, depends on the type of floating platform being used, and can be calculated for the SB and the SSP using the following equation:

$$C_m = (n_S + n_T) \cdot c_{\text{line }} \cdot L_P \cdot \frac{w_d}{\cos_L} \cdot 1,2 \tag{4.3}$$

The equation is multiplied with 1,2 to account for the increasing slack in the moorings with an increasing water depth. This will be discussed further in chapter 6.

For the TLP, the following equation can be used:

$$C_m = (n_S + n_T) \cdot c_{\text{line }} \cdot L_P \cdot (w_d - 50) \tag{4.4}$$

Where n_S is the number of substations at the wind farm, n_T is the number of turbines at the wind farm, L_P is the number of mooring lines per platform – hence this depends on the type of platform being used, w_d is the average water depth at the wind farm location, and cos_L is the cosines of the angel between the water surface and the mooring lines. This parameter depends on the type of floating platform that is used. c_{line} is the cost of the moorings per meter of line. This parameter depends on the type of floating platform being used at the wind farm.

For the SB and the SSP, I will use steel chains in the calculations. The TLP will use synthetic fiber ropes. The cost of steel chains is 250 €/m, while the synthetic fiber ropes have a cost of 92 €/m, according to Myhr et al. (2014). The number of moorings per floating platform, LP, is three for the SB, six

for the SSP, and eight for the TLP.

The cosines of the angel between the water surface and the mooring lines used in this thesis is 0,3 for the SSP and 0,35 for the SB. The cosines has been calculated using numbers from Maienza et al. (2020). In their article they are looking at a wind farm with a water depth of 135 meters, the SSP has mooring lines of 450 m, the SB has mooring lines of 390 m, and the TLP has mooring lines of 85 m. The cosines were then calculated for the SSP and the SB by dividing the water depth by the mooring lengths. The TLP's mooring lines stretches from the bottom of the submerged pontoons to the seabed, without an angel. The value 50, used in the equation above is then found by subtracting the water depth from the mooring line length in Maienza et al. (2020).

4.3.3 Cost model data for $C_{I\&T}$ and $C_{O\&M}$

In this section I will present the cost models for $C_{I\&T}$ and $C_{O\&M}$, and the data used for these cost models. The data includes a variety of parameters from price of hiring cranes and vessels, and the speed of the vessels to the cost of renting the seabed that the wind farm will make use of. It is important to remember that the parameters presented in the following tables are values that will be the same for all calculations of LCOE. Other parameters also used in the calculation of LCOE that will be used with variation in their values, such as water depth, will not be presented in the following tables. For the variable parameters, one reference wind farm has been created in Table 5.1. When the results of variations in one parameter is being explored, all other variable parameters will be used as listed in Table 5.1, describing the reference wind farm.

All tables in this section includes one column used to cite the source of the value presented in the respective row. In the first table presented in this section, table 4.2, an overview of parameters used to calculate the installation and transportation of turbines and floating platforms as a part of the total $C_{I\&T}$ can be found. $C_{I\&T}$ also includes costs for installation of moorings, anchors, cables, and substation.

Parameter	Abbrev.	Unit	Vaule	Source	nr.
Hiring cost of storage					

area	c_s	$\frac{€}{m^2 \cdot day}$	0,02	Castro-Santos et al. (2018)	1
Daily cost of cranes	C_c	€/day	811 886	Castro-Santos et al. (2018)	2
Daily cost tug	c_t	€/day	22 502	Castro-Santos et al. (2018)	3
Daily cost barge	c_b	€/day	35 000	Castro-Santos et al. (2018)	4
Mobilization cost tug	c_{tm}	€	150 000	Castro-Santos et al. (2018)	5
Mobilization cost barge	c_{bm}	€	150 000	Castro-Santos et al. (2018)	6
Mobilization cost crane	C_{cm}	€	1 049 853	Castro-Santos et al. (2018)	7
Cost of port crane	c_c	€/h	833	Castro-Santos et al. (2018)	8
Time to load turbines in the vessel	t_{LT}	h	3	Castro-Santos et al. (2018)	9
Time between movements while OWT is installed	t_{iT}	h	8	Castro-Santos et al. (2018)	10
Time to install WT offshore with lifts	t_{imT}	h	3	Castro-Santos et al. (2018)	11
Time for installing and lifting offshore	t_{iP}	h	3	Castro-Santos et al. (2018)	12
Time between movements while installing	t_{imP}	h	8	Castro-Santos et al. (2018)	13
Time to load platform in vessel	t_{LP}	h	3	Castro-Santos et al. (2018)	14
Speed of barge and tug vessels	v_t	m/s	3,6	Castro-Santos et al. (2018)	15
Speed of floating crane	v_{t1}	m/s	3	Castro-Santos et al. (2018)	16
TLP, Number of wind turbines per travel 1	$n_{BT,1}$		1	Castro-Santos et al. (2018)	17
SB, Number of wind turbines per travel 1	$n_{BT,1}$		1	Castro-Santos et al. (2018)	17
Number of wind turbines per travel 2	$n_{BT,2}$		18	Castro-Santos et al. (2018)	17
Number of wind turbines per travel 3	$n_{BT,3}$		16	Castro-Santos et al. (2018)	17
Downtime	k_t		0,75	Castro-Santos et al. (2018)	18
Number of cranes w/o storage area	n_c		1	Castro-Santos et al. (2018)	19
Number of tug vessels	n_t		2	Castro-Santos et al. (2018)	20
Bumber of barge vessels	n_b		1	Castro-Santos et al. (2018)	21
Number of floating					

cranes w/ storage area for transportation	n_{cs}		1	Castro-Santos et al. (2018)	22
Number of floating platforms per boat, 1,2	$n_{BP,1,2}$		3	Castro-Santos et al. (2018)	23
Number of floating platforms per boat, 3	$n_{BP,3}$		2	Castro-Santos et al. (2018)	23
Electric transformer length	l_{TS}	m	6	Castro-Santos et al. (2018)	24
Gas insulated Switchgear length	l_{GIS}	m	4	Castro-Santos et al. (2018)	25
SSP, Maximum freeboard	l_f	m	12	Castro-Santos et al. (2018)	26
SSP, Draft	d_{pl}	m	10	Castro-Santos et al. (2018)	27
SB, Draft	d_{pl}	m	120	Castro-Santos et al. (2018)	27
TLP, Draft	d_{pl}	m	44,89	Castro-Santos et al. (2018)	27
SSP, length of platform	l	m	76	Castro-Santos et al. (2018)	28
SB, length of platform	l	m	9,4	Castro-Santos et al. (2018)	28
TLP, lenght of platform	l	m	54	Castro-Santos et al. (2018)	28
TLP, Inferior pontoon diameter floater	d_{ip}	m	3	Castro-Santos et al. (2018)	29

Table 4.2: *Overview of parameters used to calculate the installation and transportation of turbines and floating platforms as a part of the total $C_{I\&T}$. Some of the parameters are also used in the calculation of the installation of the substations, cables, and moorings. A brief explanation for all the parameters can be found in the Appendix A. The number in the "nr."-column corresponds to the number of the parameter found in the Appendix. All values in this table has been gathered from Castro-Santos et al. (2018) and Ioannou et al. (2018).*

The values found in Table 4.2 has come from Castro-Santos et al. (2018). The article by Maienza et al. (2020) that has developed the cost model for $C_{I\&T}$ used in this thesis has also referred to Castro-Santos et al. (2018) when writing their article. Some parameters depend on what the type of floating platform is being used. Those parameters are marked with either SB, SSP or TLP to distinguish between what platform type the parameter is referring to in the table.

The next table that will be presented is Table 4.3. Here all parameters regarding the installation of cables, substations, anchors, and moorings are

presented. These values have also been taken from Castro-Santos et al. (2018), in addition two of the values (The installation rate for the array, and export cables) have been taken from Ioannou et al. (2018). Some of the values regarding the installation of the substations can also be found in the Table 4.2. This is due to some of the equations for calculating the cost of the installation of the substations, that uses some of the same values as the formulas for calculating the costs of installing the turbines.

The last table, Table 4.4 presented in this section show the values involved in the calculations of the costs of $C_{O\&M}$. These values are found in the article from Shafiee et al. (2016), Bjerkseter and Ågotnes (2013), and a selection of webpages, as referenced in the tables. As with the previous Table 4.3, some values regarding the calculations of $C_{O\&M}$ can also be found in Table 4.2.

4.3.4 Cost model for installation of floating platforms and wind turbines

In the above sections, I have explained how the average cost have been used to calculate an estimate for C_{Dev}, C_{Manuf}, and C_{Decom} in previous litterature. The parameters that are used as constant values in the calculation of $C_{I\&T}$ and $C_{O\&M}$ have also been presented. In this section I will give an overview of the equations used to calculate $C_{I\&T}$. All equations described in this section comes from Maienza et al. (2020).

$C_{I\&T}$ will be calculated by adding the sum of the 1: the cost of the installation and transportation of the wind turbines, 2: the cost of the installation and transportation of the floating platforms, and 3: the cost of the installation of cables, substations, anchors, and moorings. The cost of the installation and transportation of the wind turbines and floating platforms depends on the type of floating platforms being used. The cost of the installation of anchors and moorings also depends on the type of floating platform being used. This is due to the fact that the SB needs 3 moorings, the SSP needs 6 moorings, and the TLP needs 8 moorings. For some equations used to calculate the costs the equations will differ depending on the type of floating platform. When this is the case, a note will be made before the equation is shown.

The cost of the installation and transportation of the wind turbines will be divided into three subcategories. Firstly, the cost of the procedure taking place at the port, as described in Maienza et al. (2020). The costs associ-

Parameter	Abbrev.	Unit	Vaule	Source	nr.
Cost of soil preperation	$C_{ITS,5,1}$	€	660 192	Castro-Santos et al. (2018)	30
Cost of foundation	$C_{ITS,5,2}$	€	312 265	Castro-Santos et al. (2018)	31
Installation cost using cranes	$C_{ITS,5,1}$	€	63 646	Castro-Santos et al. (2018)	32
Daily rate of CLV	$c_{ITS,1}$	€/day	82 500	Castro-Santos et al. (2018)	33
AHV cost	$C_{IMA,1}$	€/day	48 860	Castro-Santos et al. (2018)	34
The cost of direct labour	$C_{IMA,,2}$	€/day	5 656	Castro-Santos et al. (2018)	35
Unit installation cost	$c_{ITS,3}$	€ /m	600	Castro-Santos et al. (2018)	36
Installation rate of array cables	$k_{ITS,1}$	m/day	600	Ioannou et al. (2018)	37
Installation rate of export cables	$k_{ITS,2}$	m/day	1 600	Ioannou et al. (2018)	38
Anchor installation rate	$r_{IMA,1}$	$\frac{\text{anchors}}{\text{day}}$	7	Castro-Santos et al. (2018)	39
Plan area of transformer	A_{TS}	m2	5	Castro-Santos et al. (2018)	40
Gas Insulated Switchgear GIS plan area	A_{GIS}	m2	2,5	Castro-Santos et al. (2018)	41
Time lift substation, load on vessel	t_{LIOS}	h	3	Castro-Santos et al. (2018)	42
Number of electric array cables	n_1		7	Castro-Santos et al. (2018)	43
Number of electric export cables	n_2		2	Castro-Santos et al. (2018)	44
Number of electric onshore cables	n_3		2	Castro-Santos et al. (2018)	45

Table 4.3: *Overview of parameters used to calculate the installation of cables, substations, anchors, and moorings as a part of the total $C_{I\&T}$. A brief explanation for all the parameters can be found in the Appendix A. The number in the "nr."-column corresponds to the number of the parameter found in the Appendix. All values in this table has been gathered from Castro-Santos et al. (2018) and Ioannou et al. (2018).*

Parameter	Abbrev.	Unit	Vaule	Source	nr.
Cost of crew vessel	c_{cv}	£/day	2500	Catapult Offshore (2022)	46
Price per unit energy	PE	€/MWh	37,69	SSB (2022)	47
Insurance cost per power unit	$c_{O,4}$	€/MW	17,48	Shafiee et al. (2016)	48
Transmission cost per power unit	$c_{O,5}$	€/MW	86,09	Shafiee et al. (2016)	49
Crew vessel speed	v_{cv}	m/s	10,3	4C Offshore (2022)	50
Rent percentage of wind farm revenue	ℓ	%	0,02	Shafiee et al. (2016)	51
Export cable annual failure rate	E_f	$\frac{\text{Failures}}{100\text{km}\cdot year}$	0,1	Bjerkseter and Ågotnes (2013)	52

Table 4.4: *Overview of parameters used to calculate the total COM. A brief explanation for all the parameters can be found in the Appendix. The number in the "nr."-column corresponds to the number of the parameter found in the appendix. All values in this table have been gathered from Shafiee et al. (2016), Bjerkseter and Ågotnes (2013), Catapult Offshore Renewable Energy (2022), SSB (2022), and 4C Offshore (2022).*

ated with the port procedure is the cost of hiring the port, as well as the cost of hiring a port crane. The second cost is the cost of transporting the wind turbines to the location of the offshore wind farm. These costs stem from the rental of the transportation vessels. Lastly, there is the cost of the installation of the wind turbines at the wind farm location. This cost comes from the cost of renting floating cranes that can lift the turbines into place. This can be summed up in the following equation:

$$C_{IT} = \sum_{i=1}^{3} C_{IT,i} \tag{4.5}$$

Where C_{IT} is the total cost of transporting and installing the wind turbines at the wind farm location. $C_{IT,1}$, $C_{IT,2}$, and $C_{IT,3}$ will be explained below.

For the cost of transportation and installation of the turbines that will utilize SSP, the costs will be zero. The reason for this is that the scenario described in this thesis, when utilizing SSP, the turbine will be mounted directly onto the floating platform at the harbor. Therefor all costs will be displayed in the

chapter describing the cost of installation and transportation of the floating platform, when regarding turbines utilizing SSP.

The port procedure cost regarding the wind turbines is calculated using the following equation:

$$C_{IT,1} = A_{IT,1} \cdot t_{IT,1} \cdot c_s + n_T \cdot t_{LT} \cdot c_{pc} \tag{4.6}$$

Where $C_{IT,1}$ is the cost of the port procedure regarding the turbines, $A_{IT,1}$ is the hired area of the port required for one wind turbine, $t_{IT,1}$ is the time needed to hire the port per wind turbine, c_s is the hiring cost for the port per m2 per day, n_T is the total number of wind turbines used in the wind farm. n_T is the only value in this equation that will vary depending on the wind farm being investigated. t_{LT} is the time it takes to load one wind turbine into the vessel that will carry it to the wind farm location, c_{pc} is the daily rental cost for the port crane used to lift the wind turbines. All constant values can be found in Table 4.2. Wind farm dependant values are found in table 5.1, where the reference wind farm is defined.

$A_{IT,1}$ and $t_{IT,1}$ are not constant values. $A_{IT,1}$ is calculated the following way:

$$A_{IT,1} = 3 \cdot n_T \cdot \left[l_b \cdot d_b + \pi \cdot \left(\frac{d_t}{2} \right)^2 \right] \tag{4.7}$$

Where l_b is the length of one wind turbine blade. The wind turbine blade is not a constant value and will vary with the type of wind turbine being investigated for the different locations. d_b is the diameter of a single blade, while d_t is the diameter of the wind turbine tower, values for these parameters is found in section 2.4.2 for each of the three wind turbines used in this thesis.

For $t_{IT,1}$, the time it takes to load a turbine onto the vessel depends on the type of floating platform that will be utilized. For the SB $t_{IT,1}$ this will be the sum of three other parameters as described in the following equation:

$$t_{IT,1} = t_{A,1} + t_{A,2} + t_{A,3} \tag{4.8}$$

Where $t_{A,1}$, $t_{A,2}$ and $t_{A,3}$ has to do with the waiting time for the barge, tug, and crane respectively, hence the components have to wait at the port while the vessels are being used to ship other parts of the wind farm and install them at the location. This is given in the following equations:

$$t_{A,1} = \frac{\left(\frac{2}{3600} \cdot \frac{d_p}{v_t} + n_{BT,1} \cdot t_{LT}\right) \cdot \frac{1}{k_t} \cdot \frac{n_T}{n_{BT,1}}}{24} \tag{4.9}$$

$$t_{A,2} = \frac{\left(\frac{2}{3600} \cdot \frac{d_p}{v_t}\right) \cdot \frac{1}{k_t} \cdot \frac{n_T}{n_{BT,2}}}{24} \tag{4.10}$$

$$t_{A,3} = \frac{(t_{iT} + t_{imT}) \cdot \frac{1}{k_t} \cdot n_T}{24} \tag{4.11}$$

Where d_p is the average distance from any point within the wind farm location to a harbor. This is a variable parameter depending on the location of the wind farm being investigated. v_t is the speed of the barge and tug vessels, v_{t1} is the speed of the floating crane, $n_{BT,1}$, $n_{BT,2}$, and $n_{BT,3}$ are the number of wind turbines being transported per vessel, and these depends on the type of floating platform being used. t_{iT} is the time between crane movements while the wind turbine is being installed at site, t_{LT} is the time it takes to load one wind turbine into the vessel that will carry it to the wind farm location, k_t is the downtime, and t_{imT} is the time it takes to install the turbine offshore with lifts.

For turbines utilizing the TLP, $t_{IT,1}$ is made up of $t_{A,3}$ mentioned above, and $t_{A,4}$ as shown in the next equation :

$$t_{IT,1} = t_{A,3} + t_{A,4} \tag{4.12}$$

Where $t_{A,4}$ is the time spent using the floating crane and is given as follows:

$$t_{A,4} = \frac{\left(\frac{2}{3600} \cdot \frac{d_p}{v_{t1}} + n_{BT,3} \cdot t_{LT}\right) \cdot \frac{1}{k_t} \cdot \frac{n_T}{n_{BT,3}}}{24} \tag{4.13}$$

I have now shown the equations needed for the calculation of the port procedure costs, $C_{IT,1}$ regarding the wind turbines. Next is the costs for the transportation of the wind turbines, $C_{IT,2}$. This cost is calculated differently for turbines utilizing the SB and the TLP. For the SSP all costs regarding the turbines are zero.

The wind turbine transportation costs, $C_{IT,2}$, for turbines utilizing the SB, is calculated using the following equation:

$$C_{IT,2} = n_t \cdot t_{A,1} \cdot c_t + n_b \cdot t_{A,2} \cdot c_b + C_{tm} + C_{bm} \tag{4.14}$$

Where $C_{IT,2}$ is the cost of transporting the wind turbines from the port to the wind farm location, n_t and n_b is the number of tug vessels and barge vessels used in the transportation, c_t and c_b is the daily rental cost of tug vessels and barge vessels, and C_{tm} and C_{bm} is the cost of mobilizing one tug vessel and one barge vessel.

For turbines utilizing the TLP the transportation costs are calculated as follows:

$$C_{IT,2} = n_{cs} \cdot t_{A,2} \cdot c_c + C_{cm} \tag{4.15}$$

Where n_{cs} is the number of floating cranes with a storage area used for installation at sea.

The final cost for the transportation and installation of the wind turbines is the cost of installation of the wind turbines at sea, $C_{IT,3}$ given in the following equation:

$$C_{IT,3} = n_c \cdot t_{A,3} \cdot c_c + C_{cm} \tag{4.16}$$

Where $C_{IT,3}$ is the cost of installing the wind turbines at the wind farm location, n_c is the number of floating cranes without a storage area used for installation at sea, c_c is the daily cost of the crane and C_{cm} is the cost of mobilizing a crane.

I have now shown the equations used to calculate the cost of transporting and installing the wind turbines at the location of the wind farm. Next, I will show how to calculate the cost of transporting and installation of the floating platforms, C_{IP}, at the wind farm location. The cost of transportation and installation of the floating platforms is calculated with similar steps as that of the calculation of the transportation and installation of the wind turbines. As stated previously, the wind turbines utilizing the SSP will be installed directly to the platform at the port. Therefor the cost of transporting and installing wind turbines utilizing the SSP will be included in the following equations. The cost for transporting and installing the floating platforms, C_{IP}, can be calculated with the following equation:

$$C_{IP} = \sum_{i=1}^{3} C_{IP,i} \tag{4.17}$$

Where C_{IP} is the total cost associated with the transportation and installation of the floating platforms at the wind farm location, $C_{IP,1}$, $C_{IP,2}$, and $C_{IP,3}$ will be shown below.

The cost of the port procedure associated with the floating platforms can be calculated using the following equation:

$$C_{IP,1} = A_{IP,1} \cdot t_{IP,1} \cdot c_s + n_T \cdot t_{LP} \cdot c_c \tag{4.18}$$

Where $A_{IP,1}$ is the total area of the port needed to be rented during the process of transporting and installing the floating platforms. $t_{IP,1}$ is the number of days the port will have to be rented during the installation process, and

t_{LP} is the time it takes to load one floating platform onto the vessel that will carry it to the wind farm location. The rest of the variables are described under equation 4.6.

$A_{IP,1}$ which is the area needed for storing the floating platforms during the installation process can be calculated as follows:

$$A_{IP,1} = A_{SP} + n_S \cdot (l_{TS} + l_{GIS})^2 \tag{4.19}$$

Where n_s is the number of offshore substations used in the wind farm. The number of substations used will be accounted for in the next chapter when discussing the results for each wind farm location. l_{TS} is the length of the electric transformer used in the substation and l_{GIS} is the length of the gas insulated switch gear. In the case of A_{SP}, it is calculated differently for the three floating platform types. For the the SB, A_{SP} is calculated using the following equation:

$$A_{SP} = n_T \cdot (l_f + d_P) \cdot l \tag{4.20}$$

For the SSP the following equation is used:

$$A_{SP} = n_T \cdot \frac{l^2}{2} \cdot \sqrt{3} \tag{4.21}$$

For the TLP the following equation is used:

$$A_{SP} = n_T \cdot (l_f + d_P + d_{ip}) \cdot l \tag{4.22}$$

Where l_f is the maximum freeboard of the platform, d_{pt} is the draft, l is the length of the floating platform and d_{ip} is the diameter of the inferior pontoon. The maximum freeboard for the SB was not given in Castro-Santos

et al. (2018), and A_{SP} for the SB has therefore been calculated without this value.

$t_{IP,1}$, which is the number of days the port has to be rented during the installation of the floating platforms, and also has to be calculated considering what type of floating platform will be used. For the SB, $t_{IP,1}$ can be calculated as follows:

$$t_{IP,1} = t_{A,5} + t_{A,6} + t_{A,7} \tag{4.23}$$

For the SSP, $t_{IP,1}$ can be calculated using the following equation:

$$t_{IP,1} = \frac{t_{iP}}{24} \cdot (n_T + n_s) + t_{A,8} \tag{4.24}$$

Filnally, for the TLP, $t_{IP,1}$ can be calculated using the following equation:

$$t_{IP,1} = t_{A,6} + t_{A,9} \tag{4.25}$$

Where $t_{A,5}$, $t_{A,6}$, and $t_{A,7}$, has to do with the operation time during the installation process of the floating crane, barge, and tug respectively. $t_{A,8}$ and $t_{A,9}$ is the time of crane usage. These times can be calculated using the following equations:

$$t_{A,5} = \frac{\left(\frac{2}{3600} \cdot \frac{d_p}{v_{t1}}\right) + (t_{ip} + t_{im_P}) \cdot \frac{1}{k_t} \cdot n_T}{24} \tag{4.26}$$

$$t_{A,6} = \frac{\left(\frac{2}{3600} \cdot \frac{d_p}{v_t} + n_{BP,1} \cdot t_{LP}\right) \cdot \frac{1}{k_t} \cdot \frac{n_T}{n_{BP,1}}}{24} \tag{4.27}$$

$$t_{A,7} = \frac{\left(\frac{2}{3600} \cdot \frac{d_p}{v_t}\right) \cdot \frac{1}{k_t} \cdot \frac{n_T}{n_{BP,2}}}{24} \tag{4.28}$$

$$t_{A,8} = \frac{\left(n_{BP3} \cdot t_{LT} + \frac{2}{3600} \cdot \frac{d_p}{v_t}\right) \cdot \frac{1}{k_t} \cdot \frac{n_T}{n_{BP,3}}}{24} \tag{4.29}$$

$$t_{A,9} = \frac{(t_{ip} + t_{imp}) \cdot \frac{1}{k_t} \cdot n_T}{24} \tag{4.30}$$

Where d_p is, as previous, the average distance from the wind farm location to the harbor, which is a variable parameter dependent on the wind farm location being investigated. v_t is the speed of the barge and tug vessels, v_{t1} is the speed of the floating crane, $n_{BP,1}$, $n_{BP,2}$, and $n_{BP,3}$ are the number of wind turbines being transported per vessel, and they depend on the type of floating platform being used. t_{imp} is the time between crane movements while the floating platform is being installed at site, t_{LP} is the time it takes to load one floating platform onto the vessel that will carry it to the wind farm location, k_t is the downtime, t_{iP} is the time it takes to install the turbine offshore with lifts and n_T is the number of wind turbines in the wind farm, which is a varying parameter dependent of the wind farm being investigated.

After the calculation of the port procedure cost, $C_{IP,1}$, we can now move on to the calculation of the transportation and installation cost for the floating platforms, $C_{IP,2}$ and $C_{IP,3}$. This is calculated differently for the SB and the TLP. In the case of the SSP these costs are baked into the cost of the port procedure. For the SB, the cost of transportation of the floating platform to the location of the wind farm is calculated using the following equation:

$$C_{IP,2} = n_b \cdot t_{A,6} \cdot c_b + 2 \cdot n_t \cdot t_{A,7} \cdot c_t + C_{bm} + 2 \cdot C_{tm} \tag{4.31}$$

Where n_b and n_t represents the number of barge and tug vessels used in the transportation, c_b and ct represents the daily cost of rental for the barge and

tug vessels, C_{bm} and C_{vm} represents the cost of mobilizing the barge and tug vessels.

For the TLP, $C_{IP,2}$ is calculated using the following equation:

$$C_{IP,2} = n_{cs} \cdot t_{A,6} \cdot c_{cs} + C_{csm} \tag{4.32}$$

Where n_{cs} is the number of floating cranes with storage used for transportation, c_{cs} is the daily cost for renting the crane and C_{csm} is the cost of mobilizing the crane.

The last step in the calculation of the transportation and installation costs for the wind turbines and the floating platforms is calculating the installation cost for the floating platforms, $C_{IP,3}$. For the SB this is done using the following equation:

$$C'_{IP,3} = t_{A,5} \cdot c_C + C_{cm} \tag{4.33}$$

Where c_c is the daily cost for renting the crane and C_{cm} is the cost of mobilizing the crane.

For the TLP, $C_{IP,3}$ is calculated using the following equation:

$$C_{IP,3} = t_{A,9} \cdot c_{cs} + C_{csm} \tag{4.34}$$

4.3.5 Cost model for cables, substations, and moorings

This section will give an overview of how the costs connected to the installation of the substations, cables, anchors and mooring have been calculated in the cost model developed in this thesis. All equations presented in this section comes from Maienza et al. (2020).

Cost calculations for installation of substations

I will first go through the method for calculating the cost of the offshore substations, then the cost of installation of the onshore substation. The cost of the installing of the offshore substation is calculated with the following equation:

$$C_{ITS,4} = C_{ITS,4,2} + (C_{ITS,4,1} + C_{ITS,4,3}) \cdot n_s \tag{4.35}$$

Where $C_{ITS,4}$ is the total cost of the installation process of the offshore substations, $C_{ITS,4,1}$ is the cost associated with the port procedure regarding the offshore substation, $C_{ITS,4,2}$ is the cost of transportation regarding the offshore substations, and $C_{ITS,4,3}$ is the cost of installing the substations at the wind farm location. $C_{ITS,4,1}$ is calculated using the following equation:

$$C_{ITS,4,1} = A_{ITS,4,1} \cdot t_{ITS,4,1} \cdot c_S + (n_{TS} \cdot 1 + 1 + 1) \cdot t_{LOS} \cdot c_c \tag{4.36}$$

Where $A_{ITS,4,1}$ is the total area of the port that needs to be hired for storage of the substation components during the installation of the substations, $t_{ITS,4,1}$ is the time needed to hire the port during the installation process, c_s is the cost of hiring the port, t_{LOS} is the time needed to load the substations onto the carrying vessel, and c_{pc} is the daily cost of the port crane.
The total area of the port that needs to be hired for storage of the substation components during the installation of the substations, $A_{ITS,4,1}$ is calculated as follows:

$$A_{ITS,4,1} = n_{TS} \cdot (A_{TS} + A_{GIS}) \cdot (1 + 1.5) \tag{4.37}$$

Where n_{TS} is the number of transformers, A_{TS} is the plan area of the transformer and A_{GIS} is the plan area if the insulated switch gear.
Finaly, t_{LOS} is calculated as follows:

$$t_{LOS} = (n_{TS} \cdot 1 + 1 + 1) \cdot t_{LIOS} \tag{4.38}$$

Where t_{LIOS} represents the time it takes to load one substation onto the carrying vessel.

For the cost of transportation for the substations, $C_{ITS,4,2}$, and the cost of installaltion for the substations, $C_{ITS,4,3}$, they are calculated the same way as the cost for transporting and installing floating platforms, but substituting the number of turbines, for the number of substations in the equations. See section 4.3.4 for these calculations.

I will now show how to calculate the cost of the onshore substation. It is done using the following equation:

$$C_{ITS,5} = \sum_{j=1}^{3} C_{ITS,5j} \tag{4.39}$$

Where $C_{ITS,5}$ is the cost of installing the onshore substation, $C_{ITS,5,1}$ is the cost of soil preparation, $C_{ITS,5,2}$ is the foundation cost, and $C_{ITS,5,3}$ is the cost of cranes during the installation process. These costs can be found in the table containing costs for the installation of substations, cables, and moorings, Table 4.3.

Cost calculations for installation of cables

I will in this section go through how the cost of installing all cables needed for the wind farm is calculated. This includes array cables, that connects the turbines with the substations within the wind farm, the export cable that export the generated electricity from the wind farm to the onshore substation, and lastly the onshore cable that connects the wind farm to the national electricity grid. The cost of installation of cables is calculated as follows:

$$C_{ITS} = \sum_{i=1}^{3} C_{ITS,i} \tag{4.40}$$

Where C_{ITS} is the total cost of installing all cables needed for the wind farm, $C_{ITS,1}$ is the cost of installing the array cables, $C_{ITS,2}$ is the cost of installing the export cable and $C_{ITS,3}$ is the cost of installing the onshore cables.

The cost of installing the array cables, $C_{ITS,1}$ is calculated as follows:

$$C_{ITS,1} = \frac{c_{ITS,1}}{k_{ITS,1}} \cdot l_1 \cdot n_1 \tag{4.41}$$

Where $c_{ITS,1}$ is the daily rental cost of the cable laying vessel (CLV), $k_{ITS,1}$ is the installation rate of the CLV in m/day, while l_1 is the length of the array cables, and n_1 is the number of electric cables used.

The length of the array cables, l_1 can be calculated as follows:

$$l_1 = (7 \cdot d + w_d) \cdot (n_T - 1) \tag{4.42}$$

Where d_b is the wind turbine rotor diameter, w_d is the average water depth at the wind farm location, and n_T is the number of wind turbines. All of these three parameters, d_b, w_d, and n_T, are variables that change according to the conditions of the wind farm being investigated and the location of the wind farm.

The cost of installation for the export cable, $C_{ITS,2}$ can be calculated as follows:

$$C_{ITS,2} = \frac{c_{ITS,1}}{k_{ITS,2}} \cdot l_2 \cdot n_2 \tag{4.43}$$

Where $k_{ITS,2}$ is the installation rate for export cables of the CLV, n_2 is the number of electric cables and l_2 is the length of the export cable. This parameter is given as a variable that depends on the location of the wind farm being investigated. It is given as the average length of the location to the nearest shoreline.

The cost of the installation of the onshore cables, $C_{ITS,3}$ is calculated in the following equation:

$$C_{ITS,3} = c_{ITS,3} \cdot l_3 \cdot n_3 \tag{4.44}$$

Where $c_{ITS,3}$ is the installation cost per meter of installed cable, n_3 is the number of electric cables and l_3 is the length of a single cable. The length of a single cable is in this thesis given as the length from the nearest point at

shore to the nearest grid connected transformer.

Cost calculations for installation of anchors and moorings

The last section in the method chapter about installation costs will showcase how to calculate the costs associated with installing anchors and moorings. The cost of installing anchors and moorings, C_{IMA} can be calculated using the the following equation:

$$C_{IMA} = (c_{IMA,1} + c_{IMA,2}) \cdot \frac{n_M}{r_{IMA,1}} \tag{4.45}$$

Where $c_{IMA,1}$ is the daily rental cost of the anchor handling vehicle (AHV), $c_{IMA,2}$ is the cost of the direct labor associated with the installation, $r_{IMA,1}$ is the installation rate of anchors installed per day, and finally n_M is the total number of moorings at the wind farm. n_M is not a constant parameter, and it will vary with the number of wind turbines in the wind farm being investigated.

The total number of mooring lines, n_M can be calculated as follows:

$$n_M = (n_S + n_T) \cdot L_P \tag{4.46}$$

Where n_S is the number of offshore substations used at the wind farm, n_T is the number of wind turbines and LP is the number of mooring lines per floating platform. The substations uses the same type of floating platform as the wind turbines. These parameters are not constant and all depend on the type of wind farm being investigated and the type of floating platform being used at the wind farm.

4.3.6 Cost model for O&M

In the following section I will give an overview of how the cost model for operation and maintenance (O&M) has been developed. The cost model for O&M is in some ways a much more complex calculation than that of $C_{I\&T}$,

even though the $C_{I\&T}$ consists of far more steps than $C_{O\&M}$ to get the final result. The problem with calculating $C_{O\&M}$ is a lack of available data that is needed to calculate the cost. The most hard-to-come-by data includes statistics for failure rates of wind turbine components. For this reason, I have used both Maienza et al. (2020) and Bjerkseter and Ågotnes (2013) when calculating $C_{O\&M}$. I have looked at how Maienza et al. (2020) have calculated the cost of renting the maritime property, insurance cost, and transmission costs. Because of a lack of data to calculate the costs of maintenance repairs of the $C_{O\&M}$ with the cost model developed by Maienza et al. (2020), I have looked at how Bjerkseter and Ågotnes (2013) have calculated costs associated with repairs of the turbines. Their article includes a detailed description of how the O&M process functions. In addition to the cost of repairs on the wind turbines, I have based my method of calculating $C_{O\&M}$ associated with the repairs on the wind farm cables, on the descriptions of this process in Bjerkseter and Ågotnes (2013).

To calculate $C_{O\&M}$, Bjerkseter and Ågotnes (2013) have in their paper used a specialized software developed by Energy Research Centre of the Netherlands. As I do not have access to this software, I have based the cost model developed for this thesis on the description of the O&M process associated with repairs of turbines and cables, described by Bjerkseter and Ågotnes (2013). Based on these descriptions I have developed a general way of calculating $C_{O\&M}$ for any offshore wind farm. It is worth noticing that the developed model for calculating $C_{O\&M}$ have uncertainty. This will be discussed in chapter 6.

According to Bjerkseter and Ågotnes (2013) there are three types of maintenance that occur within a wind farm: calendar-based preventative maintenance, condition-based preventative maintenance and unplanned corrective maintenance. Calendar-based and condition-based preventative maintenance can be considered part of the usual daily operation of the wind farm. This type of maintenance is done to prevent failure of any components on the wind turbines. On the other hand, unplanned corrective maintenance is done in the case of when a component of a wind turbine has already failed, and the turbine needs corrective maintenance to resume energy production. Unplanned corrective maintenance is divided further into two subcategories of minor- and major- unplanned corrective maintenance.

Table 4.5 shows the number of maintenance events per year that would occur in the scenario described by Bjerkseter and Ågotnes (2013). In their article

Type of maintenance	Number of maintenance events per year
Unplanned corrective	872
Condition-based	4
Calendar-based	120

Table 4.5: *The data in the table is gathered from Bjerkseter and Ågotnes (2013). It shows the number maintenance events per year in the reference wind farm described in Bjerkseter and Ågotnes (2013). The maintenance events has been categorized by unplanned corrective maintenance events, condition-based maintenance events, and calendar-based maintenance events.*

they are looking at a wind farm with 100 turbines. By extrapolating those numbers to the number of turbines used in the scenarios being looked at in this thesis, there is possible to get an understanding of the $C_{O\&M}$. Looking at the table one can note that condition-based maintenance only accounts for about 0,4 % of the total number of maintenance events per year. Because of the small fraction of the total number of maintenance events that come from condition-based maintenance events, I have decided to neglect the condition-based events.

To calculate the cost of the maintenance done on the wind turbines, we need an understanding of what type of equipment is required during the maintenance. For the calendar-based planed preventative maintenance, Bjerkseter and Ågotnes (2013) assumes that a crew vessel and a diving support vessel is needed. For the minor unplanned corrective maintenance, it is assumed that a crew vessel is satisfactory for the corrective maintenance. For the major unplanned corrective maintenance, it is assumed that a crane is needed to carry out the maintenance of the turbine. It is assumed that the maintenance of the turbines takes an average of 24 hours. In addition, the cost of travel back and forth between the port and the wind farm location must be accounted for.

As one can imagine the total $C_{O\&M}$ will be heavily influenced by the ratio between the minor and major corrective maintenance, due to the huge difference in rental costs between the crew vessel and the crane. This ratio will be presented in chapter 5, where I will look at how this ratio affect the LCOE of the wind farm. It will be further discussed in chapter 6.

The cost of maintenance related to the wind farm electrical cables is connected to the cable failure rate. Bjerkseter and Ågotnes (2013) assumes offshore electrical cables to have an annual failure rate of 0,1 per 100 km of

cables. The maintenance of the cables will be carried out by a CLV. The maintenance of the cables is expected to take 24 hours. During the time of the maintenance of the export cable, the wind farm will be unable to deliver electricity to the grid, and the electricity generated during this time will be lost. In the case of maintenance on the array cables the wind farm is assumed to lose 3 % of its power production during the time of the maintenance. This will therefore influence the total energy produced over the wind farm's lifetime. However, these losses is not accounted for in the method used to calculate energy production outlined in this theis.

As a summary, $C_{O\&M}$ consists of the cost of renting the maritime property, an insurance cost, a transmission cost, and the cost of maintenance on the wind farm electrical cables – in addition to the cost of direct maintenance of the turbines.

The next part of this section will show the method used to calculate $C_{O\&M}$. I will start with describing the method of calculating the cost regarding yearly maintenance events, then I will go through the rest of the costs associated with $C_{O\&M}$.

As a summary, $C_{O\&M}$ consists, in addition to the cost of direct maintenance of the turbines, also of the cost of renting the maritime property, an insurance cost, a transmission cost, and the cost of maintenance on the wind farm electrical cables. I will start with describing the method of calculating the cost regarding yearly maintenance events, then I will go through the rest of the costs associated with $C_{O\&M}$.

The total $C_{O\&M}$ will be calculated as an annual cost. This cost must be multiplied with the wind farm's lifetime to get the full cost of OM over the wind farm's lifetime.

$C_{O\&M}$ can be calculated using the following equation:

$$C_{O\&M} = \sum_{i=1}^{5} C_{O,i} \tag{4.47}$$

Where $C_{O,1}$ is the cost of calendar-based preventative maintenance, $C_{O,2}$ is the cost of unplanned corrective maintenance, $C_{O,3}$ is the annual cost of rent-

ing the maritime state property, $C_{O,4}$ is the annual insurance cost, and $C_{O,5}$ is the annual transmission cost based on the capacity of the wind farm.

The annual cost of all calendar-based preventative maintenance, $C_{O,1}$ can be calculated using the following equation:

$$C_{O,1} = n_{CBM} \cdot c_{cv} \cdot \left(1 + \frac{d_p}{v_{cv} \cdot 3600 \cdot 24}\right) \tag{4.48}$$

Where n_{CBM} is the annual number of calendar-based maintenance events. This number has been extrapolated from the numbers given in table 4.5. The number of calendar-based maintenance events will depend on the number of wind turbines in the wind farm being investigated. c_{cv} is the daily rental cost of a crew vessel, v_{cv} is the speed of the crew vessel, and d_p is the average distance between the wind farm location and the nearest harbor.

The annual cost of all unplanned corrective maintenance events, $C_{O,2}$ can be calculated using the following equation:

$$C_{O,2} = \sum_{i=1}^{2} C_{O,2,i} \tag{4.49}$$

Where $C_{O,2,1}$ is the annual cost of all minor unplanned corrective maintenance events, and $C_{O,2,2}$ is the annual cost of all major unplanned corrective maintenance events.

The annual cost of all minor unplanned corrective maintenance events, $C_{O,2,1}$ can be calculated using the following equation:

$$C_{O,2,1} = n_{UCM} \cdot \min_{UCMpct.} \cdot c_{cv} \cdot \left(1 + \frac{d_p}{v_{cv} \cdot 3600 \cdot 24}\right) \tag{4.50}$$

Where n_{UCM} is the annual number of all unplanned corrective maintenance events, and $min_{UCMpct.}$ is the minor unplanned corrective maintenance events

as a percentage of the total unplanned corrective maintenance events.

The annual cost of all major unplanned corrective maintenance events, $C_{O,2,2}$ can be calculated using the following equation:

$$C_{O,2,2} = n_{UCM} \cdot \left(1 - \min_{UCMpct.}\right) \cdot c_c \cdot \left(1 + \frac{d_p}{v_{t1} \cdot 3600 \cdot 24}\right) \tag{4.51}$$

Where c_c is the daily rental cost of a crane, and v_{t1} is the speed of the crane.

The annual cost of renting the maritime state property, $C_{O,3}$ is calculated using the following equation:

$$C_{O,3} = \ell \times E_{anno} \times P_E \tag{4.52}$$

Where ℓ is the percentage of the wind farm revenue that will be paid as the rent of the maritime property, E_{anno} is the annual energy production, and P_E is the price the wind farm will be able to sell the produced energy for. This price is the average price of electricity paid by Norwegian households the past 10 years, SSB (2022).

The annual cost of insurance, $C_{O,4}$ is calculated as follows:

$$C_{O,4} = c_{O,4} \cdot n_T \cdot p_T \tag{4.53}$$

Where $c_{O,4}$ is the insurance cost per installed MW of power capacity at the wind farm, n_T is the number of wind turbines in the wind farm, and p_T is the rated power of one turbine. The rated power of one turbine varies with the type of wind turbine being used at the wind farm.

The final part of $C_{O\&M}$ is the cost of transmission, $C_{O,5}$. This cost can be calculated using the following equation:

$$C_{O,5} = c_{O,5} \cdot n_T \cdot p_T \tag{4.54}$$

Where $c_{O,5}$ is the cost of transmission per installed MW of power capacity at the wind farm.

Finally the total cost of O&M adjusted for inflation, assuming an average of 2 % inflation can be calculated as follows:

$$C_{O\&M} = \sum_{i=1}^{5} C_{O,i} \cdot WF_{LT}^{1,02} \tag{4.55}$$

Where WF_{LT} is the lifetime of the wind farm.

4.3.7 Claculation of LCOE

The last section of this chapter will look at how LCOE can be calculated from all the parameters previously discussed. To do that we have to start with LCC. As defined in chapter 2, LCC can be calculated with the following equation:

$$\text{LCC} = C_{\text{Dev}} + C_{\text{Manuf}} + C_{\text{IT}} + C_{\text{O\&M}} + C_{\text{Decom}} \tag{4.56}$$

Where C_{Dev} is the average cost of development, C_{Dev_avg} found in table 4.1, C_{Manuf_avg} is the average cost of manufacturing found in table 4.1 added with the manufacturing cost of moorings, C_m that was calculated in section 4.3.2, The cost of installation, C_{IT} is the sum of $C_{IT,1}$, $C_{IT,2}$, $C_{IT,1}$, $C_{IP,1}$, $C_{IP,1}$, $C_{IP,1}$, $C_{ITS,1}$, $C_{ITS,2}$, $C_{ITS,3}$, $C_{ITS,4}$, $C_{ITS,5}$, and C_{IMA}, the cost of operation and maintenance, C_{OM} is the sum of $C_{O,1}$, $C_{O,2}$, $C_{O,3}$, $C_{O,4}$, $C_{O,5}$, and finally the cost of decommissioning, C_{Decom}, is the average cost of decommissioning found in table 4.1, C_{Decom_avg}. To account for the time-value of money, these costs has to be split into initial investments and operating expenditure.

The initial investment, I, includes development costs, manufacturing costs, installation and transportation costs, and decommissioning costs. The initial investment can be calculated by combining equations derived in the previous sections as follows:

$$I = \sum_{i=1}^{3} C_{IT,i} + \sum_{i=1}^{3} C_{IP,i} + \sum_{i=1}^{5} C_{ITS,i} + C_{IMA} + C_{fix} \tag{4.57}$$

From here we can derive an equation for LCC that accounts for the time-value of money:

$$LCC = FRC \cdot WF_{LT} \cdot I + C_{O\&M} \tag{4.58}$$

Where I is the initial investment, WF_{LT} is the wind farm lifetime, and FRC is the fixed charge rate, and can be calculated using the following equation:

$$FRC = \frac{r \cdot (1+r)^{WF_{LT}}}{(1+r)^{WF_{LT}} - 1} \tag{4.59}$$

Where r is the real discount rate, which is typically set to 6 % for Norwegian energy infrastructure projects, according to Buvik et al. (2019).

From here we can finally define an equation for LCOE as:

$$LCOE = \frac{LCC}{E_{month} \cdot 12 \frac{months}{year} \cdot WF_{LT}} \tag{4.60}$$

Where E_{month} is the average expected monthly energy production of a wind farm, derived in equation 4.1, in section 4.2, and WF_{LT} is the expected lifetime of the wind farm, from the start of production, until the start of its decommissioning, given in years.

Following the steps described in this chapter one should be able to derive the same results as will be presented in the next chapter, where we will explore how variations in different parameters affects the LCOE of a wind farm, discuss the results for the four different locations that has been presented in the thesis, and explore how the results in energy production for these areas compare to that found in NVE's report, Sydness et al. (2012).

Chapter 5

Results

In the introduction of this thesis I stated four questions that I wanted to inquire for this master thesis. These were the following questions:

How is the levelized cost of energy (LCOE) affected by the distance to port, the number of wind turbines in a park, the wake effect, the water depth, capacity factor and the wind farm lifetime?

Can we add to the understanding that we have from research done by for example Myhr et al. (2014), and Shafiee et al. (2016) on how different parameters influence LCOE for offshore wind farms?

Can we improve our understanding of available resources for production of wind energy and are there areas better suited for wind farms than others regarding LCOE?

Are there any significant changes in the possible energy production in the different areas looked at by NVE when using the data from NORA3-WP?

I will in this section use the data and method presented in the previous chapters, to find results that can help answering these questions. I will start definging a reference wind farm that will be used in calculations of the results. Then, I will present results of how the parameters distance to port, the number of wind turbines in a park, the wake effect, the water depth, capacity factor, and the wind farm lifetime will affect the Levelized cost of energy (LCOE) of a wind farm. I will continue by looking into results for LCOE for each of the four locations, Utsira Nord, Stadthavet, Træna Vest and Frøyabanken. I will also look at how using a 6, 10, and 15 MW wind turbine will affect the LCOE at each of the four locations. Lastly, I will

Reference wind farm parameters

Parameter	unit	value
Distance to port	km	83
Distance from shore	km	46
Distance from transformer	km	58
Water depth	m	237
Floating platform		Spar buoy
Wind turbine		SWT-6.0-154
Number of substations		3
Number of wind turbines		250
Installed capacity	MW	1500
Capacity factor	%	45
Wake effect	%	10
minUCMpct.	%	98
Discount rate	%	6
Lifetime	years	20

Table 5.1: *The table show the reference wind farm used in this thesis. Parameters from this table is used in the wind farms presented in the results chapter.*

compare results of the energy production, and LCOE estimation for the four locations, with that found by NVE, Sydness et al. (2012).

To look at the effects on LCOE of the parameters previously stated, I must define some standard parameters of a wind farm. By doing this I can measure the effect of the change in one parameter, relative to the others. The standard parameters that I have decided to measure LCOE are presented in Table 5.1.

The standard parameters presented in Table 5.1 will be used in calculations of all results presented in this chapter, unless otherwise stated. The distance from transformer, harbor and shore in Table 5.1 is the average distances of the four locations that is being investigated in this thesis. The water depth and capacity factor in Table 5.1 are also the average of the values found within the four wind farm locations. I have chosen the spar buoy platforms (SB) as the standard floating platform as it is the most familiar floating platform in the Norwegian floating wind industry, as it is used by Equinor in multiple projects, Equinor (2022a), Equinor (2022b). The SWT-6.0-154 turbine was chosen as the standard wind turbine as it is currently the only

commercially available turbine out of the three being investigated in the thesis. The total power capacity of 1500 MW for the wind farm was chosen to match the maximum power capacity investigated in NVE's report, Sydness et al. (2012). From the turbine's 6 MW rated power and the total wind farm power capacity, a total of 250 turbines was calculated to be needed. The number of substations was set to three to handle the power capacity of 1500 MW, Catapult Offshore Renewable Energy (2022). The wind farm lifetime was set to 20 years as this is a lifetime used in most academic papers about offshore wind farms. Finally, a parameter that will have a large effect on C_{OM} is minor unplanned corrective maintenance events, $min_{UCMpct.}$, as a percentage of the total unplanned corrective maintenance events. For the standard wind farm, I have chosen this to be 98 %. This decision is discussed in chapter 6.

Now that the standard parameters for wind farms being discussed in this thesis has been set, we can look at the LCOE of this standardized floating wind farm. By following the method described in the previous chapter, and using the parameters given in the table for the standard wind farm parameters we can calculate the LCOE of this wind farm to be 103 €/MWh. This is in line with that found by Maienza et al. (2020), of 100 €/MWh, and Ioannou et al. (2018), of 109 €/MWh.

In Table 5.2 we can see of how the total Life Cycle Cost (LCC) for the reference windfarm is distributed amongst the five cost categories. It is worth noting that the majority of the LCC comes from manufacturing, while C_{OM} takes up just over 15 % of the total costs. As we will see later, C_{OM} is a parameter that is heavily influenced by distance to harbor, and wind farm lifetime. It is therefore worth to keep in mind that with an increasing distance to harbor, and wind farm lifetime the C_{OM} will increase its total contribution to the wind farm LCC.

5.1 Effects of the wind farm parameters on LCOE

We have now established what results in terms of LCOE that the model for calculating LCOE presented in chapter 4, gives while using the reference wind farm. We will now investigate the change in LCOE with variations in the standardized parameters given for the reference wind farm. To do this,

Cost category	LCC (M€)
CI&T	767
CO&M	1 506
CManuf	7 268
CDecom	611
CDev	592

Table 5.2: *The table show how LCC is divided over the five cost categories that make up LCC. The results shown in this table is derived using the standard parameters for the reference wind farm found in Table 5.1*

one parameter found in Table 5.1 is changed, while the others remain unchanged as found in the table.

All results presented in this chapter will be discussed in chapter 6. The results will be presented in graphs where LOCE will be plotted against the changing parameter. LCOE will be displayed on the y-axis, and the respective parameter on the x-axis. The first parameter to be explored is variations in the distance to harbor. The results can be found in Figure 5.1.

In Figure 5.1 we can see how the LCOE increases from just under 100 €/MWh, to between 110 and 120 €/MWh for all three platform types. We can see how the Tension Leg Platforms (TLP). is increasing its LCOE faster with the changing distance, than the Spar Buoy platforms (SB) and the Semi-Submersible platforms (SSP). It is also worth noting that the SSP consistently has a lower LCOE at any given distance, than that of the SB.

The faster change in LCOE for the TLP can also be seen in Figure 5.2, where the percentage change in LCOE for each platform type can be seen. In this figure one can easily see which platform is the most affected by the change in distance to harbor, since all platforms are compared from 0 % change in LCOE, at 0 km from the harbor.

In Figure 5.3, I describe how LCOE is affected by change in water depth.

In Figure 5.3 we can see that SSP starts out as the platform with the best LCOE, but as the water depth gets deeper, the TLP overtakes as the platform with the best LCOE. This is reflected in Figure 5.4, where we can see that TLP has the smallest percentage change in LCOE with an increasing water depth.

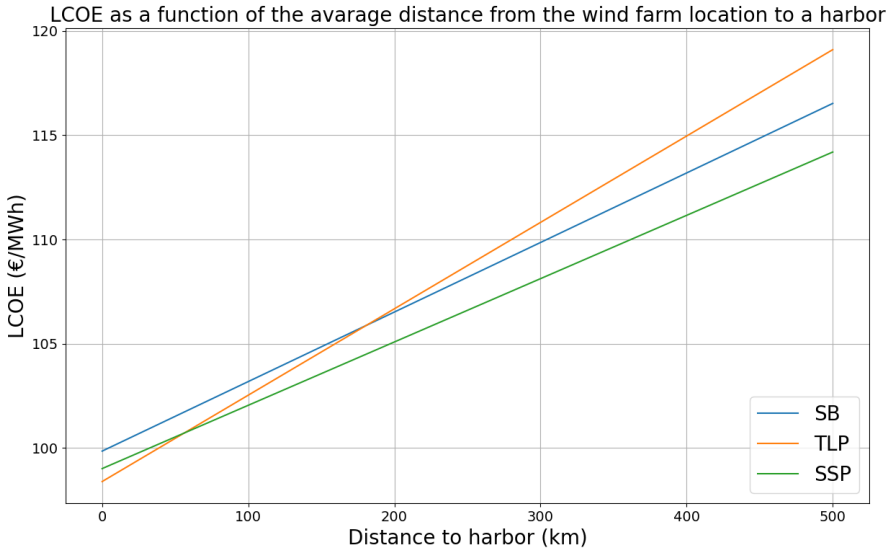

Figure 5.1: *The graph shows LCOE of a wind farm as a function of distance to the closest harbor. All other wind farm parameters than the distance to harbor used in the results in this figure can be found in table 5.1, which gives an overview of the reference wind farm. LCOE (€/MWh) is shown on the y-axis, while the distance to harbor (km) is shown on the x-axis. The graph displays the LCOE of three different wind farms, using the SB (blue line), the TLP (orange line), and the SSP (green line) as the floating platform.*

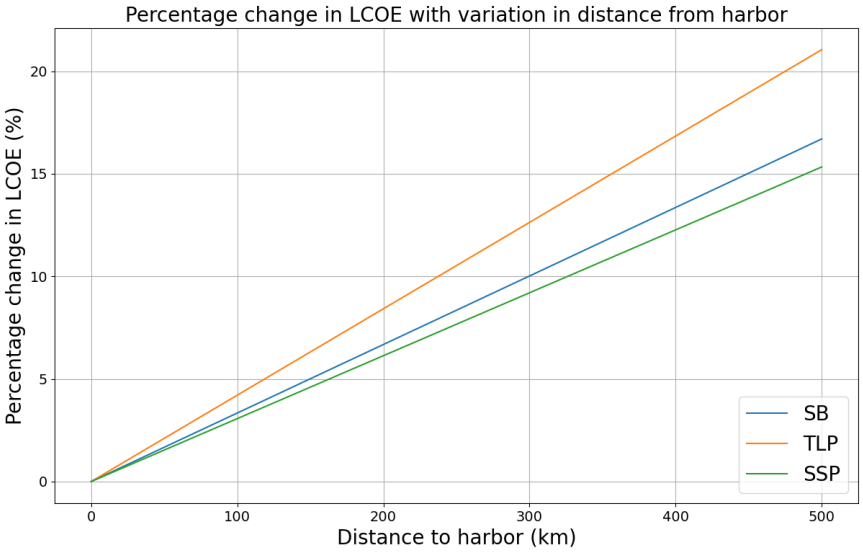

Figure 5.2: *The graph shows the percentage change in LCOE of a wind farm as a function of distance to the closest harbor. All other wind farm parameters than the distance to harbor used in the results in this figure can be found in table 5.1, which gives an overview of the reference wind farm. The percentage change in LCOE (%) is shown on the y-axis, while the distance to harbor (km) is shown on the x-axis. The graph displays the change in LCOE of three different wind farms, using the SB (blue line), the TLP (orange line), and the SSP (green line) as the floating platform.*

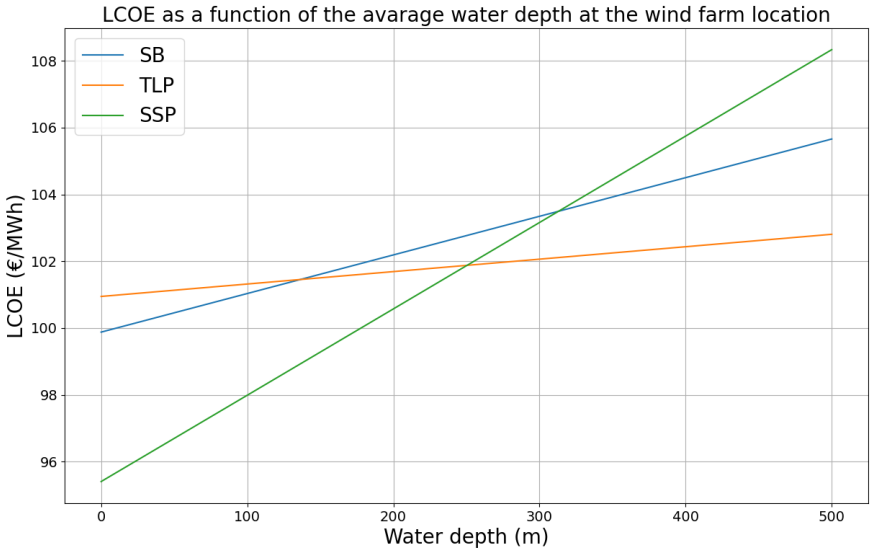

Figure 5.3: *The graph shows LCOE of a wind farm as a function of water depth. All other wind farm parameters than the water depth used in the results in this figure can be found in table 5.1, which gives an overview of the reference wind farm. LCOE (€/MWh) is shown on the y-axis, while the water depth (m) is shown on the x-axis. The graph displays the LCOE of three different wind farms, using the SB (blue line), the TLP (orange line), and the SSP (green line) as the floating platform.*

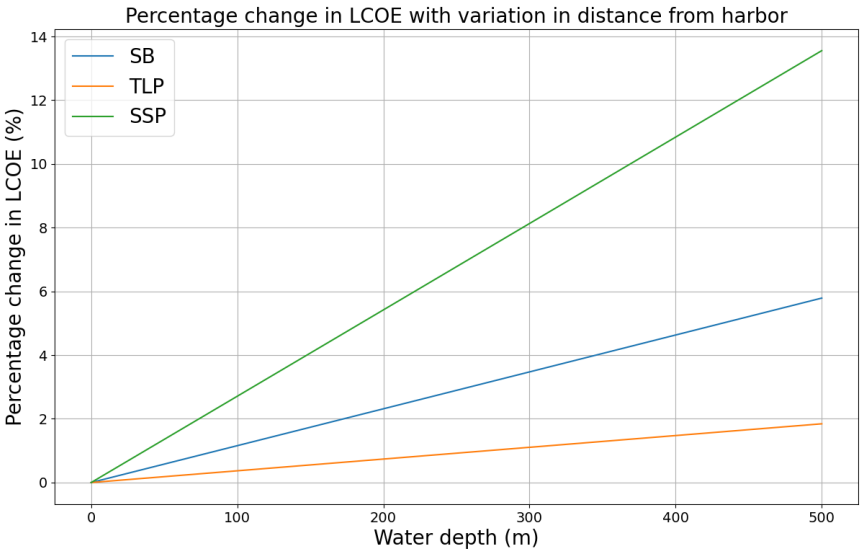

Figure 5.4: *The graph shows the percentage change in LCOE of a wind farm as a function of water depth. All other wind farm parameters than the water depth used in the results in this figure can be found in table 5.1, which gives an overview of the reference wind farm. The percentage change in LCOE (%) is shown on the y-axis, while the water depth (m) is shown on the x-axis. The graph displays the change in LCOE of three different wind farms, using the SB (blue line), the TLP (orange line), and the SSP (green line) as the floating platform.*

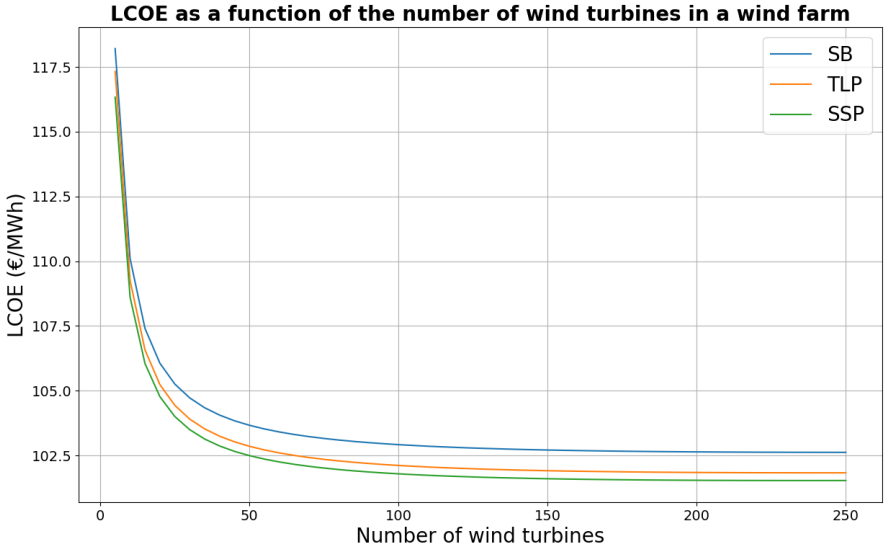

Figure 5.5: *The graph shows LCOE of a wind farm as a function of the number of wind turbines in the wind farm. All other wind farm parameters than the number of wind turbines used in the results in this figure can be found in table 5.1, which gives an overview of the reference wind farm. The exception is the total power capacity of the wind farm. This parameter also changes with the number of wind turbines in the results shown in the figure. LCOE (€/MWh) is shown on the y-axis, while the number of turbines is shown on the x-axis. The graph displays the LCOE of three different wind farms, using the SB (blue line), the TLP (orange line), and the SSP (green line) as the floating platform.*

We will now look at how the LCOE behaves with a lower number of turbines, without reducing the rated power of the turbines, and therefore decreased total power capacity for the wind farm.

From Figure 5.5, we can see that the increase in the total number of wind turbines in a wind farm contributes to reduce the LCOE of the farm. The effect is greatest until the wind farm reaches a size of about 50 wind turbines. Here the effect on LCOE starts to level off and stabilizes around 100 €/MWh.

Next, Figure 5.6 will give an overview of the change in LCOE caused by variations in a wind farm's wake effects.

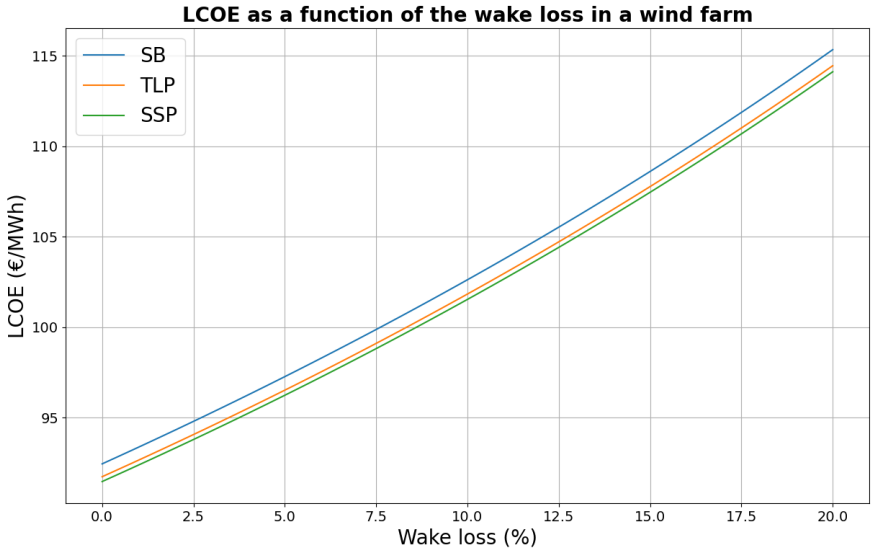

Figure 5.6: *The graph shows LCOE of a wind farm as a function of wake loss. All other wind farm parameters than the wake loss used in the results in this figure can be found in table 5.1, which gives an overview of the reference wind farm. LCOE (€/MWh) is shown on the y-axis, while the wake loss (%) is shown on the x-axis. The graph displays the LCOE of three different wind farms, using the SB (blue line), the TLP (orange line), and the SSP (green line) as the floating platform.*

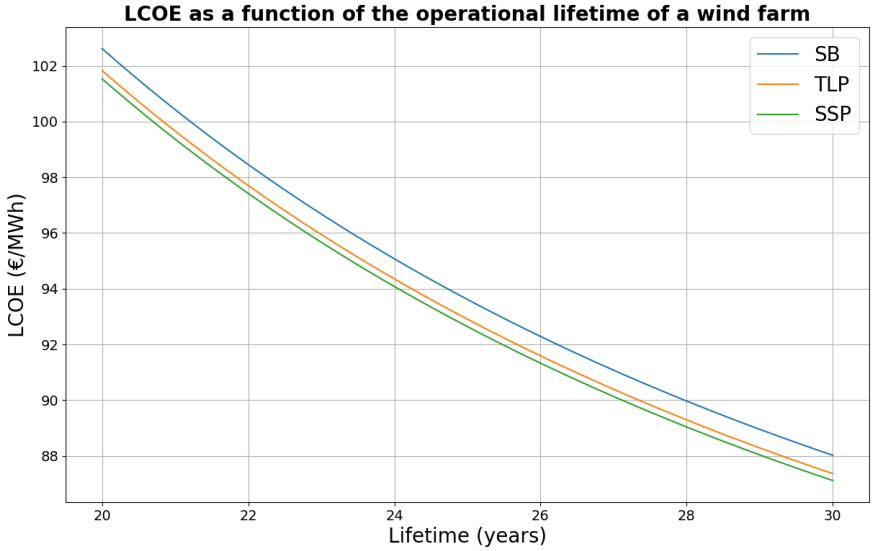

Figure 5.7: *The graph shows LCOE of a wind farm as a function of the wind farm's operational lifetime. All other wind farm parameters than the lifetime used in the results in this figure can be found in table 5.1, which gives an overview of the reference wind farm. LCOE (€/MWh) is shown on the y-axis, while the lifetime (years) is shown on the x-axis. The graph displays the LCOE of three different wind farms, using the SB (blue line), the TLP (orange line), and the SSP (green line) as the floating platform.*

As seen in Figure 5.6, an increase of the total wake effect of a wind farm affects the LCOE of the wind farm slightly exponentially, in positive direction. The LCOE moves from just under 95 €/MWh at 0 % wake loss, to about 115 €/MWh at 20 % wake loss.

Next, we will have a look at the effect of the wind farm's lifetime on LCOE. This is presented in Figure 5.7.

From Figure 5.7, we see that an increasing wind farm lifetime reduces the wind farm's LCOE. Here we can see that a wind farm with a lifetime of about 28 years and older brings the LCOE down to under 90 €/MWh, which is the lowest LCOE seen from all scenarios that has been investigated.

The result of the final wind farm parameter described in this chapter is how capacity factor affects LCOE. This can be seen in Figure 5.8.

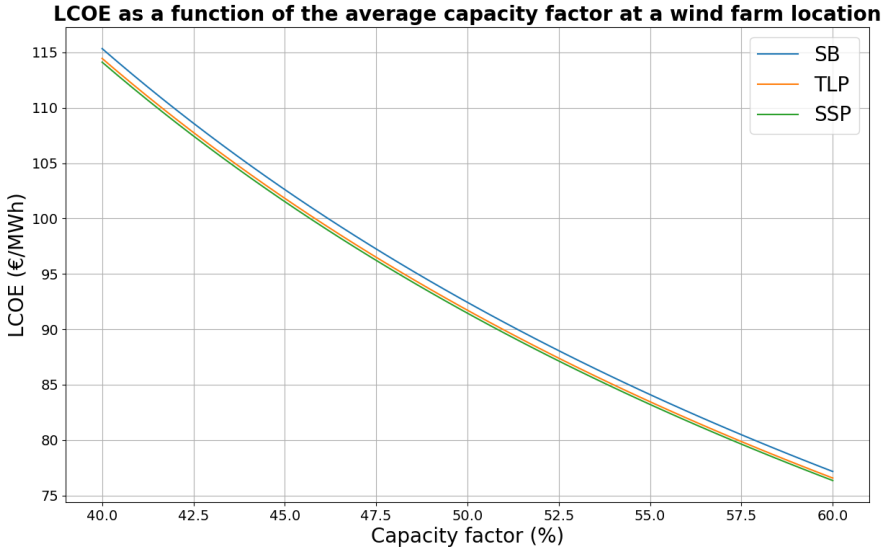

Figure 5.8: *The graph shows LCOE of a wind farm as a function of capacity factor. All other wind farm parameters than the capacity factor used in the results in this figure can be found in table 5.1, which gives an overview of the reference wind farm. LCOE (€/MWh) is shown on the y-axis, while the capacity factor (%) is shown on the x-axis. The graph displays the LCOE of three different wind farms, using the SB (blue line), the TLP (orange line), and the SSP (green line) as the floating platform.*

As seen, the capacity factor can bring the LCOE down under 80 €/MWh. Looking back at Table 3.1, in chapter 3, one can see that Stadthavet with a 15 MW turbine yields just over 60 % capacity factor, which is necessary to bring the LCOE under 80 €/MWh with the standard wind farm parameters defined in the beginning of this thesis in Table 5.1.

We have discussed the results how the LCOE of a wind farm is affected for three different floating platforms by changes in the parameters of the distance from a harbor, water depth, the total number of wind turbines, wake effect, capacity factor and the change in the wind farms lifetime. To get a even better understanding of what parameters that has the greatest effect on the LCOE they will be presented together in a single graph shown in Figure 5.9. In this graph the percent change in LCOE is shown, compared with a normalized change in the distance from the nearest harbor, water depth, to-

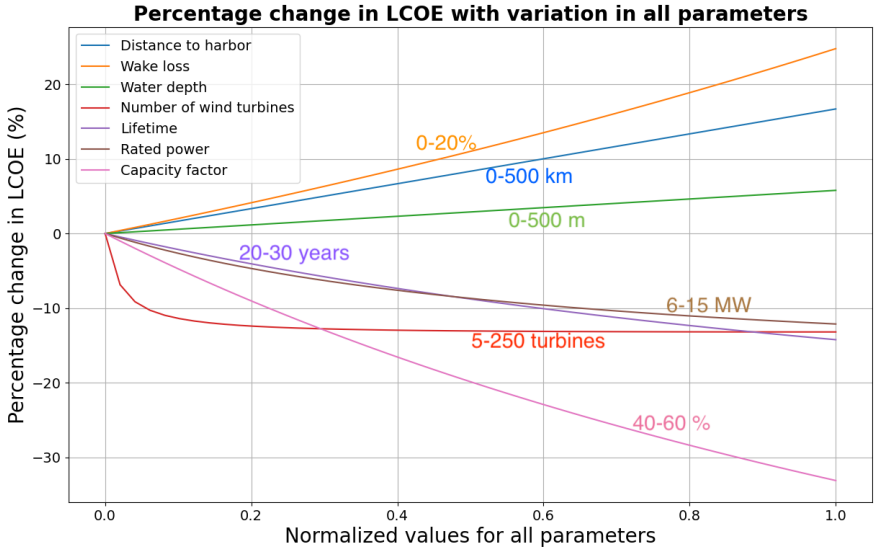

Figure 5.9: *The graph shows the percentage change for LCOE when changing the values of the wind farm parameters: number of wind turbines in the wind farm (red), the average distance from the wind farm location to a harbor (blue), the average depth at the wind farm location (green), the total wake loss in a wind farm (orange), the operational lifetime of the wind farm (purple), and the average capacity factor in a wind farm (pink). All values have been normalized so that 0 represents the smallest value and 1 represents the greatest value on the x-axis. All values written on the graph next to a line of the same color, represents the change in that parameter's native unit from 0 to 1 on the x-axis. This figure can be found in the attachments where it appears rotated, so it is easier to see all the lines.*

talt number of wind turbines, wake effect, capacity factor and the change in the wind farms lifetime. The change in the parameters has been normalized so that the lowest value shown in the above graphs (Figure 5.1, 5.3, 5.7, 5.8, 5.5, and 5.6) for the respective parameter will be equal to zero, while the greatest value will be equal to 1. That will be 5-250 for the number of wind turbines, 20-30 years for the lifetime, 0-500 km for the average distance to a harbor, 0-500 m for the average depth at location, 0-20 % energy loss for the wake effect, and 40-60 % average capacity factor at the wind farm location.

A rotated version of Figure 5.9 where the lines are easier to see can be found in the attachments. When looking at the graph in Figure 5.9, it is important

to note that the values chosen to be normalized for each wind farm parameter could have been chosen for any amount of change in the parameter value. For example, in Figure 5.9 distance to harbor is shown with less effect on the percentage change for LCOE, than the wake loss. However, the effect of distance to harbor on LCOE could have been greater than the wake loss, if the distance from harbor was normalized for a greater distance, for example 0 to 1000 km. One should therefore be cautious to draw conclusions about effects of different parameters on LCOE relative to each other, based on the graph in Figure 5.9.

5.2 Locations

Now that we have shown how much the different parameters affect the LCOE of a wind farm, we can start investigating the four different locations that were presented in chapter 3. All of the four locations will be presented with the distance-, depth-, and capacity factor values presented in Table 3.1 in chapter 3. All other values that have been presented as variable parameters in chapter 5 will be designated the standard values presented in Table 5.1 for all four locations. The locations will be displayed showing LCOE as a function of the wind farm lifetime. The three wind turbine types SWT-6.0-154, DTU-10.0-Reference, and IEA-15-240-RWT will be presented for all four locations. The locations will be shown in the order from highest to lowest LCOE. All scenarios presented represents a wind farm with a 1500 MW power capacity. The results can be seen in Figure 5.10.

A rotated version of Figure 5.10 where the lines are easier to see can be found in the Appendix B. From Figure 5.10, there are a few things to note. firstly, the impact on LCOE of the wind turbine chosen, secondly, the effect on LCOE from the location itself.

When it comes to the power capacity, one can see the great impact choosing a wind turbine with a greater power capacity has on the LCOE of the wind farm. Looking at the solid blue line, representing 250 turbines with a power capacity of 6 MW at Utsira Nord, the LCOE starts at just under 100 €/MWh for a 20-year lifetime, while the solid green line also representing Utsira Nord, but with 100 turbines of 15 MW power capacity starts just under 70 €/MWh for a 20-year lifetime. Therefore, an increase from 6 MW turbines to 15 MW turbines will contribute to decrease LCOE with about 30 €/MWh. This is mainly due to the increased capacity factor with the

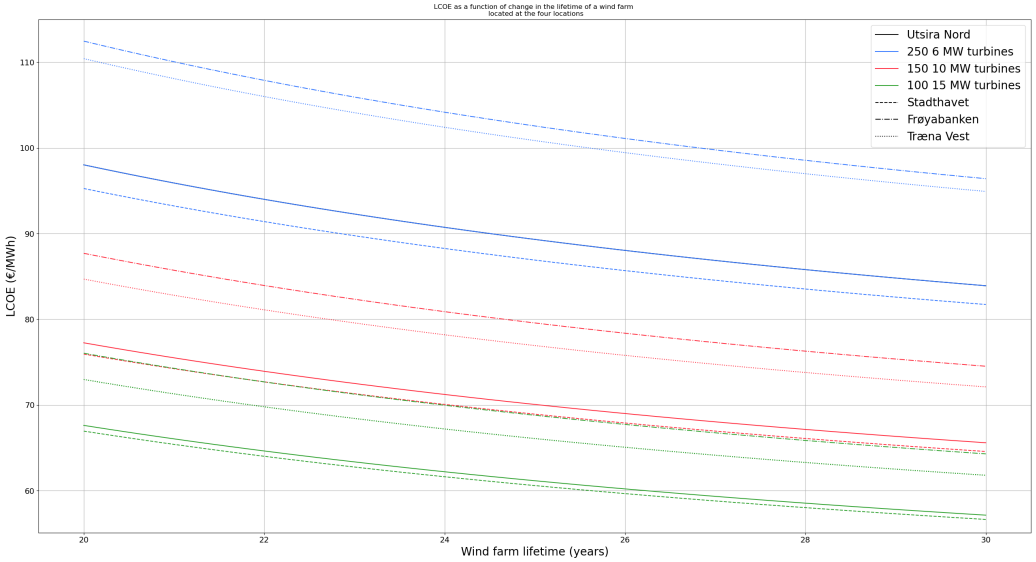

Figure 5.10: *The graph in this figure shows LCOE as a function of the lifetime of a wind farm between 20 and 30 years. In this figure all the four locations that has been investigated in this thesis is presented. Utsira Nord is presented as solid lines, Stadthavet is presented as dashed lines, Frøyabanken is presented as dash-dot lines, and Træna Vest is presented as dotted lines. Each location is presented as a wind farm with 250 6 MW turbines, 150 10 MW turbines, and 100 15 MW turbine. For all locations the 6 MW turbines are colored blue, the 10 MW turbines are colored red, and the 15 MW turbines are colored green. This figure can be found in the Appendix B where it appears rotated, so it is easier to see all the lines.*

increased turbine size. This can be seen in Table 3.1.

Further, increasing the lifetime of a wind farm will reduce the LCOE of the windfarms with about 10 to 15 €/MWh. Therefore, trying to increase the lifetime of the wind farm can also be an important contributor to reducing a wind farm's LCOE.

Lastly, looking at the different locations that is represented by different colors in Figure 5.10. For each color there are four lines with Utsira Nord represented by solid lines, Stadthavet represented by dashed lines, Frøyabanken represented by dash-dot lines, and Træna vest represented by dotted lines. These four lines show that the location chosen for the wind farm has a great impact on the LCOE of the wind farm. We can also note that the four locations can be devided into two groups, Utsira Nord and Stadthavet in group 1 and Frøyabanken and Træna Vest in group 2. Here we can see that group 1 has a considerably lower LCOE than group 2. This pattern can be seen for all three turbine types. Looking at the four blue lines, we can see that the order of the locations in terms of high to low LCOE is Frøyabanken, Træna Vest, Utsira Nord, and Stadthavet. Figure 3.12, showed the variability in capacity factor between the turbine types for each location, where the result showed that the order of locations from low- to high-capacity factor was Frøyabanken, Træna Vest, Utsira Nord, and Stadthavet. Lastly, we can note that Træna Vest is on average about 60 km further from the nearest harbor than Frøyabanken, and it has on average of about 60 meters deeper waters than Frøyabanken. These factors should contribute to a lower LCOE for Frøyabanken than Træna Vest. Despite this, Træna Vest has a lower LCOE than Frøyabanken for all turbine types. This is the result of the greater capacity factor at Træna Vest, and will be discussed further in the next chapter.

5.3 Comparisons with the findings in the NVE reports

Having looked at the results for how the LCOE looks for the four locations, we can now compare the findings with what was found by NVE, Sydness et al. (2012). In Table 5.3, results found in this thesis is compared with the results found by Sydness et al. (2012). For easier visualization of the comparison, the results found in Table 5.3 can be seen in Figure 5.11, 5.12, and 5.13. The results include capacity factor, and annual energy production

	Utsira Nord		Stadthavet	
	NVE	This thesis	NVE	This thesis
Capacity factor (%)	47	46	48	49
Annual energy production (GWh)	6210	6096	6348	6402
LCOE deviation from mean (%)	-9	-4,3	-7,0	-8,8
LCOE (€/MWh)		98		93,4
	Frøyabanken		Træna Vest	
	NVE	This thesis	NVE	This thesis
Capacity factor (%)	42	41	44	43
Annual energy production (GWh)	5508	5358	5615	5598
LCOE deviation from mean (%)	5,0	8,8	2,0	4,2
LCOE (€/MWh)		111,4		106,7

Table 5.3: *The table compare results from the NVE report by Sydness et al. (2012) with results found in this thesis. The loactions Utsira Nord, Stadthavet, Frøyabanken, and Træna Vest is compared in the table. The results of capacity factor (%), calculated annual energy production (GWh), and deviation from mean LCOE (%) is shown. For the NVE report, mean LCOE refers to the mean LCOE of all the 15 locations that has been investigated in their report, which includes Utsira Nord, Stadthavet, Frøyabanken, and Træna. The mean LCOE in this thesis is the mean LCOE of Utsira Nord, Stadthavet, Frøyabanken, and Træna. In addition, the LCOE (€/MWh) found for each location in this thesis is included in the table.*

for the four locations. It also includes a percentage deviation from the mean LCOE of all locations. For the results found in this thesis the mean LCOE is a mean of the four locations. For the results presented in the NVE report, Sydness et al. (2012), the mean LCOE is a mean of 15 locations that was investigated in their report. All the four location investigated in this thesis, Utsira Nord, Stadthavet, Frøyabanken, and Træna Vest, are included in the NVE report, Sydness et al. (2012). Hence, they have not presented the values found for LCOE in €/MWh, only a deviation from the mean LCOE as a percentage. That is the reason why the LCOE found by NVE is not presented in €/MWh in Table 5.3.

The results described in this thesis is based on the calculations of 6 MW wind turbines, and the SB floating platforms. The 6 MW turbine is used as, Sydness et al. (2012) also used a 6 MW turbine in their calculations.

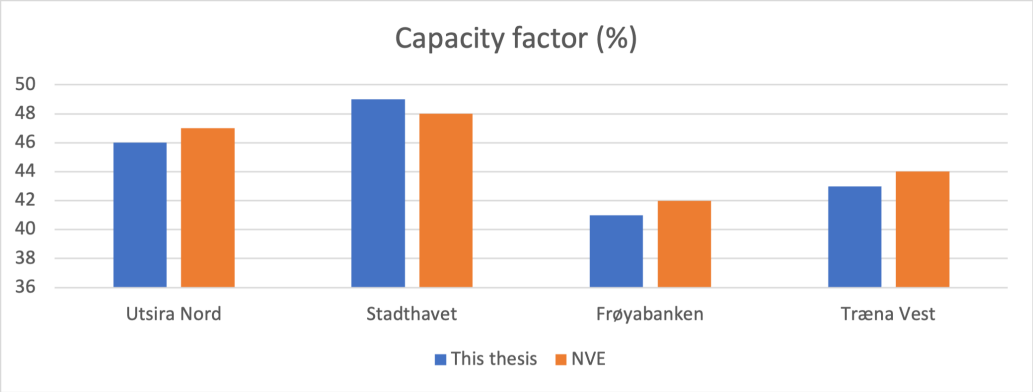

Figure 5.11: *The clustered column chart compares the capacity factor found in the NVE report, Sydness et al. (2012), with that found when using the dataset NORA3-WP. The results are shown for the four locations: Utsria Nord, Stadthavet, Frøyabanken, and Træna Vest. The results are shown using a 6 MW turbine. The capacity factor is given in percent (%) on the y-axis. The blue columns represent results from the NVE report, while the orange columns represent results found in this thesis.*

5.3.1 Capacity factor comparison

Starting with the capacity factors for each location found by NVE, we can see that it only deviates by one percentage point for all four locations, when comparing to the capacity factor used in this thesis, which was found using the NORA3-WP dataset. For Stadthavet, NVE uses a lower capacity factor, than used in this thesis, while for the remaining three locations, NVE uses a larger capacity factor than that of this thesis. This is most likely due to differences in the datasets used in this thesis, and the dataset used by NVE.

5.3.2 Annual energy production comparison

The annual energy production is calculated for a wind farm with a 1500 MW power capacity for both this thesis and NVE. The energy production found by NVE is, like with the capacity factor, also very similar to that found in this thesis. The greatest deviation is found at Frøyabanken where NVE calculated a production of 150 GWh more energy produced each year. The smallest deviation was found at Træna Vest where NVE calculated a production of 17 GWh more energy produced each year. We can also see that the same pattern is found for the energy production, as the capacity factor, with

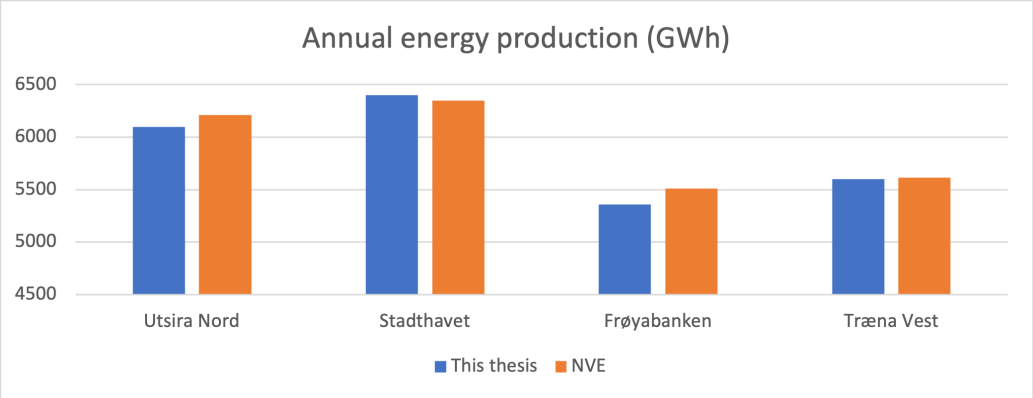

Figure 5.12: *The clustered column chart compares the annual energy production found in the NVE report, Sydness et al. (2012) with that found when using the dataset NORA3-WP. The results are shown for the four locations: Utsria Nord, Stadthavet, Frøyabanken, and Træna Vest. The results are shown using a 6 MW turbine. The annual energy production is given in GWh on the y-axis. The blue columns represent results from the NVE report, while the orange columns represent results found in this thesis.*

Stadthavet being the only location with a higher energy production found in this thesis, than in the report by NVE.

5.3.3 LCOE deviation from mean comparison

When comparing the LCOE, it is not possible to compare it in terms of €/MWh, but the LCOE can be compared in percentage deviation from the mean LCOE amongst the locations. We can note that the NVE report has a smaller percentage deviation from the mean LCOE compared with three out of the four locations. Once again, we can see that Stadthavet is the outlier, with a higher value for the percentage deviation found in the NVE report, Sydness et al. (2012), compared with this report. This is probably linked with the higher energy production found by this thesis for Stadthavet, that pulls down the LCOE more for Stadthavet than what was found by NVE. We can also note that Frøyabanken was found to have the highest LCOE out of the four locations. This was reported both NVE, and is also the results found and presented in this thesis. Træna Vest was found to have the second highest LCOE, both found by NVE and the results found in this theises. Stadthavet has been found to have the lowest LCOE, and Utsira Nord, the second lowest, based on the results presented in this theises. The

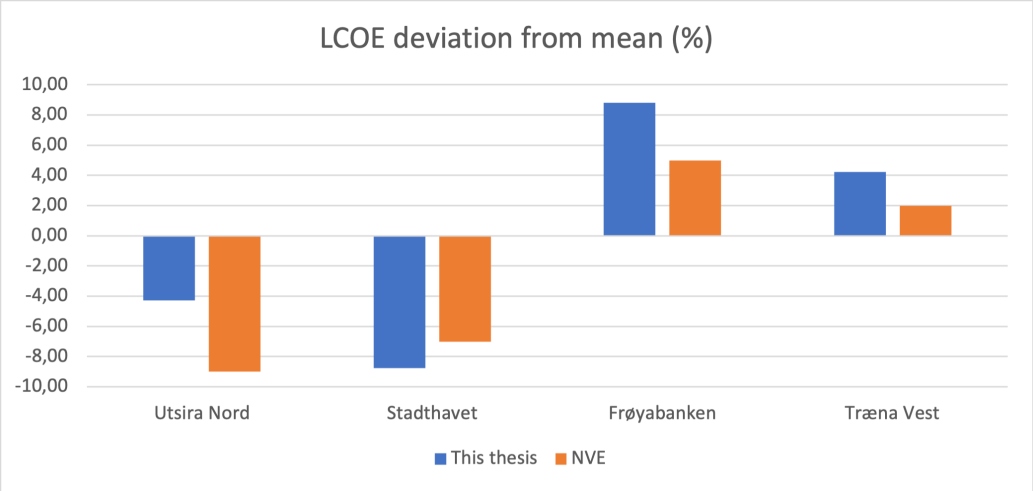

Figure 5.13: *The clustered column chart compares the deviation from the mean LCOE found in the NVE report, Sydness et al. (2012) with that found when using the dataset NORA3-WP. The results are shown for the four locations: Utsria Nord, Stadthavet, Frøyabanken, and Træna Vest. The results are shown using a 6 MW turbine. The deviation from the mean LCOE is given in percent (%) on the y-axis. The blue columns represent results from the NVE report, while the orange columns represent results found in this thesis.*

opposite was found by NVE with Utsira Nord being the location with the lowest LCOE, and Stadthavet with the second lowest LCOE. These findings will be discussed in the next chapter.

5.4 LCOE compared with Maienza et al. (2020)

Since a large part of the method used in this thesis is based on the method found in Maienza et al. (2020) it is useful to compare the results for the LCOE for each floating platform type, with the findings from their article. The comparison can be seen in Table 5.4.

In the comparison the same wind farm parameters used in Maienza et al. (2020) is used for the method of calculating LCOE in this thesis. This includes a water depth of 135 meters, a distance to shore of 16 km, a distance to harbor of 165 km, and 25 wind turbines in the wind farm. Any other parameters are used as described in Table 5.1, where the standardized pa-

LCOE comparison with Maienza et al.

	Maienza et al.	This thesis
TLP	106,7	106,35
SB	94,17	105,63
SSP	91,97	102,35

Table 5.4: *The table compare results of the LCOE calculation from Maienza et al. (2020) with results found in this thesis. The Three floating platform types of SB, TLP, and SSP is compared in the table. The LCOE is given in €/MWh. The table compares the LCOE of a wind farm with the same parameters used by the reference wind farm found in Maienza et al. (2020)*

rameters for the reference wind farm used in this thesis can be found.

As seen in Table 5.4, the LCOE found in both Maienza et al. (2020) and this thesis, for each of the floating platforms can be ranked from high to low as the TLP, the SB, and the SSP. For Maienza et al. (2020) a larger variation for the LCOE between the floating platforms is found, ranging from 91,97 to 106,70 €/MWh, while for LCOE found with the method used in thesis the range goes from 102,46 to 106,35 €/MWh.

The results presented in this chapter show how different parameters affect the LCOE of a wind farm. They also show differences in LCOE between four different locations, using three different wind turbines. This was done by using a method for life cycle cost analysis developed through the work with this thesis. The results also show whether there were any changes in the possible energy production of that found by NVE, when using the open-source dataset NORA3-WP. As we could see in the results there were some differences, and in the following chapter this will be discussed.

Chapter 6

Discussion

By now we have seen how one can calculate the levelized cost of energy (LCOE) for a wind farm, and how variations in different parameters of the wind farm affect the LCOE of the wind farm. We have also seen the results of these calculations used on some potential locations for wind farms along the Norwegian sea, and what the LCOE of these wind farm could potentially be in different scenarios.

In this chapter I want to discuss the method used to calculate LCOE in this thesis, and the assumptions that was made to do those calculations. I also want to discuss the results presented in the previous chapter and see how they compare to other research done in the same area.

6.1 Discussion of assumptions

To inquire the goal, I will start by discussing the assumptions made in chapter 4. I will go through each of the assumptions in the same order as listed in chapter 4. Starting with the 1st assumption that there has been no loss of power in the cables of the wind farms. We can discuss this assumption by looking at the effect it would have made on LCOE, if the power loss from the cables had been calculated. Power loss from cables can be compared to the power loss from wake loss. Each percentage point of power loss in the cables would have the same effect on the energy production, as each percentage point of wake loss. Looking at figure 5.6, which gives an overview of the effect of wake loss on LCOE, we can see that a 1 % increase in the wake loss increase the LCOE by approximately 1 €/MWh. This is the effect we could have expected, had power loss in the cables not being neglected. Therefore,

a power loss of 1,8 % as used by Myhr et al. (2014) would have a small effect on the LCOE.

The 2nd assumption stated that power loss from wake effects is 10 %. This number comes from looking at the assumed wake loss in other articles, where the wake loss in Maienza et al. (2020) was set to 5 %, Myhr et al. (2014) set it to 7 %, and Skeie et al. (2012) set to between 6 and 13 %. I therefore decided that 10 % was a reasonable number to round to when setting up the parameters for a standard wind farm.

The 3rd assumption was to simplify mooring line length calculations. After a literature search regarding mooring line length calculations, it was found difficult to find the most appropriate calculation for each floating type's mooring line lengths. Therefore, it was decided that due to the complexity of the calculations, a simplification would be appropriate. This task should be persuaded in further research. The simplification assumes a constant angel between the water surface and the mooring lines, regardless of the water depth. To account for the increasing slack that the mooring lines would experience in a real world, the mooring lines length has been multiplied by 1,2 to increase the length by 20 %. This is only done for the moorings of the SB and the SSP, as the TLP's moorings is at a 90 degree angle. When looking at the effects of mooring line length on LCOE, using the method outlined in this thesis, the change in LCOE is 3 €/MWh per 1000 meters of longer mooring lines. This means that even if the approximation is wrong, it will not have a remarkable effect on the LCOE.

The 4th assumption was that O&M would be carried out equally throughout the different seasons of the year. The effects of this assumption on the LCOE is unknown, but it is reasonable to assume that carrying out maintenance throughout the year, as assumed in this thesis, will increase the LCOE of the wind farm compared to a scenario where maintenance is mostly carried out in the summer months. This is because the summer months on average has lower wind speeds and therefore carrying out maintenance in the summer months would compromise less of the total energy production, thereby allowing the wind farm to produce more total energy, and thus decrease the LCOE of the wind farm. The assumption of equal maintenance throughout the year was made to simplify the process of calculating the total energy production of the wind farm.

The 5th assumption states that the mooring costs make up 3 % of the total

manufacturing costs. To be able to see the effect of lengthening mooring lines with deepening waters on LCOE, the manufacturing costs of mooring lines had to be a variable dependant on water depth. I therefore looked at the total cost of manufacturing mooring lines in Maienza et al. (2020). This cost was found to be 3 % of the total manufacturing cost in their article. I therefore assumed that this would apply to the method of calculating costs in this thesis as well.

The 6th assumption states that the maintenance work on cables would take 24 hours to complete. The description regarding how maintenance work is carried out that the method outlined in this thesis is based on is found in Bjerkseter and Ågotnes (2013). In this article maintenance work performed on a wind turbine is described to take an average of 24 hours. No description was given for the cables, and therefore the time was assumed to be equal to that of the wind turbines.

6.2 Discussion of the method

6.2.1 Choice of cost categories to impact LCOE

The method for calculating the Life Cycle Cost (LCC) for wind farms in this thesis is based on how changes in parameters regarding the wind farm affect the cost of installation and transportation and the cost of operation and maintenance. I want to discuss why these two cost categories was chosen as the main cost categories to impact variations in LCOE.

One of the objectives of the thesis is to investigate how wind farm parameters such as the distance to a port, the number of wind turbines in a farm, the wake effect, the water depth, the capacity factor, and the wind farm lifetime would affect the LCOE of a wind farm. I also wanted to investigate how three different platform types and three wind turbines of different power capacity would affect the LCOE. Out of these parameters the wake effect, and the capacity factor are two parameters that does not affect the cost side of the LCOE equation, but rather the total energy production side of the LCOE equation. The remaining parameters will affect the cost categories by varying degrees. How each parameters affect LCOE will be discussed further in the following sections.

When starting to write this thesis I hypothesized that the cost of installation

and transportation and the cost of operation and maintenance would be the two categories that would be the most affected by changes in the distance from a harbor, and the water depth. These are the two wind farm parameters that are directly impacted by the location of the wind farm, and at the same time influences the cost of building the wind farm. One could also argue that the cost of decommissioning is just as much a function of the distance from a port, as the cost of transportation and installation and the cost of operation and maintenance. However, the removal of a structure is generally a much less complex operation, than the installation of that same structure. Therefore, I hypothesized that the decommissioning of a wind farm would be more or less the same job, regardless of the specifications of the wind farm. Due to this line of thought it was decided to simplify the calculation of the cost of decommissioning by not looking into how parameters such as distance to a harbor, or water depth would affect this cost. However, this decision does affect the accuracy in the results regarding how much the distance to a harbor, or the water depth affect the LCOE off a wind farm.

When it comes to the number of wind turbines in a wind farm, this number does affect all cost categories. However, Wind turbines with larger power capacity has generally not been manufactured in large quantities yet and therefore the cost benefit of producing fewer turbines when choosing a larger turbine type would arguably be eaten up by the increased cost of this technology. Therefore, it was thought that simplifying the cost of manufacturing to only be affected by the total power capacity of the wind farm, rather than also the number of wind turbines in that wind farm, would be a reasonable simplification.

At the time of writing this thesis there has never been built floating platforms for wind turbines at a large scale. Therefore, the costs of manufacturing the different platform types is largely unknown. The same goes for the wind turbines where 10 and 15 MW turbines has never been built for commercial use. Because of this, looking into variations in the manufacturing costs due to different types of floating platforms and wind turbines has been neglected in this thesis.

At the time of writing this thesis there has never been built floating platforms for wind turbines at a large scale. Therefore, the costs of manufacturing the different platform types are largely unknown. The same goes for the wind turbines where 10 and 15 MW turbines has never been built for commercial use. Because of this lack of cost data for large scale production of floating

platforms for wind turbines, looking into variations in the manufacturing costs, due to different types of floating platforms and wind turbines has been neglected in this thesis.

6.2.2 Choice of supporting articles for the method used

This thesis has based a lot of its method on the work done by Maienza et al. (2020) for the C_{IT} and in Bjerkseter and Ågotnes (2013) for the C_{OM}. The main work in this thesis has been to build a cost model for offshore floating wind farms, with emphasis the effects on LCOE by change in various wind farm parameters. Since the change in these parameters would mainly come from the cost of installation and transportation, and operation and maintenance, a method for calculating these costs thoroughly was needed.

For calculating C_{IT} a very useful method was found in Maienza et al. (2020) that covered all the details needed for the investigations set out to be done in this thesis. The article covered cost calculations for the three floating platform types that was to be discussed in this thesis. At the same time, it included the effects from parameters such as the number of wind turbines in the wind farm, the distance from a harbor, and the water depth. Maienza et al. (2020) also got the values for most parameters used from Castro-Santos et al. (2018). Therefore, it was easy to find reliable values for all parameters, such as vessel speeds, and vessel day rates. For these reasons, it was decided to use the method from Maienza et al. (2020) for the calculation of C_{IT}.

For the calculations of the C_{OM} it was harder to find a method that could be replicated. Maienza et al. (2020) could be replicated to a certain degree, but a large amount of their work used a method which relied on statistics, of how often various wind turbine components would break down. The statistical calculations of the maintenance operations needed for the method used by Maienza et al. (2020) has not been replicated in because it would mean moving into a subject field outside the focus of this thesis. Another article by Bjerkseter and Ågotnes (2013) relied on a specialized software to calculate the C_{OM}. This article also included detailed description of how the operation and maintenance was carried out. It was therefore decided that based on the description by Bjerkseter and Ågotnes (2013), a method for calculating the C_{OM} would be built.

6.3 The results

6.3.1 Floating platform types

In the following part, I want to start by discussing the results regarding the three platform types, the Spar Buoy (SB), the Tension Leg Platform (TLP), and the Semi-Submersible Platform (SSP). The results for the three platforms can be seen in figures 5.1-5.8. As discussed earlier, the cost of manufacturing is not affected by the type of floating platform in the method used. This cost of installation and transportation is the only cost category that is affected by the platform type, which can be seen from the equations in chapter 4.

For variations in the wind farm parameters capacity factor, wind farm lifetime, turbine rated power, wake effect, and number of turbines in a wind farm, the most effective floating platform type, regarding LCOE, does not change. For all five parameters the SSP gives the lowest LCOE, then TLP gives the second lowest LCOE, while using the SB results in the highest LCOE for the wind farm.

The reason SSP is barely cheaper than the TLP for all other parameters is because 237 m water depth is used for the standard wind farm. Looking at Figure 5.3, one can see that this is the water depth just before TLP overtakes the SSP as the cheapest platform. The same goes for the distance to harbor, where 84 km is used for the standard wind farm. Looking at Figure 5.1, one can see that this is the distance just after the SSP overtakes the TLP as the cheapest platform.

For variations in water depth, and the distance from a harbor the most LCOE-effective floating platform type does change. Starting with the water depth, the SSP starts out as the most cost effective, but at around 250 m depth the TLP takes over as the most cost-effective floating platform. The SB is consistently more expensive than the TLP and the SSP for all water depths. The variations in the cost with water depth comes down to mooring lines specifications.

The cost of mooring lines, first referenced in section 4.3.2, where we can see that the SSP is the cheapest at shallow waters, but due to its six mooring lines made of steel chains at a cost of 250 €/m the cost increase faster than that of the SB and the TLP. The three steel chains of the SB and the eight fiber ropes at a price of 92 €/m of the TLP, comes out to a cost of about

750 €/m for both platforms. But since the SB moorings is at an angle, more meters of moorings are needed per meter of water depth compared with the TLP, who's moorings go straight down. The assumption of a 1,2 multiplier for the SP and the SSP to make up for the lack of slack in the moorings with the calculation of mooring line lengths also affect the LCOE to increase quicker for the SP and the SSP compared with the TLP.

When it comes to the distance from a harbor, this variation changes the TLP to go from having the lowest LCOE, to the highest LCOE at around 200 km, for all three platform types. The reason for this can be found in the equations for calculating the cost of transportation for the floating platforms, $C_{IP,2}$. Here we can see that in the equation used for the SB, tug and barge vessels are used for the transportation. However, for the TLP a floating crane is used for the transportation. The daily rental cost for the floating crane is about 800 000 €. For the barge it is about 35 000 € and for the tug it is about 22 000 €. With an increased distance to the harbor, and thereby increased time spent transporting, one can see how the costs add up quickly for the installation of the TLP. When it comes to the SSP it has no costs associated with the equation for calculating $C_{IP,2}$. The reasoning for this will be discussed next.

The method for calculation of C_{IT} presented in Maienza et al. (2020) which is used in this article assumes that when installing the wind turbines while using the Semi-Submersible Platform type, the wind turbine will be installed onto the platform at the harbor. The platform will then be transported, already installed on the floating platform, to the location of the wind farm. This way all installation costs regarding the wind turbine, is baked into the costs regarding the floating platform when it is calculated. This includes the cost of the port procedure, $C_{IT,1}$, the cost of transportation, $C_{IT,2}$, and the cost of installation at sea, $C_{IT,3}$, and all three costs therefore equal to zero. However, the cost of transportation, $C_{IP,2}$, and installation at sea, $C_{IP,3}$ for the floating platform is also baked into the cost of the port procedure, $C_{IP,1}$ for the SSP, according to one of the co-authors of the Maienza et al. (2020), Francesco Ricciardelli. Ricciardelli explained that "*Accordingly, the installation cost shares $C_{IP,2}$ and $C_{IP,3}$ for SSP are directly included in the cost share $C_{IP,1}$*" (personal correspondence, 30.01.22), when asked about the $C_{IP,2}$ and $C_{IP,3}$ for the SSP. This means the entire cost of the installation and transportation of wind turbines and floating platforms for the SSP is included in the cost of the port procedure, $C_{IP,1}$.

While the SSP can be transported and installed as one structure at the wind farm, the SB and the TLP must be carried to the installation site without wind turbines, and then have the turbines transported and installed at sea. This significantly reduces the cost of transportation and installation for the wind farms using SSP, and thereby reducing the LCOE for those wind farms.

6.3.2 Effects of $C_{O\&M}$ on the results

A large part of the $C_{O\&M}$, as it has been calculated in this thesis, comes from the cost of unplanned corrective maintenance, which was divided into the sub-categories minor- and major- unplanned corrective maintenance. The ratio of this division has the potential to have large effects on the LCOE of a wind farm. The ratio describes the number of minor unplanned corrective maintenance (UCM) events, as a the percentage of the total number of UCM events, called $min_{UCMpct.}$. The reason this affects the total LCOE, is because in major UCM events, a crane is used to do the maintenance, while for the minor UCM events only a crew vessel is needed. The day rate for a crane is about 800 000 €, while it is 2 500 € for the crew vessel. Because UCM makes up the majority of the maintenance events, and because $C_{O\&M}$ is the second largest cost category, an increase in the total number of major UCM events will have a large effect on the LCOE. The ratio has been set to 98 % minor UCM events for all cases discussed in this thesis. But having a look at Figure 6.1, the impact on LCOE by a change in this ratio can be seen.

Here the change in ratio is shown from 95 to 100 % minor UCM events of the total number of UCM events, for a standard wind farm as defined in this thesis. One can clearly see how this ratio affects the LCOE of the wind farm, decreasing the LCOE by more than 20 €/MWh for a 5 % increase in the ratio. The ratio was set to 98 % in this thesis, as having one major UCM event out of every 50 events seemed reasonable. However, this ratio is set at 98 % based on subjective reasoning for a reasonable ratio value. When looking at the LCOE found for different wind farms in this thesis, this should be kept in mind.

6.3.3 Effects of wind farm parameters on LCOE

In this section I will discuss how the wind farm parameters distance to a harbor, water depth, number of wind turbines in the wind farm, capacity factor, wake effect, and the wind farm lifetime, affects the LCOE of a wind

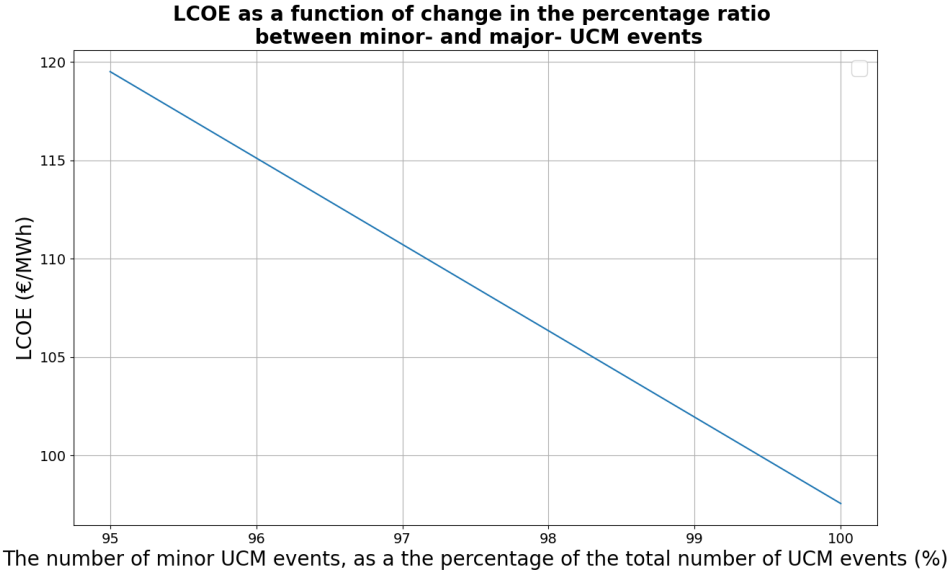

Figure 6.1: *The graph shows the LCOE of a wind farm as a function of* $min_{UCMpct.}$. $min_{UCMpct.}$ *Is defined as all minor unplanned corrective maintenance events as a percentage of the total number of unplanned corrective maintenance events. All wind farm parameters used in the results in this figure can be found in table 5.1, which gives an overview of the reference wind farm. LCOE (€/MWh) is shown on the y-axis, while the* $min_{UCMpct.}$ *(%) is shown on the x-axis.*

farm. For the distance to harbor, water depth, the number of wind turbines, and wind farm lifetime, Myhr et al. (2014) has done a similar investigation of how these parameters influence LCOE. I will discuss how the results found in this thesis, compares to that of Myhr et al. (2014).

Distance to harbor

Looking at Figure 5.1, we can see that an increase in the average distance of a wind farm location to a harbor, will increase the LCOE of a wind farm. Increasing the distance from 0 to 500 km will increase the LCOE with 15 – 20 €/MWh for the standard wind farm as it is defined in this thesis, depending on the type of floating platform that is used. Considering that the economic zone of a county stretches 370 km from shore, and there will usually not be a harbor directly at shore opposed to the wind farm, a wind farm a few hundred kilometers from a harbor is not outside the realm of possibilities, and therefor worth investigating.

Myhr et al. (2014) found an increase from 150 to 190 €/MWh for 100 to 500 km to a harbor for most platforms they looked at. This is an increased LCOE of about 26 %. This is double the percentage-wise increase in LCOE, which is found in my calculations to be about a 13 % increase from 0 to 500 km. It is hard to say what causes this difference of change in the LCOE. One factor could be the fact that the distance from a harbor was not included as a variable in the calculation of the cost of decommissioning. Generally large infrastructure projects have a lot of uncertainty connected to the calculation of the costs. This is even more so when it comes to floating wind farms, which has never been built at the scale which is being discussed. This uncertainty is arguably a large part of the difference that can be seen between this thesis and Myhr et al. (2014).

The increase in LCOE, that stems from an increase in the distance from a harbor can be found by looking at the equations found in chapter 4 used in this thesis. The distance is used as a variable in a multitude of equations. For the $C_{I\&T}$ it is used in the calculation of the amount of time spent traveling during the installation process. This way, an increased distance results in increased time spent, which increases the cost of installation and transportation. The distance to a harbor can also be found as a variable in the calculation of $C_{O\&M}$, in the equations used to calculate the cost of calendar-based maintenance events, and UCM events. An increase in the distance results in an increase in these costs leading to a raise of the total

$C_{O\&M}$. Further, an increase in $C_{O\&M}$ and $C_{I\&T}$ results in increased LCC in equation 4.60. In the fraction in equation 4.60, LCC is defined as the numerator, meaning an increase in LCC will increase the LCOE. Therefore, an increase in the distance from a harbor result in an increased LCOE.

Water depth

The results of how water depth impacts the LCOE of a wind farm can be seen in Figure 5.3. For wind farms using the SSP the increase in LCOE is 95 €/MWh to 108 €/MWh from 0 to 500 meters of water depth. On the other hand, the LCOE for a wind farm using TLP only increases from 101 €/MWh to 103 €/MWh for the same difference in water depth. As previously discussed, this difference comes from the different materials used in the moorings, the number of moorings per platform, and the smaller angel between the water surface and the moorings for the SSP and the SB, compared with that of the TLP.

When investigating effects of water depth on LCOE, Myhr et al. (2014) has some varying results for the different types of platforms, with large variations in LCOE with variations in water depth for some platforms they investigated, and little variation in LCOE for other platforms. However, we can note that four out of the six platform types investigated by Myhr et al. (2014) results in similar changes in LCOE of about 2 to 10 €/MWh over a depth spanning from 100 to 500 meters.

The contribution to increased LCOE from increased water depth can be found by looking at the equations of chapter 4. Here we see that in the C_{IT} water depth can be found as a variable in the equation for calculating the cost of installation of array cables, equation 4.41. The water depth can also be found as a variable in the equation for calculating the manufacturing costs of the moorings, equations 4.3, and 4.4. The impact of water depth on the cost of mooring manufacturing, and array cables can be seen in Figure 6.2.

As seen in Figure 6.2, most of the change in LCOE due to the water depth comes from the mooring costs. The cost of the moorings ranges from 0 € to over 30 million € at a 500 m water depth. On the other hand, the array cable contributes with an increased cost of about 12 million €.

Going back to the equations, array costs are part of the equations for $C_{I\&T}$. $C_{I\&T}$ and mooring costs, C_m can be found as a part of the equation for LCC

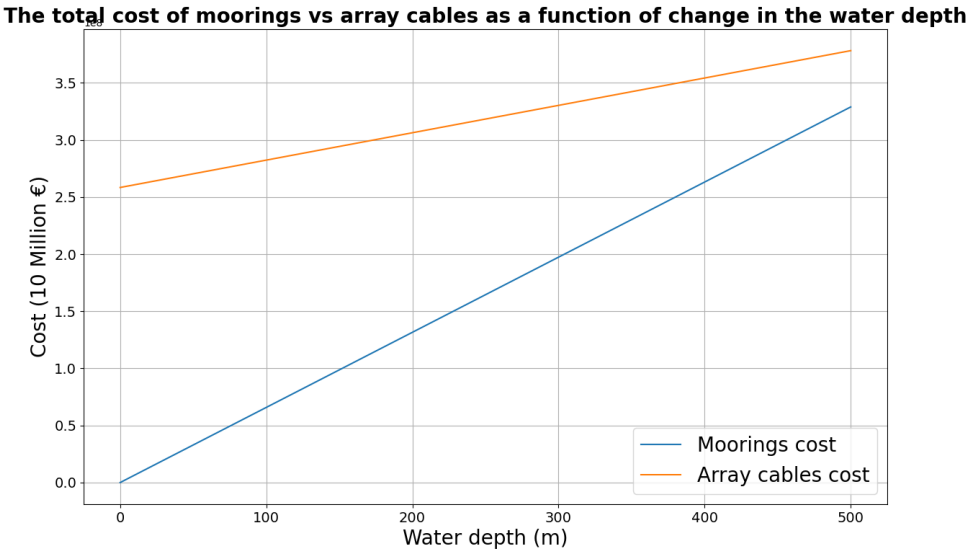

Figure 6.2: *The graph shows the cost of mooring manufacturing (blue line), and the cost of array cables (orange line) as a function of water depth. All other wind farm parameters than the water depth used in the results in this figure can be found in table 5.1, which gives an overview of the reference wind farm. The cost is shown on the y-axis and is given in 108 €, while the water depth (m) is shown on the x-axis.*

in equation 4.58. Therefore, an increase in the average depth at a wind farm location will lead to increased mooring and array costs, which again increases the LCC of the wind farm, which in turn increases the LCOE of the wind farm.

Number of wind turbines

The results of LCOE as a function of the number of wind turbines in a park can be seen in Figure 5.5. Here the LCOE is decreasing logarithmically with increasing number of wind turbines. The LCOE starts at about 117 €/MWh for 5 wind turbines and is rapidly reduced before it levels off at about 102 €/MWh for 50 wind turbines. From here the LCOE is static with increasing number of wind turbines.

When comparing with the results found by Myhr et al. (2014) and their investigation of effects of changing number of wind turbines on LCOE, there are both similarities and differences in the results. First, we can see how both graphs found in this thesis, and in Myhr et al. (2014) are decreasing logarithmically with an increasing number of wind turbines, before leveling off at a stable LCOE. The difference is seen in the number of wind turbines it takes before the LCOE stabilizes. Second, we also register that the LCOE drops rapidly while changing from 5 to 50 turbines, before leveling off. In Myhr et al. (2014) this change happens from 100 to 400 turbines, before leveling off.

Looking at the results found in Shafiee et al. (2016), we see a very similar result to that found in my work. In Shafiee et al. (2016) a rapid decline in LCOE is seen, until 50 turbines is reached. At this point the LCOE starts to level off, very similar to that found in this thesis, seen in Figure 5.5.

To find out why the drop in LCOE happens so rapidly as shown in Figure 5.5, a look into how the number of wind turbines behaves as a variable in the equations that the calculation of LCOE is based on. Looking at equation 4.1, which describes the calculation of monthly energy production, the number of wind turbines is found as a variable in the numerator of the fraction. Therefore, an increasing number of wind turbines will lead to a linear increase in energy production. As energy production is found in the denominator of calculation of LCOE in equation 4.60, a linear increase in energy production will lead to a logarithmic decline in LCOE.

Further, the number of wind turbine also increases the total power capacity

of the wind farm leading to linear increase in C_{Dev}, C_{Decom}, and $CManuf.$ However, looking at the increase in $C_{O\&M}$ due to increasing number of wind turbines, a logarithmic increase is found. For $C_{I\&T}$ an exponential increase is found. The expanding growth in $C_{I\&T}$ can be found to be faster than the slowing growth of $C_{O\&M}$, leading the overall LCC of the wind farm to be growing slightly exponentially with an increase in the number of wind turbines. This exponential growth in LCC is for a low number of wind turbines slower than the linear increase of the energy production, leading to the fast drop in LCOE for a low number of wind turbines in the farm. However, with an increasing number of wind turbines, the growth in LCC increases more than the growth in energy production, leading to eventually ending the logarithmic decline in LCOE.

With the exponential growth in LCC, a limitation of the method of calculating LCOE for higher number of wind turbines using the method outlined in this thesis, can be found. Because of the exponential growth in LCC, at around 400 wind turbines and above the LCOE will stop decreasing and start increasing with an increasing number of wind turbines in a park.

Because of the economies of scale, one would expect a cost advantage of creating larger wind farms. At more than 400 wind turbines, the cost advantage stops, and becomes a disadvantage by increasing the LCOE. Therefore, the method for calculating LCOE outlined in this thesis should be noted to have limitations when it comes to using the method for estimating LCOE for large scale wind farms.

Wake loss

The results of LCOE as a function of wake loss can be seen in Figure 5.6. Here LCOE is seen to increase slightly exponentially with an increased wake loss. Increased LCOE with increasing wake loss is to be expected as wake loss leads to less energy production, and therefore an increased LCOE.

The reason for the exponential growth in LCOE with an increasing wake loss is because the wake loss is found in the denominator of the equation for monthly energy production, equation 4.1. This leads to a logarithmic decrease in energy production with an increased wake loss. Looking at the equation for LCOE, equation 4.60, we find E_{month} in the denominator. Since E_{month} decreases logarithmically, with increased wake loss, LCOE will increase exponentially with E_{month} in the denominator, thus resulting in the

exponential growth in LCOE, as seen in Figure 5.6.

Wind farm lifetime

The results of LCOE as a function of the wind farm lifetime can be seen in Figure 5.7. The x-axis is set from 20 to 30 years, because most wind farms are assumed to have a lifetime of about 20 to 25 years. Setting the x-axis to 30 years allows us to see what would happen to LCOE, if the lifetime of a wind farm could be increased with five years from the assumed lifetime of most wind farms.

Since most of the costs included in the LCC of the wind farm is a one-time investment, one would expect the LCOE of the wind farm to decrease if the lifetime is expanded, as is reflected in Figure 5.7. An expansion in lifetime results in more years to distribute costs over, and therefore a decreased LCOE. Because of the discount rate, the drop in LCOE is not as steep as it would have been without it. This is because an increase in lifetime leads to a higher total cost for the payment on the interest rate, when assuming the payback will last the entire duration of the wind farm lifetime.

Results found by Myhr et al. (2014) shows a similar slope in the curve as that found the results in this thesis regarding the lifetime of a wind farm, seen in Figure 5.7. The difference is found in the value of the LCOE, as shown i Figure 5.7, decreases from about 102 to 88 €/MWh. The results found in Myhr et al. (2014) shows a reduction of about 160 to 145 €/MWh for most floating platforms.

Lifetime as a variable can be found in many of the equations used to calculate the LCOE of the wind farm. Firstly, it is used to calculate the total energy production during the wind farm lifetime. For this calculation it is found in the denominator in the equation for LCOE, equation 4.60. This means that the increased lifetime causes the logarithmic decline in the LCOE. When looking at the change in total LCC for the wind farm, the LCC increases linearly with increasing lifetime. The percentage change in LCC with increasing lifetime is slower than the percentage change in energy production, as seen in Figure 6.3. This causes the LCOE to decrease with increased lifetime, which we see in Figure 5.7.

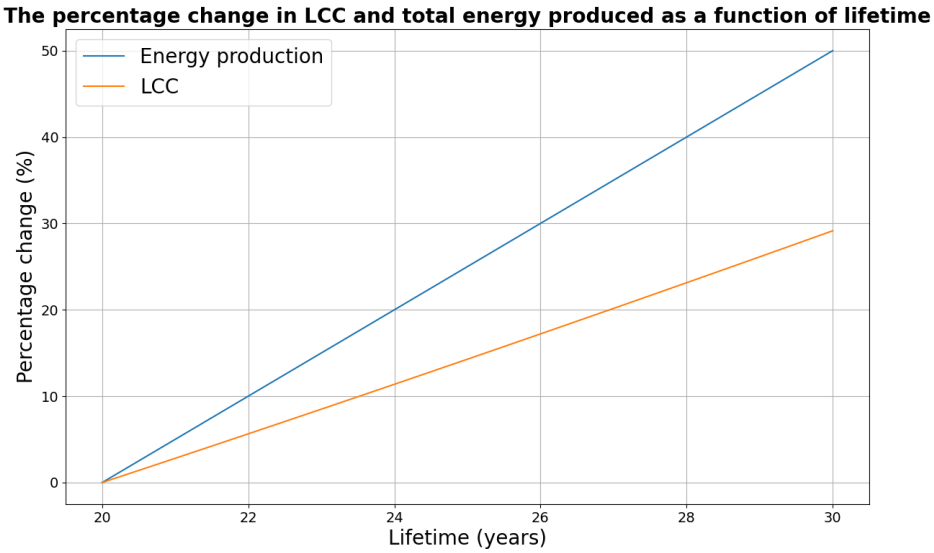

Figure 6.3: *The graph shows percentage change in LCC (orange line) and energy production (blue line) of a wind farm as a function of the wind farm's operational lifetime. All other wind farm parameters than the lifetime used in the results in this figure can be found in table 5.1, which gives an overview of the reference wind farm. The percentage change (%) is shown on the y-axis, while the lifetime (years) is shown on the x-axis.*

Capacity factor

The results of LCOE as a function of the average capacity factor at the wind farm can be seen in Figure 5.8. The x-axis is set from 40 % to 60 % as the capacity factors found in Table 3.1, which shows capacity factors for the four locations for each of the three turbine types, is found within this range.

As with the wind farm lifetime, LCOE can be seen to decrease logarithmically with increasing capacity factor. The reason for this can be explained with the same equations as for the lifetime. Capacity factor determines the amount of energy that will be produced, seen in equation 4.1, where the capacity factor is found in the numerator of the equation for monthly energy production. As previously discussed, increasing energy production with increasing capacity factor leads to a logarithmic decrease in the LCOE from 4.60 with increasing capacity factor.

Comparison of wind farm parameters

In Figure 5.9, a comparison of the percentage change in LCOE as a function of the six parameters discussed, can be seen. As stated in the description of this figure in chapter 5, it is important to remember that the percentage change seen for each parameter is decided by the start- and end- point that each parameter has had the x-axis normalized by. For example, the distance to harbor has been normalized between 0 and 500 km. However, all the locations that has been investigated lays within 150 km of a harbor. One could therefore argue that the approximately 15 % change in LCOE seen by the increase in distance to harbor, is unrealistic when compared to the change in LCOE caused by the change in capacity factor. Capacity factor is normalized between 40 % and 60 %. These values are all seen for the four locations that has been investigated in this thesis and is therefore realistic values. However, as mentioned previously, the economic zone of a country stretches 370 km from shore, and a country could be interested in establishing wind farms far from shore to minimize any conflicts with other industries using areas close to shore. Therefore, it is interesting to see how a wind farm located far from shore could possibly affect the LCOE of the wind farm.

Keeping in mind that the change in the x-axis largely influences the amount of change in LCOE when comparing the different wind farm parameters, we can try to get an idea on what wind farm parameters has the most influence over LOCE.

Starting with the water depth which, as the distance to harbor, varies by far more in depth over the x-axis in Figure 5.9, than compared with the water depth variation seen between the locations. Even though the depth over the x-axis is much deeper than the depth seen in any of the locations, the change in LCOE when the depth goes from 0 to 500 m is only 5,9 %.

Looking at the wake effect, a 20 % wake loss is arguably unrealistic, as the largest wake loss seen in any article used to find realistic wake loss for the standard wind farm in this thesis was 13 %. Even so, the change seen in LCOE with a change from 0 to 20 % wake loss is 24,8 %. But looking at a more realistic range of wake loss from 5 % to 10 %, the wake loss would account for a 5,5 % increase in the LCOE.

The change in the LCOE when increasing the distance from harbor from 0 to 500 km is 16,7 %. While looking at a range between 50 km and 250 km, that might be a more common interval to find different potential wind farm locations within, a change in LCOE of 6,7 % increase is found.

The three remaining parameters all causes negative change in the LCOE. Negative change can only go from 0 to -100 %, while positive change can go from 0 to infinity. Therefore, it is reasonable to convert the negative change using the following formula:

$$\text{Positive change} = \left(1 - \frac{1}{1 - \text{negative change}}\right) \cdot 100\% \tag{6.1}$$

Where negative change is the actual change in LCOE, given as a number between 0 and 1, and positive change is the comparable positive change in LCOE, given in %.

This would result in a 50 % decline in LCOE equaling a 100 % increase in the LCOE. Alternatively, this would be the same as looking at the change in LCOE that happens when moving from the right side of the x-axis to the left.

Going forward using this method of comparison we can first see a negative change of 14,2 % in the LCOE when going from 20 to 30 years for the wind farm lifetime. This is comparable to a 16,6 % positive change, when using

equation 6.1.

Furthermore, a negative change of 13,2 % is found for the LCOE, when going from 5 to 250 wind turbines. This equals to a positive change in LCOE of 15,2 %. When looking at these results (shown in Figure 5.9) one should keep in mind that almost the same change in LCOE would have been seen going from 5 to 50 wind turbines. This makes the number of wind turbines the only parameter that does not continuously affect the LCOE with an increase in the parameter. This also means that if the alternative when designing a park is 100 or 200 turbines, this would have neglectable influence over the LCOE of the wind farm, according to the analysis carried out in this thesis.

Lastly, a change in capacity factor from 40 % to 60 % leads to a 33,1 % negative change in the LCOE, which is comparable to a 49,4 % positive change. This makes capacity factor by far the most influential parameter when looking at changes in the LCOE, using the start and end values for the x-axis that has been chosen to be used in this thesis.

6.3.4 Locations

The results of the comparison of the LCOE between the four locations, Utsira Nord, Stadthavet, Frøyabanken, and Træna Vest can be found in Figure 5.10. The primary objective of this comparison is to see at which of the four locations it makes more economical sense to establish a wind farm. It is important to remember that other industries with conflicting interests in the areas has not been considered in this analysis.

There are several key takeaways from the analysis of the locations. Firstly, we can note that judging solely by LCOE, the four locations can be arranged from most suitable to least suitable in the following order: Stadthavet, Utsira Nord, Træna Vest, and Frøyabanken. The reasoning for this order can be found by looking at the discussion of the influence of the various wind farm parameters on LCOE, from the previous section.

First, we can note that some parameters do not influence the LCOE of a wind farm, based on the location of that wind farm. These parameters include the wake effect, the number of wind turbines, and the wind farm lifetime.

The distance from a harbor ranges from 45,4 km for Utsira Nord, to 131,8

km for Træna Vest. This change in distance accounts for a percentage change in the LCOE of 2,8 %. The difference in water depth accounts for even less of the difference in LCOE between the locations. The variation in depth for the locations ranges from both Stadthavet and Frøyabnken with the shallowest depth of 207 m, to 269 m for Træna Vest with the deepest average depth. This variation in depth accounts for 0,7 % change in the LCOE of a wind farm. A different story can be told for the effects from the variations in capacity factor between the locations. Looking at the 6 MW turbine, the capacity factor ranges from 40,8 % at Frøyabanken, to 48,7 % at Stadthavet. This difference in capacity factor accounts for a negative change in LCOE of 16,1 %, which is comparable to a 19,2 % positive change in the LCOE.

With these drastic differences in effects on LCOE from changes in water depth, distance to harbor, and capacity factor between the four locations, most of the variation in LCOE seen between the four locations, can be attributed the contribution from capacity factor.

6.3.5 Comparison of results with NVE report, Sydness et al. (2012)

I will in this section discuss the comparison of the results found in this thesis with the results found in the NVE report, Sydness et al. (2012). When looking at the comparison between the capacity factor found by using NORA3-WP, with that of NVE, one can note that they are about the same. Using the capacity factor in the calculation of energy production yields a result for the energy production that is about the same for the NVE report and that found in the calculations for this thesis.

Regarding the results for LCOE, the actual values of LCOE was not disclosed in Sydness et al. (2012). However, they included numbers for the change from the mean LCOE of the 15 locations that was investigated in the report. To be able to compare with the results found by Sydness et al. (2012) in the change from mean LCOE, I have looked at how each of the four locations investigated in this thesis differs from the mean LCOE of the four locations. The results found when doing this, seen in Figure 5.13, is similar to that found by NVE. In the figure, one can see that the LCOE of Frøyabanken and Træna Vest is greater than the mean LCOE for both the NVE report, and this thesis. The LCOE of Utsira Nord and Stadthavet is less than the mean LCOE for both the NVE report and the work presented in my work.

One thing to be noticed is that for Utsira Nord, Frøyabanken, and Træna Vest, the deviation from the mean is a larger number in Sydness et al. (2012), than in this thesis. This could be a result of Sydness et al. (2012) including 15 locations when calculating the mean LCOE, which could have raised the mean LCOE higher than the mean LCOE for the four locations, investigated in this thesis. Therefore, the four locations have a higher value relative to the mean LCOE found by Sydness et al. (2012), than the mean LCOE found in this thesis.

The exception to the trend discussed in the previous paragraph is found in Stadthavet. For Stadthavet, the calculations show a deviation from the mean LCOE, that has a smaller value than that of the value for deviation from the mean LCOE found by Sydness et al. (2012). This also results in Sydness et al. (2012) finding a greater LCOE, in terms of €/MWh, for Stadthavet, than Utsira Nord. Considering that Sydness et al. (2012) also operates with the largest capacity factor for Stadthavet amongst the four locations, this can only mean that they have put greater emphasis on some other factors, affecting the LCOE, than what has been done for the work presented in my thesis. This could be the distance from a harbor, since Stadthavet is located at double the distance compared with Utsira Nord. However, if that was the case, one would possibly expect to see a more similar LCOE between Træna Vest and Frøyabanken, or possibly a higher LCOE for Træna Vest than Frøyabanken found by Sydness et al. (2012), considering that Træna Vest has an average distance to a harbor double that of Frøyabanken. Also, water depth can be ruled out as a reason for the larger LCOE at Stadthavet compared with Utsira Nord, in terms of €/MWh, found by Sydness et al. (2012). This is because Stadthavet has an average depth of 207 m, while Utsira Nord has one of 264. This should contribute to a greater LCOE in terms of €/MWh.

Chapter 7

Conclusion

To answer the four questions addressed in the instruction, I developed a cost model for offshore floating wind farms, with emphasis on the effects on LCOE by change in various wind farm parameters. To conclude, I will try to answer the four questions by connecting the discussion and the presented findings.

How is the levelized cost of energy (LCOE) affected by the distance to port, the number of wind turbines in a park, the wake effect, the water depth, capacity factor and the wind farm lifetime?

We have seen the different effects of the wind farm parameters mentioned, through the results presented in this thesis. The results showed varying effects on LCOE by the various parameters. Water depth was shown to have the smallest effect on LCOE out of the parameters that has been discussed, with a change in LCOE of 5,9 % by a change of 500 meters. Taking into account that the four locations that has been investigated in this thesis, all has an average water depth between 200 and 300 meters, the real effect on LCOE, when comparing different locations, is in reality only 1,2 % for wind farms within that range of water depth.

The distance to harbor, and wake effect is two parameters that when comparing values within a large interval has a large effect on LCOE. But when looking at two different parks within a more reasonable interval of 50 to 250 km, and 5 to 10 % wake loss, the changes occurring in LCOE is about 6 % for each respective change in parameter-interval. Arguably, the effects of these parameters on LCOE are greater than the effect of water depth, but this of course depends on the interval that is compared for each parameter.

The impact of the number of wind turbines in a wind farm on LCOE, de-

pends on the size of the wind farm that is being planned. If the wind farm is small, ranging from 5 to 50 turbines, adding as many turbines as possible up to 50, will have a positive effect on LCOE. However, if the wind farm in question is one of larger size, greater than 100 turbines, going from for example 100 to 200 turbines would only decrease the LCOE by only a few €/MWh.

One of the larger effects on LCOE is seen by the impact of the wind farm lifetime. If the wind farms lifetime was increased by 10 years, from 20 to 30 years, this would result in a 14,2 % decrease in LCOE, the equivalent of a 16,6 % increase in LCOE.

Arguably, the most important parameter when designing a wind farm, is the average capacity factor one can achieve for the wind farm. As seen in Table 3.1, a good capacity factor is achieved by selecting a wind turbine with great rated power, combined with a wind farm location with ideal wind conditions. With a percentage change in LCOE comparable to a positive change of about 50 %, capacity is a huge driver in the LCOE of a wind farm. Looking at these results, capacity factor should be a decisive factor when choosing a location for a wind farm if a low LCOE is a primary goal.

Can we add to the understanding that we have from research done by for example Myhr et al. (2014), and Shafiee et al. (2016) on how different parameters influence LCOE for offshore wind farms?

The conclusions found in the articles mentioned above, states that distance from shore and water depth are factors with significant contribution to the LCOE of a wind farm. While those parameters were found to contribute to LCOE also in this master thesis, some other parameters such as wind farm lifetime, and especially capacity factor was found to be major driver in the LCOE of offshore floating wind farms. Capacity factor being one wind farm parameter which effects on LCOE was not investigated by either Myhr et al. (2014), Shafiee et al. (2016), or any other articles as far as I have noticed. Therefore, the effects of the capacity factor on LCOE is an area that should be investigated more thoroughly in further research.

Can we improve our understanding of available resources for production of wind energy and are there areas better suited for wind farms than others regarding LCOE?

As seen in the results found in Figure 5.10, we can see that there are indeed

areas more suited for wind farms than others, when LCOE is the only criteria to judge by. As we have seen, water depth and distance to a harbor does play a part in the resulting LCOE for a wind farm location, however judging by the results of this thesis, the most important criteria to look at when choosing a wind farm is the possible capacity factor of the location.

Are there any significant changes in the possible energy production in the different areas looked at by NVE (Sydness et al. (2012)) when using the data from NORA3-WP?

One of the objects of this thesis was to investigate whether there were any changes in the possible energy production of that found by Sydness et al. (2012), when using the open-source dataset NORA3-WP. As seen in the comparison in Figure 5.11, the capacity factor of that found by NVE and by using NORA3-WP, lays within one percentage point of each other. However, this is when assuming 6 MW turbines. Since the NVE report, Sydness et al. (2012) were written more than 10 years ago, it was at the time unrealistic to look at turbines larger than 6 MW. When using 10 or 15 MW turbines in the analysis, a significantly better capacity factor can be found than that found by NVE. However, the better capacity factor can solely be attributed to advances in technology. Had NVE looked at turbines of the same rated power, they probably would have found the same capacity factor for the equivalent turbines.

To say that the building an offshore floating wind farm is a huge undertaking would be an understatement. Equally to the construction, estimating the costs of such a project is a complex task, including competences and calculations based on knowledge from many different fields of study. A multitude of variable parameters influence the end-cost, as well as a large variety of costs, and fixed parameters, from different industries and stakeholders. A lack of good data can be stated as one of the main problems trying to get a good estimation of the actual LCOE of a floating wind farm. When it comes to floating wind farms of larger power capacity, there exists no real data at all, as such a farm has never been created before. However, as more and more floating wind farms are built, and the size increases, more and more reliable data will be created. This will allow future estimations of LCOE within floating wind farms to be even more robust. Hence, further research will have to be conducted to inform such projects and the decisions to be made.

List of Figures

2.1 *Proportion of new installed wind turbines each year by wind turbine rated power for onshore wind. Each color represents the share of total annual installed capacity for each "power capacity group" ranging from 0-500 kW, all the way to greater than 5 MW turbines. Figure is taken from Wind Monitor (2022a).* 14

2.2 *Proportion of annualized installed offshore wind turbines categorized by wind turbine rated power. Each color represents the share of total annual installed capacity for each "power capacity group" ranging from 0-500 kW, all the way to greater than 5 MW turbines. Figure is taken from Wind Monitor (2022b).* 15

2.3 *The graph shows the power curves of three wind turbine types: the 6 MW SWT-6.0-154 turbine, the 10 MW DTU-10.0-Reference turbine, and the 15 MW IEA-15-240-RWT turbine. The solid line represents the 6 MW turbine, the dashed line represents the 10 MW turbine, and the dash-dot line represents the 15 MW turbine. The figure shows normalized wind power on the y-axis, and wind speed on the x-axis, and is useful to compare the cut-in wind speeds of each turbine. The black arrowed line represents the cut-out wind speed. The red, and blue arrowed lines represent storm control 1, and 2, and are nor relevant for this thesis. Figure from Solbrekke and Sorteberg (2021).* . 16

2.4 *Five SWT-6.0-154 are used in Hywind Scotland, the first commercial floating wind farm ever to be built. Here represented by a SWT-6.0-154 from Hywind Scotland. Other turbines from the farm can be seen in the background. Picture from Wind Europe (2022)* 18

2.5 *The Figure shows a wind turbine installed on a Spar Buoy. Most of the SB stays under the water surface, using its weight to balance the wind turbine. The moorings can be seen as black angled lines. They connect the turbine to the anchors holding the turbine in place. The figure from Energy Facts (2022)* . . . 20
2.6 *The figure shows a wind turbine installed on a Tension Leg Platform. The platform, seen as a yellow structure on the figure, has high buoyancy keeping the structure afloat. The high buoyance creates tension on the moorings, which raises vertically from the seabed, keeping the floating platform connected to the anchors. Figure from Energy Facts (2022)* 22
2.7 *The picture shows three wind turbines in the WindFloat Atlantic wind farm outside Portugal. All three wind turbines are installed on Tension Leg Platforms. Picture from EDP (2022)* 23
2.8 *The figure shows a wind turbine installed on a Semi-Submersible Platform. As seen, the platform is partly under, and partly over the water surface, hence the name "Semi-Submersible". The mooring lines can be seen stretching to the seabed with slack in the lines. Picture from Energy Facts (2022)* 24

3.1 *The total area the NORA3-WP dataset covers is shown with color. The map shows capacity factor for a 6 MW turbine. The color representing the capacity factor can be seen in the legend, where the capacity factor is a percentage between 0 and 90 %. A low capacity factor is shown in dark blue, while the color gets lighter with higher capacity factor.* 28
3.2 *All 15 locations analyzed by NVE. The locations with deep waters, suitable for floating wind are colored pink. Picture from NVE's 2010 report, Espegren et al. (2010).* 29
3.3 *The location of Utsira Nord with location coordinates. Picture from NVE's 2012 report, Sydness et al. (2012).* 32
3.4 *Key data for Utsira Nord. The table show the closest distance to transformer, harbor, shore, and the water depth. Longitude and latitude for the mapped area are displayed on the x- and y-axis respectively. The legends display distance as lighter color the larger the distance is. Distance is displayed in km. Water depth is displayed as lighter colors the shallower it gets. Water depth is displayed as meters below sea level.* 33
3.5 *The location of Stadthavet with location coordinates. Picture from NVE's 2010 report, Espegren et al. (2010).* 34

3.6 *Key data for Stadthavet. The table show the closest distance to transformer, harbor, shore, and the water depth. Longitude and latitude for the mapped area are displayed on the x- and y-axis respectively. The legends display distance as lighter color the larger the distance is. Distance is displayed in km. Water depth is displayed as lighter colors the shallower it gets. Water depth is displayed as meters below sea level.* 35
3.7 *The location of Frøyabanken with location coordinates. Picture from NVE's 2012 report, Sydness et al. (2012).* 36
3.8 *Key data for Frøyabanken. The table show the closest distance to transformer, harbor, shore, and the water depth. Longitude and latitude for the mapped area are displayed on the x- and y-axis respectively. The legends display distance as lighter color the larger the distance is. Distance is displayed in km. Water depth is displayed as lighter colors the shallower it gets. Water depth is displayed as meters below sea level.* 37
3.9 *The location of Træna Vest with location coordinates. Picture from NVE's 2012 report, Sydness et al. (2012)* 38
3.10 *Key data for Træna Vest. The table show the closest distance to transformer, harbor, shore, and the water depth. Longitude and latitude for the mapped area are displayed on the x- and y-axis respectively. The legends display distance as lighter color the larger the distance is. Distance is displayed in km. Water depth is displayed as lighter colors the shallower it gets. Water depth is displayed as meters below sea level.* 39
3.11 *The figure show water depth at Utsira Nord, Stadthavet, Frøyabanken, and Træna Vest. The y-axis display water depth as meters below sea level (MBSL). For each location the water depth at the shallowest point is marked with a blue square, the average water depth is marked with a gray square, and the deepest water depth is marked with an orange square.* 40
3.12 *The figure show capacity factor at Utsira Nord, Stadthavet, Frøyabanken, and Træna Vest. The y-axis display capacity factor as a percentage (%). The capacity factor is shown for three wind turbines. For each location the capacity factor for the 6 MW turbine is marked with a blue square, the capacity factor for the 10 MW turbine is marked with a gray square, and the capacity factor for the 15 MW turbine is marked with an orange square.* 41

3.13 *The figure show distance to the closest harbor at Utsira Nord, Stadthavet, Frøyabanken, and Træna Vest. The y-axis display distance in kilometers (km). For each location the closest distance to harbor within the location is marked with a blue square, the average distance to harbor within the location is marked with a gray square, and the furthest distance to harbor within the location is marked with an orange square.* 42

4.1 *The graph shows potential monthly energy production for a 1,5 GW capacity wind farm with 250 6 MW turbines, located at Frøybanken. The y-axis shows the monthly energy production in GWh. The time is shown in years on the x-axis, but keep in mind that the energy production is monthly values. Energy production can be seen to spike and crash every year. This is due to the winter months being naturally windier than the summer months, and thereby the production being significantly higher during the winter, than the summer.* 46

5.1 *The graph shows LCOE of a wind farm as a function of distance to the closest harbor. All other wind farm parameters than the distance to harbor used in the results in this figure can be found in table 5.1, which gives an overview of the reference wind farm. LCOE (€/MWh) is shown on the y-axis, while the distance to harbor (km) is shown on the x-axis. The graph displays the LCOE of three different wind farms, using the SB (blue line), the TLP (orange line), and the SSP (green line) as the floating platform.* 83

5.2 *The graph shows the percentage change in LCOE of a wind farm as a function of distance to the closest harbor. All other wind farm parameters than the distance to harbor used in the results in this figure can be found in table 5.1, which gives an overview of the reference wind farm. The percentage change in LCOE (%) is shown on the y-axis, while the distance to harbor (km) is shown on the x-axis. The graph displays the change in LCOE of three different wind farms, using the SB (blue line), the TLP (orange line), and the SSP (green line) as the floating platform.* 84

5.3 *The graph shows LCOE of a wind farm as a function of water depth. All other wind farm parameters than the water depth used in the results in this figure can be found in table 5.1, which gives an overview of the reference wind farm. LCOE (€/MWh) is shown on the y-axis, while the water depth (m) is shown on the x-axis. The graph displays the LCOE of three different wind farms, using the SB (blue line), the TLP (orange line), and the SSP (green line) as the floating platform.* . 85

5.4 *The graph shows the percentage change in LCOE of a wind farm as a function of water depth. All other wind farm parameters than the water depth used in the results in this figure can be found in table 5.1, which gives an overview of the reference wind farm. The percentage change in LCOE (%) is shown on the y-axis, while the water depth (m) is shown on the x-axis. The graph displays the change in LCOE of three different wind farms, using the SB (blue line), the TLP (orange line), and the SSP (green line) as the floating platform.* 86

5.5 *The graph shows LCOE of a wind farm as a function of the number of wind turbines in the wind farm. All other wind farm parameters than the number of wind turbines used in the results in this figure can be found in table 5.1, which gives an overview of the reference wind farm. The exception is the total power capacity of the wind farm. This parameter also changes with the number of wind turbines in the results shown in the figure. LCOE (€/MWh) is shown on the y-axis, while the number of turbines is shown on the x-axis. The graph displays the LCOE of three different wind farms, using the SB (blue line), the TLP (orange line), and the SSP (green line) as the floating platform.* 87

5.6 *The graph shows LCOE of a wind farm as a function of wake loss. All other wind farm parameters than the wake loss used in the results in this figure can be found in table 5.1, which gives an overview of the reference wind farm. LCOE (€/MWh) is shown on the y-axis, while the wake loss (%) is shown on the x-axis. The graph displays the LCOE of three different wind farms, using the SB (blue line), the TLP (orange line), and the SSP (green line) as the floating platform.* 88

5.7 *The graph shows LCOE of a wind farm as a function of the wind farm's operational lifetime. All other wind farm parameters than the lifetime used in the results in this figure can be found in table 5.1, which gives an overview of the reference wind farm. LCOE (€/MWh) is shown on the y-axis, while the lifetime (years) is shown on the x-axis. The graph displays the LCOE of three different wind farms, using the SB (blue line), the TLP (orange line), and the SSP (green line) as the floating platform.* 89

5.8 *The graph shows LCOE of a wind farm as a function of capacity factor. All other wind farm parameters than the capacity factor used in the results in this figure can be found in table 5.1, which gives an overview of the reference wind farm. LCOE (€/MWh) is shown on the y-axis, while the capacity factor (%) is shown on the x-axis. The graph displays the LCOE of three different wind farms, using the SB (blue line), the TLP (orange line), and the SSP (green line) as the floating platform.* 90

5.9 *The graph shows the percentage change for LCOE when changing the values of the wind farm parameters: number of wind turbines in the wind farm (red), the average distance from the wind farm location to a harbor (blue), the average depth at the wind farm location (green), the total wake loss in a wind farm (orange), the operational lifetime of the wind farm (purple), and the average capacity factor in a wind farm (pink). All values have been normalized so that 0 represents the smallest value and 1 represents the greatest value on the x-axis. All values written on the graph next to a line of the same color, represents the change in that parameter's native unit from 0 to 1 on the x-axis. This figure can be found in the attachments where it appears rotated, so it is easier to see all the lines.* . . 91

5.10 *The graph in this figure shows LCOE as a function of the lifetime of a wind farm between 20 and 30 years. In this figure all the four locations that has been investigated in this thesis is presented. Utsira Nord is presented as solid lines, Stadthavet is presented as dashed lines, Frøyabanken is presented as dash-dot lines, and Træna Vest is presented as dotted lines. Each location is presented as a wind farm with 250 6 MW turbines, 150 10 MW turbines, and 100 15 MW turbine. For all locations the 6 MW turbines are colored blue, the 10 MW turbines are colored red, and the 15 MW turbines are colored green. This figure can be found in the Appendix B where it appears rotated, so it is easier to see all the lines.* 93

5.11 *The clustered column chart compares the capacity factor found in the NVE report, Sydness et al. (2012), with that found when using the dataset NORA3-WP. The results are shown for the four locations: Utsria Nord, Stadthavet, Frøyabanken, and Træna Vest. The results are shown using a 6 MW turbine. The capacity factor is given in percent (%) on the y-axis. The blue columns represent results from the NVE report, while the orange columns represent results found in this thesis.* 96

5.12 *The clustered column chart compares the annual energy production found in the NVE report, Sydness et al. (2012) with that found when using the dataset NORA3-WP. The results are shown for the four locations: Utsria Nord, Stadthavet, Frøyabanken, and Træna Vest. The results are shown using a 6 MW turbine. The annual energy production is given in GWh on the y-axis. The blue columns represent results from the NVE report, while the orange columns represent results found in this thesis.* 97

5.13 *The clustered column chart compares the deviation from the mean LCOE found in the NVE report, Sydness et al. (2012) with that found when using the dataset NORA3-WP. The results are shown for the four locations: Utsria Nord, Stadthavet, Frøyabanken, and Træna Vest. The results are shown using a 6 MW turbine. The deviation from the mean LCOE is given in percent (%) on the y-axis. The blue columns represent results from the NVE report, while the orange columns represent results found in this thesis.* 98

6.1 *The graph shows the LCOE of a wind farm as a function of $min_{UCMpct.}$. $min_{UCMpct.}$ Is defined as all minor unplanned corrective maintenance events as a percentage of the total number of unplanned corrective maintenance events. All wind farm parameters used in the results in this figure can be found in table 5.1, which gives an overview of the reference wind farm. LCOE (€/MWh) is shown on the y-axis, while the $min_{UCMpct.}$ (%) is shown on the x-axis.* 108

6.2 *The graph shows the cost of mooring manufacturing (blue line), and the cost of array cables (orange line) as a function of water depth. All other wind farm parameters than the water depth used in the results in this figure can be found in table 5.1, which gives an overview of the reference wind farm. The cost is shown on the y-axis and is given in 108 €, while the water depth (m) is shown on the x-axis.* 111

6.3 *The graph shows percentage change in LCC (orange line) and energy production (blue line) of a wind farm as a function of the wind farm's operational lifetime. All other wind farm parameters than the lifetime used in the results in this figure can be found in table 5.1, which gives an overview of the reference wind farm. The percentage change (%) is shown on the y-axis, while the lifetime (years) is shown on the x-axis.* 115

B.1 *Figure text for this figure found under Figure 5.9* 139

B.2 *Figure text for this figure found under Figure 5.10* 140

List of Tables

3.1 *Key data for the locations Utsira Nord, Stadthavet, Frøyabanken and Træna Vest. Turbine capacity factor is a measure of the average capacity factor each location, using 6 MW turbines, 10 MW turbines, and 15 MW turbines. Distances is shown for the average, closest and furthest distance to the closest harbor, transformer, and shoreline. The capacity factor data is gathered from the dataset NORA3-WP, Solbrekke and Sorteberg (2021). The distance to harbor data is gathered from the geonorge (NMA) dataset, Kystverket (2022). The water depth data is gathered from the GEBCO Grid, GEBCO (2021). The distance to transformer data is gathered from geonorge (NVE) dataset, Geonorge (2022). The distance to shore data is gathered from the geonorge (POD - Norge 1:50000 (land)) dataset, Kartverket (2022)* 30

4.1 *The table show values for costs of development costs (C_{Dev}), manufacturing costs (C_{Manuf}), installation and transportation costs ($C_{I\&T}$), operation and maintenance costs ($C_{O\&M}$) and decommissioning costs (C_{Decom}). The table shows values in euros (€) collected from five articles and one master's theses, referenced in the table. The values have been adjusted after they were collected and cannot be found as they are shown in this table in their respective papers. The values have first been adjusted for inflation since the year of the publication of the respective paper. The values have been extrapolated from the power capacity of the wind farm being investigated in the respective paper, to a 1,5 GW wind farm (The power capacity of the farms investigated in this thesis). The values seen under "Average" is an average of the values from the articles, for each category. Note that $C_{I\&T}$ and $C_{O\&M}$ are not used to calculate LCC in this thesis. They are there as a reference to compare the costs of these two categories that will be calculated later in the thesis.* 50

4.2 *Overview of parameters used to calculate the installation and transportation of turbines and floating platforms as a part of the total $C_{I\&T}$. Some of the parameters are also used in the calculation of the installation of the substations, cables, and moorings. A brief explanation for all the parameters can be found in the Appendix A. The number in the "nr."-column corresponds to the number of the parameter found in the Appendix. All values in this table has been gathered from Castro-Santos et al. (2018) and Ioannou et al. (2018).* 55

4.3 *Overview of parameters used to calculate the installation of cables, substations, anchors, and moorings as a part of the total $C_{I\&T}$. A brief explanation for all the parameters can be found in the Appendix A. The number in the "nr."-column corresponds to the number of the parameter found in the Appendix. All values in this table has been gathered from Castro-Santos et al. (2018) and Ioannou et al. (2018).* 57

4.4 *Overview of parameters used to calculate the total COM. A brief explanation for all the parameters can be found in the Appendix. The number in the "nr."-column corresponds to the number of the parameter found in the appendix. All values in this table have been gathered from Shafiee et al. (2016), Bjerkseter and Ågotnes (2013), Catapult Offshore Renewable Energy (2022), SSB (2022), and 4C Offshore (2022).* 58
4.5 *The data in the table is gathered from Bjerkseter and Ågotnes (2013). It shows the number maintenance events per year in the reference wind farm described in Bjerkseter and Ågotnes (2013). The maintenance events has been categorized by unplanned corrective maintenance events, condition-based maintenance events, and calendar-based maintenance events.* . . . 72

5.1 *The table show the reference wind farm used in this thesis. Parameters from this table is used in the wind farms presented in the results chapter.* 80
5.2 *The table show how LCC is divided over the five cost categories that make up LCC. The results shown in this table is derived using the standard parameters for the reference wind farm found in Table 5.1* 82
5.3 *The table compare results from the NVE report by Sydness et al. (2012) with results found in this thesis. The loactions Utsira Nord, Stadthavet, Frøyabanken, and Træna Vest is compared in the table. The results of capacity factor (%), calculated annual energy production (GWh), and deviation from mean LCOE (%) is shown. For the NVE report, mean LCOE refers to the mean LCOE of all the 15 locations that has been investigated in their report, which includes Utsira Nord, Stadthavet, Frøyabanken, and Træna. The mean LCOE in this thesis is the mean LCOE of Utsira Nord, Stadthavet, Frøyabanken, and Træna. In addition, the LCOE (€/MWh) found for each location in this thesis is included in the table.* 95
5.4 *The table compare results of the LCOE calculation from Maienza et al. (2020) with results found in this thesis. The Three floating platform types of SB, TLP, and SSP is compared in the table. The LCOE is given in €/MWh. The table compares the LCOE of a wind farm with the same parameters used by the reference wind farm found in Maienza et al. (2020)* 99

Appendix A

Parameter explanation for tables 4.2, 4.3, and 4.4

1. cs is the hiring cost for the port per m2 per day
2. cc is the daily rental cost of a crane, and
3. cb is the daily rental cost of barge vessels
4. ct represents the daily cost of rental for tug vessels
5. Ctm is the cost of mobilizing one tug vessel
6. Cbm is the cost of mobilizing one barge vessel
7. Ccm is the cost of mobilizing a crane
8. cpc is the daily rental cost for the port crane used to lift the wind turbines
9. tLT is the time it takes to load one wind turbine into the vessel that will carry it to the wind farm location
10. tiT is the time between crane movements while the wind turbine is being installed at site
11. timT is the time it takes to install the turbine offshore with lifts
12. tiP is the time it takes to install the turbine offshore with lifts
13. timp is the time between crane movements while the floating platform is being installed at site

14. tLP is the time it takes to load one floating platform onto the vessel that will carry it to the wind farm location
15. vt is the speed of the barge and tug vessels
16. vt1 is the speed of the crane.
17. nBT,1,2, and 3 are the number of wind turbines being transported per vessel
18. kt is the downtime between work
19. nb represents the number of barge vessels used in the transportation
20. nt represents the number of tug vessels used in the transportation
21. ncs is the number of floating cranes with a storage area used for installation at sea
22. nc is the number of floating cranes without a storage area used for installation at sea
23. nBP,1, 2 and 3 are the number of floating platforms being transported per vessel
24. lTS is the length of the electric transformer used in the substation
25. lGIS is the length of the gas insulated switch gear used in the substation
26. lf is the maximum freeboard of the platform
27. dP is the draft of the platform
28. l is the length of the floating platform
29. dip is the diameter of the inferior pontoon
30. CITS,5,1 is the cost of soil preparation
31. CITS,5,2 is the foundation cost
32. CITS,5,3 is the cost of cranes during the installation process
33. cITS,1 is the daily rental cost of the cable laying vessel (CLV)
34. cIMA,1 is the daily rental cost of the anchor handling vehicle (AHV)

35. cIMA,2 is the cost of the direct labour associated with the installation
36. cITS,3 is the installation cost per meter of installed cable
37. kITS,1 is the installation rate for array cables of the CLV
38. kITS,2 is the installation rate for export cables of the CLV
39. rIMA,1 is the installation rate of anchors installed per day
40. ATS is the plan area of the transformer
41. AGIS is the plan area if the insulated switch gear
42. tLIOS represents the time taken to load one substation onto the carrying vessel
43. n1 is the number of electric cables used for the array cables
44. n2 is the number of electric cables used for the export cables
45. n3 is the number of electric cables used for the onshore cables
46. ccv is the daily rental cost of a crew vessel
47. PE is the price the wind farm will be able to sell the produced energy for
48. cO,4 is the insurance cost per installed MW of power capacity at the wind farm
49. cO,5 is the cost of transmission per installed MW of power capacity at the wind farm
50. vcv is the speed of the crew vessel
51. ℓ is the rent paid as a percentage of the wind farm's revenue
52. Ef is the annual number of failures on the wind farm cables per 100 km of cable

Appendix B

Enlarged figures

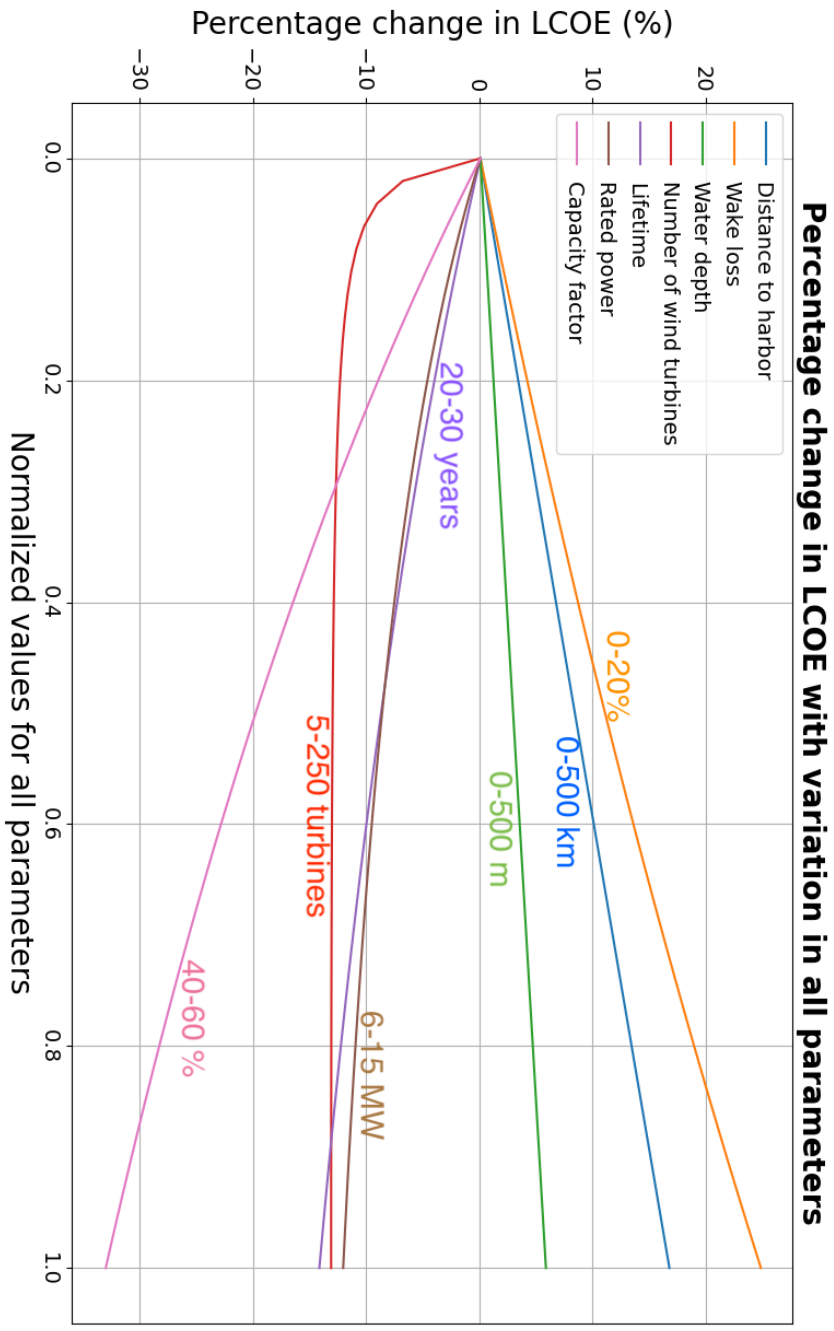

Figure B.1: *Figure text for this figure found under Figure 5.9*

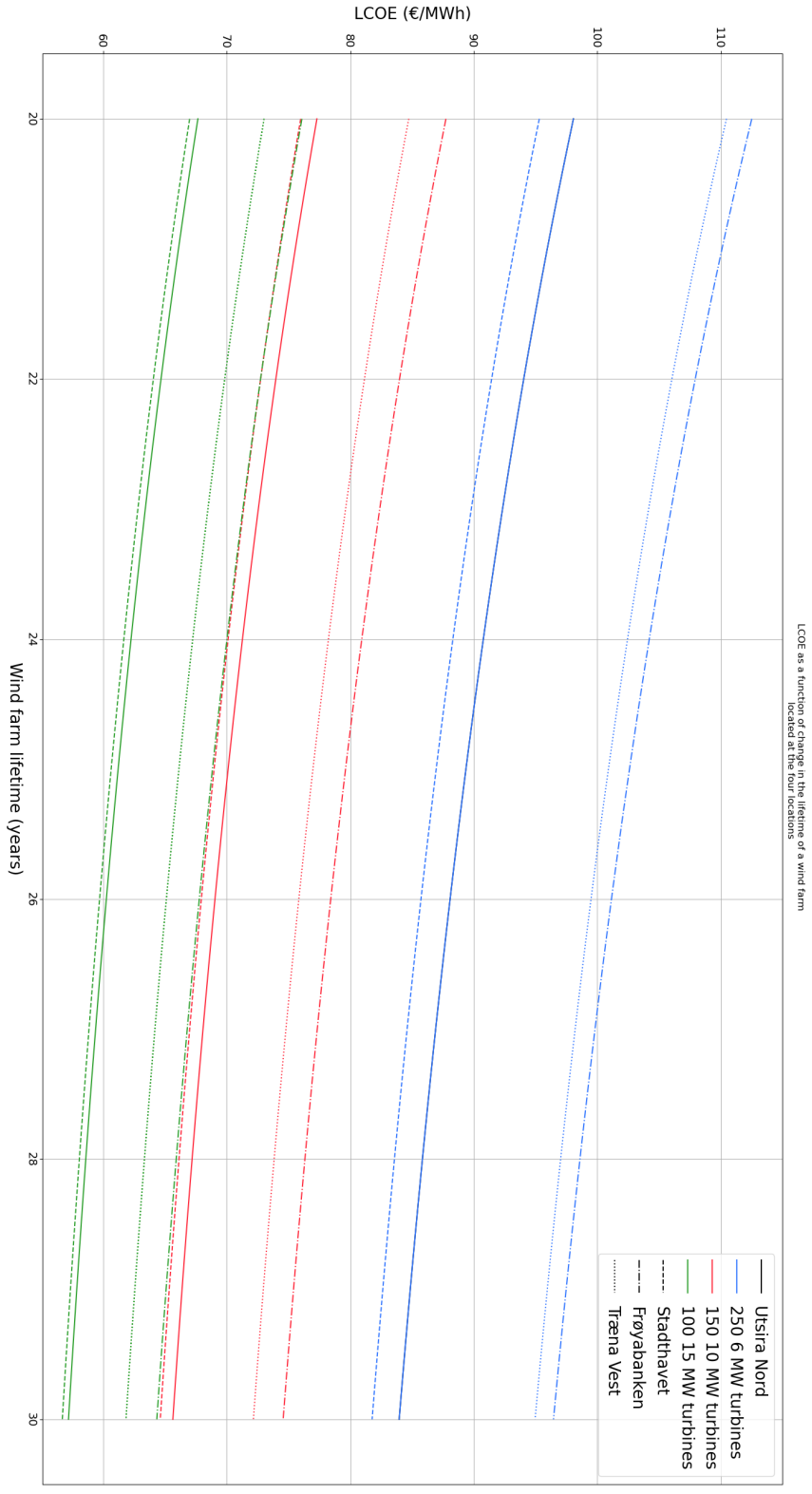

Figure B.2: *Figure text for this figure found under Figure 5.10*

Bibliography

4C Offshore (2022). An Introduction To Crew Transport Vessels, https://www.4coffshore.com/support/an-introduction-to-crew-transfer-vessels-aid2.html.

Bak, C., Bitsche, R., Yde, A., Kim, T., Hansen, M. H., Zahle, F., Gaunaa, M., Blasques, J., Døssing, M., Heinen, J. J. W., and Behrens, T. (2012). Light rotor: The 10-MW Reference Wind Turbine. *Eur. Wind Energy Conf. Exhib. 2012, EWEC 2012*, 1:532–541.

BarentsWatch (2012). Havnestrukturen i Norge, https://www.barentswatch.no/artikler/Havnestrukturen-i-Norge/.

Bjerkseter, C. and Ågotnes, A. (2013). Levelised cost of energy for offshore floating wind turbine concepts.

Buvik, M., Hole, J., Østenby, A. M., Koestler, V., Isachsen, O. K., and Ericson, T. B. (2019). Kostnader for kraftproduksjon 2018. *Teknol. 2019*, (7):1–2.

Castro-Santos, L. and Diaz-Casas, V. (2015). Sensitivity analysis of floating offshore wind farms.

Castro-Santos, L., Filgueira-Vizoso, A., Lamas-Galdo, I., and Carral-Couce, L. (2018). Methodology to calculate the installation costs of offshore wind farms located in deep waters. *J. Clean. Prod.*, 170:1124–1135.

Catapult Offshore Renewable Energy (2022). Guide to an Offshore Wind Farm, https://guidetoanoffshorewindfarm.com/guide#O_1_3_1.

Cobra (2022). Kincardine Floating Offshore Wind Farm, https://www.grupocobra.com/en/proyecto/kincardine-offshore-floating-wind-farm/.

EDP (2022). Windfloat Atlantic Project, https://www.oceanwinds.com/projects/windfloat-atlantic-project/.

Energy Facts (2022). Floating Wind Structures And Mooring Types, https://www.energyfacts.eu/floating-wind-structures-and-mooring-types/.

Equinor (2022a). Hywind Scotland, https://www.equinor.com/energy/hywind-scotland.

Equinor (2022b). Hywind Tampen, https://www.equinor.com/energy/hywind-tampen.

Espegren, N. M., Bartnes, G., Drivenes, A., Eirum, T., Johnson, N. H., Mindeberg, S. K., Lunde, S., Undem, L. S., Veggeland, K., Veie-Rosvoll, B., and Voksø, A. (2010). Havvind Forslag til utredningsområder. pages 1–204.

Gaertner, E., Rinker, J., Sethuraman, L., Anderson, B., Zahle, F., and Barter, G. (2020). IEA Wind TCP Task 37: Definition of the IEA 15 MW Offshore Reference Wind Turbine. pages 1–44.

GEBCO (2021). The GEBCO_2021 Grid, https://www.gebco.net/data_and_products/gridded_bathymetry_data/gebco_2021/.

Geonorge (2022). Transformatorstasjoner, https://kartkatalog.geonorge.no/metadata/transformatorstasjoner/ae55f901-480d-4fdc-8f1e-58ef3004d169.

Hvidevold, A. E. and Karlsen, M. (2020). *Økonomiske utsikter for utbygging av Utsira Nord*. PhD thesis, Norges Handelshøyskole.

Ioannou, A., Angus, A., and Brennan, F. (2018). A lifecycle techno-economic model of offshore wind energy for different entry and exit instances. *Appl. Energy*, 221(November 2017):406–424.

Kartverket (2022). https://kartkatalog.geonorge.no/metadata/pod-norge-150000-land/3e2ca03a-0978-4d1a-894f-83866b3a0b5a.

Kystverket (2022). ISPS Havneanlegg, https://data.kystverket.no/dataset/dc9b4d63-8597-4971-92a4-9f665abc3e21.

Lerch, M., De-Prada-Gil, M., Molins, C., and Benveniste, G. (2018). Sensitivity analysis on the levelized cost of energy for floating offshore wind farms. *Sustain. Energy Technol. Assessments*, 30:77–90.

Maienza, C., Avossa, A. M., Ricciardelli, F., Coiro, D., Troise, G., and Georgakis, C. T. (2020). A life cycle cost model for floating offshore wind farms. *Appl. Energy*, 266:114716.

Myhr, A., Bjerkseter, C., Ågotnes, A., and Nygaard, T. A. (2014). Levelised cost of energy for offshore floating wind turbines in a life cycle perspective. *Renew. Energy*, 66:714–728.

Rinaldi, G., Garcia-Teruel, A., Jeffrey, H., Thies, P. R., and Johanning, L. (2021). Incorporating stochastic operation and maintenance models into the techno-economic analysis of floating offshore wind farms. *Appl. Energy*, 301(June):117420.

Shafiee, M., Brennan, F., and Espinosa, I. A. (2016). A parametric whole life cost model for offshore wind farms. *Int. J. Life Cycle Assess.*, 21(7):961–975.

Simens Gamesa (2022a). SG 14-222 DD Turbine, https://www.siemensgamesa.com/products-and-services/offshore/wind-turbine-sg-14-222-dd.

Simens Gamesa (2022b). SWT-6.0-154, https://www.siemensgamesa.com/products-and-services/offshore/wind-turbine-swt-6-0-154.

Skeie, P., Steinskog, D. J., and Näs, J. (2012). Kraftproduksjon og vindforhold. Technical report.

Solbrekke, I. M. and Sorteberg, A. (2021). NORA3-WP: A high-resolution offshore wind power dataset for the Baltic, North, Norwegian, and Barents Seas. *NIRD Res. data Arch.*, 2019.

SSB (2022). Elektrisitetspriser, https://www.ssb.no/statbank/table/09364/tableViewLayout1/.

Sydness, G. S., Berg, K. S., Carlsen, M., Eirum, T., Jakobsen, S. B., Johnson, N. H., Mindeberg, S. K., and Nybakke, K. (2012). *Havvind Strategisk konsekvensutredning*. Oslo.

Wind Europe (2022). Hywind Scotland, https://windeurope.org/newsroom/press-releases/ ywind d-awards-seabed-rights-for-massive-amounts-of-offshore-wind-most-of-it-floating/attachment/ ywind-scotland-floating-wind-turbine-backlit-sun-rays-foreground-background/.

Wind Monitor (2022a). Capacity classes, http://windmonitor.iee.fraunhofer.de/windmonitor_en/3_Onshore/2_technik/2_leistungsklasse/

Wind Monitor (2022b). Turbine Size, http://windmonitor.iee.fraunhofer.de/windmonitor_en/4_Offshore/2_technik/3_Anlagengroesse